

10725

THE DYNAMIC BEHAVIOUR OF ROTAMETERS

BIBLIOTHEEK
LABORATORIUM VOOR
TECHNISCHE FYSIKA
DELFT

PROEFSCHRIFT

TER VERKRIJGING VAN DE GRAAD VAN DOCTOR
IN DE TECHNISCHE WETENSCHAP AAN DE TECH-
NISCHE HOGESCHOOL TE DELFT OP GEZAG VAN DE
RECTORMAGNIFICUS Ir. H. J. DE WIJS, HOGLERAAR
IN DE AFDELING DER MIJNBOWWKUNDE, TE VER-
DEDIGEN OP WOENSDAG 19 JUNI 1963
DES NAMIDDAGS TE 2 UUR

DOOR

HARMEN HEIN DIJSTELBERGEN

ELECTROTECHNISCH EN NATUURKUNDIG INGENIEUR
GEBOREN TE ROTTERDAM



Bibliotheek TU Delft



C 0003183944

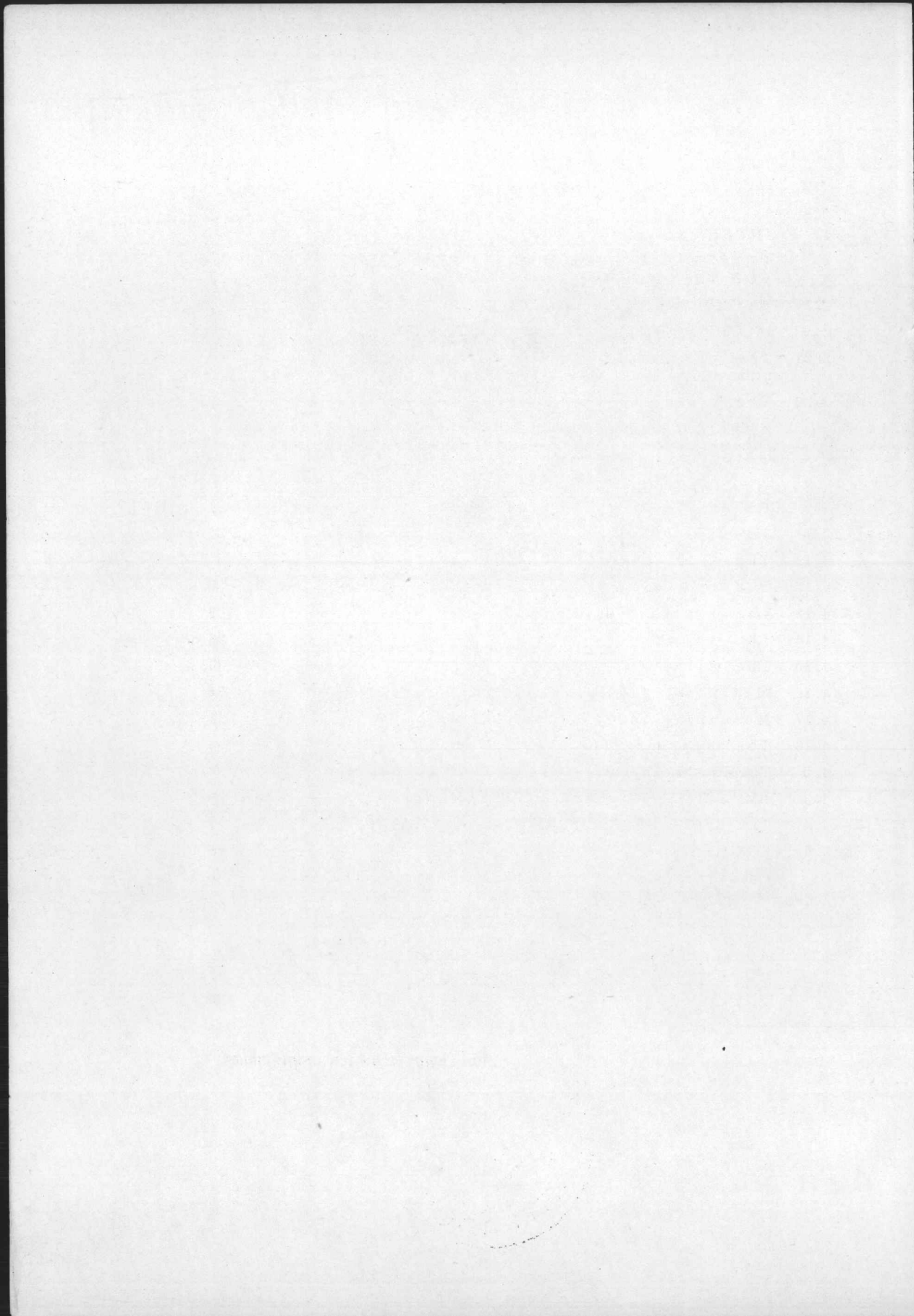
8255
716
9

DIT PROEFSCHRIFT IS GOEDGEKEURD DOOR DE PROMOTOR
PROF. DR. IR. C. J. D. M. VERHAGEN

BIBLIOTHEEK
LABORATORIUM VOOR
TECHNISCHE FYSIKA
DELFT



Aan mijn vrouw en mijn ouders



CONTENTS

1.	INTRODUCTION.	1
2.	PRESSURE DIFFERENCE TYPE FLOWMETERS FOR INCOMPRESSIBLE FLUIDS.	3
2.1	INCOMPRESSIBLE FLOW WITH FIXED RESTRICTIONS.	3
2.2	INCOMPRESSIBLE FLOW IN ROTAMETERS.	6
2.21	The velocity of the fluid in a rotameter under dynamic conditions.	9
2.22	The equation of motion for the float.	12
3.	APPROXIMATE SOLUTIONS OF THE EQUATION OF MOTION FOR SMALL SINUSOIDAL PULSATIONS.	19
4.	MEASUREMENTS FOR INCOMPRESSIBLE FLUID FLOW.	24
4.1	THE TEST SET-UP.	24
4.11	The water circuit.	24
4.12	The pulsator.	26
4.13	The magnetic flowmeter.	26
4.14	The switch.	28
4.15	The measuring vessel.	30
4.16	Measuring the frequency of pulsation.	31
4.17	Measuring the phase of the float.	31
4.18	The measuring procedure.	33
4.2	TUBES AND FLOATS.	36
4.3	AMPLITUDE AND PHASE MEASUREMENTS.	38
4.4	THE ERROR IN THE INDICATED MEAN VALUE.	41
4.5	CONCLUSION.	45
5.	FLOWMETERS FOR COMPRESSIBLE MEDIA.	46
5.1	FIXED ORIFICES.	46
5.2	ROTAMETERS.	50
5.21	Approximations for sinusoidal pulsations.	50
5.22	The impedance of the float and the rotameter tube.	53
5.23	The stability of the float.	56



6.	MEASUREMENTS FOR COMPRESSIBLE FLOW.	60
6.1	THE MEASURING CIRCUITS.	60
6.11	The measuring circuit for high flow rates.	60
6.111	The ventilator.	61
6.112	The sine generator.	61
6.113	The hot wire anemometer.	62
6.114	The measuring procedure.	64
6.12	The measuring circuit for low flow rates.	66
6.121	The sine generator.	67
6.122	The hot wire anemometer.	68
6.123	Measurement of the float movement.	69
6.124	The positive displacement meter.	70
6.125	The measuring procedure.	71
6.2	TUBES AND FLOATS.	72
6.3	AMPLITUDE AND PHASE MEASUREMENTS.	74
6.4	THE ERROR IN THE INDICATED MEAN VALUE.	77
6.5	MEASUREMENTS ABOUT BOUNCING.	79
6.6	CONCLUSION.	84
7	THE FLOW PATTERN IN A ROTAMETER.	86
7.1	THE CONTRACTION COEFFICIENT.	86
7.2	THE APPARATUS FOR OBSERVING THE FLOW PATTERN IN A ROTAMETER WITH PULSATING FLOW.	87
7.3	MEASUREMENTS.	90
7.4	CONCLUSION.	90
	SUMMARY.	94
	SAMENVATTING.	95
	REFERENCES	96

1. INTRODUCTION.

To measure a liquid or gas flow in pipes several types of instruments are available. They can be divided into some groups depending on their operating principle.

One of the largest groups comprises the instruments based on the existence of a pressure drop over some kind of restriction. The change in area of the stream tube can be gradual as in a venturi tube, or quite sudden as with sharp edged orifices or rotameters. We can roughly divide the flowmeters based on a pressure difference into two categories: the constant area and variable area meters. The first one contains all meters with a fixed restriction, i.e. venturies, orifices, and nozzles. With these instruments the pressure difference is measured directly with the aid of some type of manometer. The second one contains meters in which the area of the restriction is determined by the flow, i.e. rotameters and vane-meters. In these devices the pressure difference results in a force that is balanced by gravity.

For many years papers have been published on the dynamic behaviour of flowmeters. The main reason for the activity in this field is the error which occurs when metering non-steady flow. Some authors report errors of as much as one-hundred percent.

Although many designs have appeared in publications for flowmeters which are insensitive to pulsations *1, the dynamic behaviour of flowmeters of the pressure difference type is still of interest because the insensitivity to pulsations is obtained by means of considerable mechanical and/or electronic equipment making these devices fairly costly. The simple devices, therefore, remain preferable in cases of steady flow and for measurements not requiring great precision or when the pulsations in the flow are not too serious. Many authors *2, 3 have attempted to theoretically define criteria for the seriousness of pulsations. Others proposed measuring devices for determining the degree of pulsations *4. However there remain many aspects of these phenomena to be explained.

Another reason to investigate the dynamic behaviour of flowmeters is the use of these meters in control systems. Adequate design of a control system requires the response of the meters to be known.

The purpose of this study is to extend the theory of the process of metering pulsating flow with rotameters, to verify experimentally the results, and in some cases to indicate a way for improving the performance of the instruments. In particular, two aspects of the

behaviour of the instrument are treated : the response of the instrument to sinusoidal pulsations, and the mean reading of the instrument under these conditions. This thesis will deal with both incompressible and compressible flow in rotameters.

The work is based on investigations carried out since 1955 in the Instrumentation Laboratory of the Technological University at Delft. Subsequently Schneiders *5, Ury *6, Kramers *7, v.d. Biggelaar, Rachmad Mohamad*8, de Groot*9, Koopmans*10, and the author worked on the subject.

2. PRESSURE DIFFERENCE TYPE FLOWMETERS FOR INCOMPRESSIBLE FLUIDS.

2.1 INCOMPRESSIBLE FLOW WITH FIXED RESTRICTIONS.

We start by considering incompressible flow in a fixed restriction (fig. 2.1.1).

From Bernoulli's equation

$$\frac{p_1}{\rho} - \frac{p_2}{\rho} = \frac{1}{2}(v_2^2 - v_1^2) ,$$

and the continuity equation

$$w = v_1 a_1 = v_2 a_2 ,$$

we find

$$v_1^2 = \frac{(p_1 - p_2)}{\rho} \frac{2a_2^2}{a_1^2 - a_2^2} , \quad (2.1.1)$$

which results in

$$w = v_1 a_1 = K \sqrt{p_1 - p_2} . \quad (2.1.2)$$

In these equations w is the volumetric flow, ρ the density of the fluid and K a constant. v_1 and v_2 are the velocities, p_1 and p_2 the pressures, a_1 and a_2 the areas of the jet at the two points where the pressure is measured ¹. Eq. (2.1.2) only holds when the conditions necessary for applying Bernoulli's equation are satisfied.

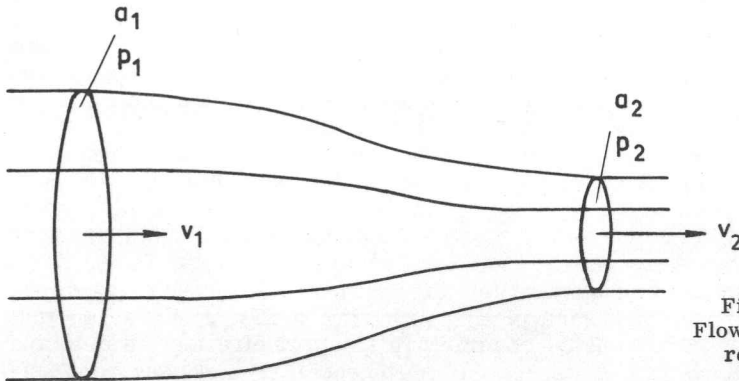


Fig. 2.1.1
Flow in a fixed
restriction.

Often the pressure is measured with a damped manometer. After extracting the square root, we do not find the mean value of the flow but

¹In this publication "a" will be written for area.

$$w_{\text{indicated}} = K \sqrt{p_1 - p_2} .$$

To obtain the mean value of the flow it would be necessary to measure

$$\bar{w} = K \sqrt{p_1 - p_2} .$$

Many investigators propose measuring the pressure difference with a fast manometer *4, 11. The mean value of the root of this signal will be proportional to the value of the mean flow.

Although this method may serve as a valuable approach in cases of low frequency pulsation, it is not exact. This can be seen by realising that Bernoulli's equation only holds for steady state flow. For dynamic conditions the pressure difference has to be increased by a quantity corresponding to the net force required to accelerate the fluid in the jet. The pressure difference must be corrected by a quantity

$$\rho \int_1^2 \frac{\partial v}{\partial t} \cdot dl$$

so that

$$p_1 - p_2 = \frac{\rho}{2} (v_2^2 - v_1^2) + \rho \int_1^2 \frac{\partial v}{\partial t} \cdot dl . \quad (2.1.3)$$

This equation only holds for incompressible frictionless fluids in horizontal pipes.

A difficulty which arises by application of this equation to nozzles and orifices is that we are not concerned with the pressure at well defined points in the velocity field, but at points in the dead water zones of the restriction. Even if this difficulty did not exist and the pattern of flow lines was known it would be very difficult to evaluate the behaviour of v from the behaviour of $p_1 - p_2$. By simplifying the flow pattern it is, however, possible to estimate the effect of this term as will be done in the next sections.

To avoid the complication of the integral term in Bernoulli's equation, it is theoretically possible to eliminate this term by subtracting a pressure difference proportional to the term *12 or to reduce its effect by choosing more suitable mechanical configurations in which the mass of the accelerated fluid is negligible *13. In those designs, measurement of the pressure difference has to be carried out with pressure pick-ups having a fast response so that the maximum frequencies occurring in the pressure can be detected without attenuation. This signal is subjected to a square root extracting apparatus which will generally be an electronic one, the maximum frequencies involved often being too high for mechanical devices. These complex electronic instruments are relatively undeveloped for large scale industrial application.

The correction term in Bernoulli's equation can be derived from Euler's equation for frictionless fluids

$$\frac{D\underline{v}}{Dt} = -\frac{\nabla p}{\rho} + \underline{g} \quad , \quad (2.1.4)$$

which is in fact the equation of motion for an infinitesimal element of the fluid. In this equation \underline{v} is the velocity vector, $\frac{D}{Dt}$ the time differential, measured at a point which is moving along with the element under consideration. ∇ is the differential operator

$$\underline{i} \frac{d}{dx} + \underline{j} \frac{d}{dy} + \underline{k} \frac{d}{dz}$$

wherein \underline{i} , \underline{j} and \underline{k} are the unit vectors.

The term $\frac{D\underline{v}}{Dt}$ in Euler's equation can be changed by substituting

$$\frac{D\underline{v}}{Dt} = \frac{\partial \underline{v}}{\partial t} + (\underline{v} \cdot \nabla) \underline{v} \quad (2.1.5)$$

where $\frac{\partial \underline{v}}{\partial t}$ is the time differential measured at a point fixed with respect to the coordinates. By omitting the influence of gravity we find

$$\frac{-\nabla p}{\rho} = \frac{\partial \underline{v}}{\partial t} + (\underline{v} \cdot \nabla) \underline{v} \quad (2.1.6)$$

For curl free velocity fields in incompressible flow it can be shown that

$$(\underline{v} \cdot \nabla) \underline{v} = \frac{1}{2} \nabla (v^2), \quad)^1 \quad (2.1.7)$$

which leads to

$$-\frac{\nabla p}{\rho} = \frac{\partial \underline{v}}{\partial t} + \frac{1}{2} \nabla (v^2) \quad . \quad (2.1.8)$$

Integrating between two points for incompressible fluids leads to

$$p_1 - p_2 = \frac{\rho}{2} (v_2^2 - v_1^2) + \rho \int_1^2 \frac{\partial \underline{v}}{\partial t} \cdot d\underline{l} \quad (2.1.9)$$

From this derivation it follows that application of the corrected Bernoulli equation is restricted to frictionless, incompressible, curl free flow or to flow where these conditions are approximated.

)¹ In this publication $(\underline{v} \cdot \nabla)$ is written as v^2 .

2.2 INCOMPRESSIBLE FLOW IN ROTAMETERS.

In the case of steady flow an approximate equation for the position of the float can easily be derived.

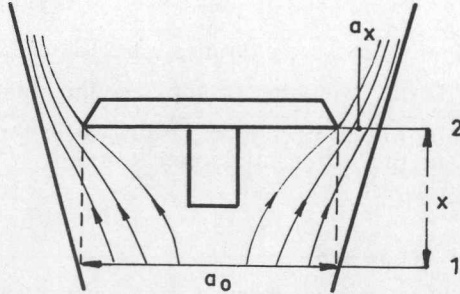


Fig. 2.2.1
Flow pattern in a rotameter.

The flow through the annular orifice between tube and float gives a pressure drop over the float. As a result of the sharpness of the float, the flow pattern will be as indicated in fig. 2.2.1.

When the area of the annular orifice between tube and float is a_x , the area of the narrowest cross section of the jet will be $C_c a_x$, where C_c is the contraction coefficient. The pressure difference over the float is usually computed with the assumptions that the pressure in the dead water zone above the float is equal to the pressure in the narrowest part of the jet and that the pressure under the float is equal to the pressure in an undisturbed cross section upstream. Because the tube is only tapered very little, the pressure in the undisturbed region upstream from the float will be approximately independent of x , apart from buoyancy. For steady flow these assumptions have led to a satisfactory description of the behaviour of the float.

With these assumptions and approximations we find for eq. (2.1.1) with

$$a_2 = C_c a_x \quad \text{and} \quad a_1 = a_0$$

$$v_1^2 = \frac{p_1 - p_2}{\rho} \frac{2 C_c^2 a_x^2}{a_0^2 - C_c^2 a_x^2}, \quad (2.2.1)$$

where a_0 is the cross section of the tube at $x=0$.

After rearranging terms we find for the pressure difference over the float with $v_1 a_0 = w$

$$p_1 - p_2 = \frac{\rho}{2} \frac{a_0^2 - C_c^2 a_x^2}{C_c^2 a_x^2 a_0^2} w^2. \quad (2.2.2)$$

The float and tube diameters are always chosen such that a_x is small in comparison with a_0 , so we can write for eq. (2.2.2)

$$p_1 - p_2 = \frac{Kw^2}{a_x^2}, \quad (2.2.3)$$

where K is approximately a constant.

The pressure difference over the float results in a force which is balanced by the weight of the float minus the buoyant force

$$g(\rho_{fl} - \rho)V_{fl} = K' \frac{w^2}{a_x^2}. \quad (2.2.4)$$

In (2.2.4) ρ_{fl} is the density of the float, V_{fl} the volume of the float and g the acceleration of gravity. In a tapered tube a_x is very nearly proportional to x , so

$$w = K''x. \quad (2.2.5)$$

The situation with pulsating flow and moving float is much more difficult. The pressure difference now also depends on the forces due to the inertia of the float. Eq. (2.2.5) is no longer applicable to a rotameter. It is also easy to see, that by putting a float in a cylindrical tube and moving the float with a constant velocity \underline{v}' , the pressure difference over the float will be determined by the velocity of the fluid relative to the float, $\underline{v}_1 - \underline{v}'$ and not by the velocity \underline{v}_1 of the fluid at a point in the undisturbed region of the float.

It will be shown that for a rotameter Bernoulli's equation has to be written as

$$p_1 - p_2 = \frac{1}{2} \rho (u_2^2 - u_1^2) + \rho \int_1^2 \left(\frac{d\underline{v}}{dt} \right)_{\underline{v}'} \cdot d\underline{l} \quad (2.2.6)$$

In this equation u_1^2 and u_2^2 are the squared velocities relative to the float at two reference points, to be specified later on, and $\left(\frac{d\underline{v}}{dt} \right)_{\underline{v}'}$ is the acceleration of the fluid measured at a point moving with velocity \underline{v}' in the fluid.

At first glance it seems rather awkward that in eq. (2.2.6) $\left(\frac{d\underline{v}}{dt} \right)_{\underline{v}'}$ has to be used instead of $\frac{\partial \underline{u}}{\partial t}$, which would follow from eq. (2.1.9)

by simply substituting \underline{u} for \underline{v} . It is however easy to understand that this substitution is not justified. Picture a cylindrical tube with constant diameter, with a float having the same specific mass as the fluid surrounding it. Now $\underline{v}' = \underline{v}$ ($\underline{u} = 0$) at each moment and this substitution would lead to $p_1 - p_2 = 0$. Hence no acceleration would

be possible. On the other hand substituting $\underline{v}' = \underline{v}$ in eq. (2.2.6) results in

$$p_1 - p_2 = \int_1^2 \rho \left(\frac{d\underline{v}}{dt} \right)_{\underline{v}' = \underline{v}} \cdot d\underline{l} = \int_1^2 \rho \frac{D\underline{v}}{Dt} \cdot d\underline{l} ,$$

because $\left(\frac{d\underline{v}}{dt} \right)_{\underline{v}' = \underline{v}}$ is defined as $\frac{D\underline{v}}{Dt}$.

The latter equation is the integral form of eq. (2.1.4), gravity omitted.

In 2.1 we used the time differentials $\frac{D}{Dt}$ and $\frac{\partial}{\partial t}$.

In eq. (2.2.6) we introduced a new time differential $\left(\frac{d}{dt} \right)_{\underline{v}'}$.

The following situation is used to illustrate the differences between these differentials.

Standing beside a highway we assume we can look at the speedometers of all cars passing by.

Suppose that the weather is going bad, we will note a change in the mean velocity that the speedometers read. In this case we are measuring $\frac{\partial \underline{v}}{\partial t}$. Now suppose ourselves driving a car at the mean velocity of \underline{v}' the cars that surround us. Looking at our speedometer we

will note accelerations and decelerations. This is the $\frac{D\underline{v}}{Dt}$ we are measuring. A helicopter-pilot surveying the road with a velocity \underline{v}' would, however, if he were able to look at the speedometers, note a different change in velocity. The latter is the $\left(\frac{d\underline{v}}{dt} \right)_{\underline{v}'}$.

Note, that in all these time differentials the velocity \underline{v} is measured with respect to the road.

We will now derive eq. (2.2.6).

In 2.1 it has been shown that Euler's equation can be written as

$$\frac{-\nabla p}{\rho} = \frac{\partial \underline{v}}{\partial t} + (\underline{v} \cdot \nabla) \underline{v} . \quad (2.2.7)$$

This equation only holds for $\frac{\partial \underline{v}}{\partial t}$ measured at a fixed point.

We are interested in $\frac{d\underline{v}}{dt}$ at a point, moving with the velocity \underline{v}' , the velocity of the float.

Now $\left(\frac{d\underline{v}}{dt} \right)_{\underline{v}'}$ can be written as $\left(\frac{d\underline{v}}{dt} \right)_{\underline{v}'} = \frac{\partial \underline{v}}{\partial t} + (\underline{v}' \cdot \nabla) \underline{v}$. (2.2.8)

Euler's equation in this case is

$$\frac{-\nabla p}{\rho} = \left(\frac{d\underline{v}}{dt} \right)_{\underline{v}'} + \left\{ (\underline{v} - \underline{v}') \cdot \nabla \right\} \underline{v} . \quad (2.2.9)$$

Substitution of $\underline{v} - \underline{v}' = \underline{u}$ leads to

$$\begin{aligned} \frac{-\nabla p}{\rho} &= \left(\frac{d\underline{v}}{dt}\right)_{\underline{v}'} + (\underline{u} \cdot \nabla)\underline{v} = \left(\frac{d\underline{v}}{dt}\right)_{\underline{v}'} + (\underline{u} \cdot \nabla)(\underline{v} - \underline{v}') = \\ &= \left(\frac{d\underline{v}}{dt}\right)_{\underline{v}'} + (\underline{u} \cdot \nabla)\underline{u}, \end{aligned} \quad (2.2.10)$$

because \underline{v}' is independent of x, y, z .
For curl free fields we can write

$$(\underline{u} \cdot \nabla)\underline{u} = \frac{1}{2}(\nabla u^2). \quad (2.2.11)$$

Substituting eq. (2.2.11) in (2.2.10) gives

$$\frac{-\nabla p}{\rho} = \left(\frac{d\underline{v}}{dt}\right)_{\underline{v}'} + \frac{1}{2}\nabla u^2. \quad (2.2.12)$$

Integrating along an arbitrary line from point 1 to point 2, moving with velocity \underline{v}' , we find for incompressible fluids

$$p_1 - p_2 = \frac{1}{2}\rho(u_2^2 - u_1^2) + \rho \int_1^2 \left(\frac{d\underline{v}}{dt}\right)_{\underline{v}'} \cdot d\underline{l} \quad (2.2.13)$$

2.21 The velocity of the fluid in a rotameter under dynamic conditions.

To apply the equation of Bernoulli to a rotameter, the situation has to be idealized.

The most important part of the float is the head. As a first approximation, consider only this part and neglect the effect of the rest of the body.

The actual flow pattern in the jet (seen in sec.7) is indicated in fig. 2.21.1 (right). The taper of the tube in this figure is exaggerated.

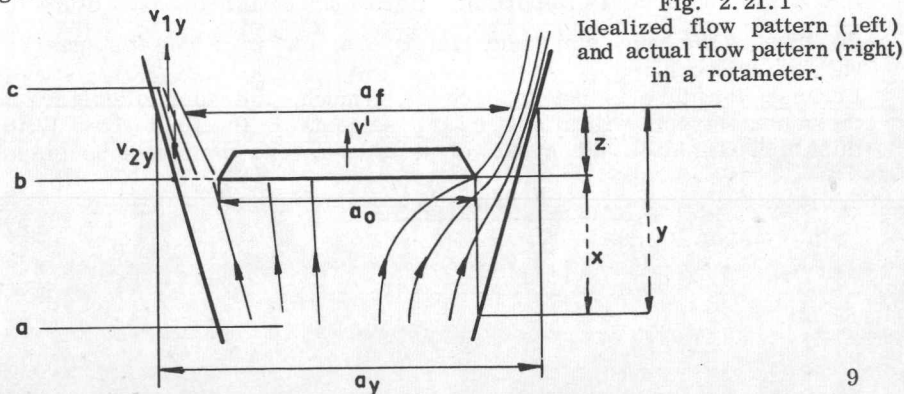


Fig. 2.21.1
Idealized flow pattern (left)
and actual flow pattern (right)
in a rotameter.

The cross section of the tube at a height $x + z = y$ is called a_y . The cross section of the float head a_0 is chosen equal to the value of a_y for $y = 0$. The cross section of the dead water zones behind the float at height y is called a_f , which is dependent on x and z .

Consider a stationary flow with a velocity v_0 at $y = 0$ and a stationary float. When the vertical component of the velocity has a constant value over a cross section perpendicular to the tube, this component of the velocity in the jet is

$$v_{1y} = \frac{v_0 a_0}{a_y - a_f} . \quad (2.21.1)$$

Now consider the float moving with a velocity v' in the tube (fig. 2.21.1), the net flow through the pipe being zero. Assume the flow pattern to be the same as above and the contraction coefficient to be the same as for stationary flow.

Because the total volume going through the section a_y has to be zero, the vertical component of the velocity at y must be

$$v_{2y} = \frac{v' a_f}{a_y - a_f} . \quad (2.21.2)$$

In general, with a flow $w = v_0 a_0$, and the float moving with a velocity v' the resulting velocity at y will be

$$v = v_{1y} - v_{2y} = \frac{w - v' a_f}{a_y - a_f} . \quad (2.21.3)$$

For the velocity relative to the float we find

$$u = v - v' = \frac{w - v' a_y}{a_y - a_f} . \quad (2.21.4)$$

In particular the value of u in the narrowest part of the jet at c , the vena contracta, is important. Here a_y is the cross section of the tube at the vena contracta and $a_y - a_f = C_c a_x$. The distance bc will be called h .

Because the tube is not tapered very much, the tube diameter at the vena contracta will almost be the same as at the float edge. With this approximation the value of u at the vena contracta becomes

$$u_2 = \frac{w - v' (a_0 + a_x)}{C_c a_x} . \quad (2.21.5)$$

Making the same assumptions for pulsating flow as were made in sec. 2.2 for stationary flow the term $(u_2^2 - u_1^2)$ in eq. (2.2.13) can be computed. Since $u_2 \gg u_1$, u_1^2 can be neglected in comparison with u_2^2 ,

$$u_2^2 - u_1^2 \approx u_2^2 = \left\{ \frac{w - v'(a_0 + a_x)}{C_c a_x} \right\}^2. \quad (2.21.6)$$

To compute the integral term of eq. (2.2.13) it is necessary, moreover, to make the assumption that the contraction coefficient is the same as for stationary flow. Furthermore the streamline pattern has to be known. We will idealize the streamline pattern to the one indicated in fig. 2.21.1 (left). In fig. 2.21.2 the value of $|v|$ for the idealized flow pattern is drawn (solid). The actual value of $|v|$ will correspond to a curve like the dotted line.

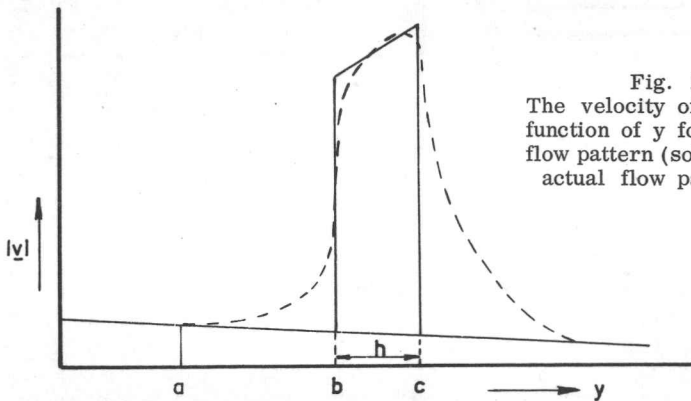


Fig. 2.21.2
The velocity of the fluid as a function of y for the idealized flow pattern (solid) and for the actual flow pattern (dotted).

As the increase in velocity is proportional to the velocity, it is easy to see that the part of the fluid between points b and c in fig. 2.21.2 will give the largest contribution to the integral term of eq. (2.2.13). Thus the integral term of eq. (2.2.13) can be computed from the idealized flow pattern between points b and c , the pressure drop between points a and b in the idealized pattern of fig. 2.21.2 being neglected.

Strictly speaking, neglecting the velocity in the region upstream from the float compared with the velocity in the jet is only possible with a stationary float. However, the velocity of the fluid in the jet will also be much larger than the velocity of the fluid in front of the float for a moving float, if the velocity of the float is low compared with that of the fluid as we will assume.

2.22 The equation of motion for the float.

Before giving a detailed derivation of the equation of motion, a general impression of this derivation will be given. A simplified form of eq. (2.2.13) can be used by neglecting radial components, and putting \dot{x} for v' , the velocity of the float. Substituting the coordinates indicated in fig. 2.22.1 and applying eq. (2.2.13) to the line indicated in this figure, we find, using eq. (2.21.6),

$$p_x - p_c = \frac{1}{2} \rho \left\{ \frac{w - \dot{x} (a_o + a_x)}{C_c a_x} \right\}^2 + \rho \int_0^h \left(\frac{dv}{dt} \right) \dot{x} dz, \quad (2.22.1)$$

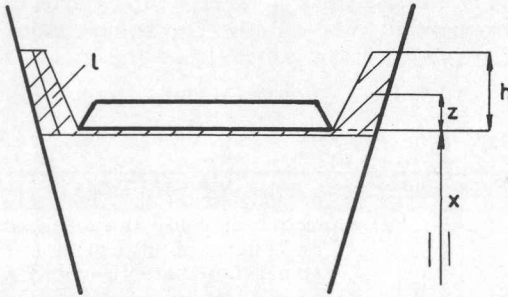


Fig. 2.22.1
The line over which the acceleration integral is integrated.

where p_x is the pressure just beneath the float, p_c the pressure in the jet at the vena contracta and h the distance between the float edge and the vena contracta. We will show later on that by computing the integral of eq. (2.22.1) and rearranging the terms we can find the following expression for the pressure difference over the float,

$$p_x - p_c = B'w^2 - C'w\dot{x} + D'\dot{x}^2 + E'\dot{w} - F'\ddot{x}, \quad (2.22.2)$$

where the coefficients B' , C' and D' result from the first term on the right of (2.22.1), and E' and F' result from the second term.

The force resulting from this pressure difference has to cancel the force caused by the inertia of the float plus the force caused by gravity which was also present for the stationary case (eq. 2.2.4).

$$(p_x - p_c) a_o = g (\rho_{fl} - \rho) V_{fl} + \ddot{x} V_{fl} \rho_{fl}. \quad (2.22.3)$$

By combining eq. (2.22.2) and eq. (2.22.3) it is possible to derive the equation of motion for the float

$$w^2 - C w \dot{x} + D \dot{x}^2 + E \ddot{w} - F \ddot{x} = G, \quad (2.22.4)$$

where again the terms with C and D are the consequence of u_c^2 , while the terms with E and a part of F account for the acceleration of the fluid $\int (\frac{dv}{dt})_{\dot{x}} dz$. The rest of F is the contribution of the inertia of the float and G is the effect of gravity. The coefficients C.....G can be expressed as follows:

$$\left. \begin{aligned} C &= 2(a_0 + a_x) & &= c_0 + c_1 x \\ D &= (a_0 + a_x)^2 = \frac{C^2}{4} & &= d_0 + d_1 x + d_2 x^2 \\ E &= 2h a_x C_c^2 \frac{\ln C_c}{C_c - 1} + \frac{2h' C_c^2 a_x^2 a_b}{(a_0 + a_x - a_b) a_0} & &= e_1 x + e_2 x^2 \\ F &= 2a_0 h C_c^2 a_x \frac{\ln C_c}{C_c - 1} + \frac{2V_{fl} \rho_{fl} C_c^2 a_x^2}{\rho a_0} & &= f_1 x + f_2 x^2 \\ G &= \frac{2g(\rho_{fl} - \rho) V_{fl} C_c^2 a_x^2}{\rho a_0} & &= g_2 x^2 \end{aligned} \right\} \quad (2.22.5)$$

In these equations a_0 is the cross section of the float head, a_x the cross section of the annular orifice between float and tube, and C_c the contraction coefficient. The second term in E results from the effect of the float body as will be explained at the end of this section. The notation h' is the length of the float body and a_b the cross section of the float body. As can be seen from the equation for E, e_2 is dependent on x .

The derivation of eq. (2.22.4) will now be given in detail. First consider the integral term

$$\int_0^h \left(\frac{dv}{dt}\right)_{\dot{x}} dz. \quad (2.22.6)$$

and float, a_x , is the difference of the cross sections of the tube at $y=x$ and the float so

$$a_x = bx \quad \text{and} \quad \frac{da_x}{dx} = b. \quad (2.22.13)$$

From eq. (2.2.8) we find for one dimensional flow

$$\left(\frac{dv}{dt}\right)_{\dot{x}} = \frac{\partial v}{\partial t} + \dot{x} \frac{\partial v}{\partial x}.$$

Substituting eq. (2.22.13) in (2.22.11) and differentiating results in

$$\left(\frac{dv}{dt}\right)_{\dot{x}} = \frac{\dot{w} - \ddot{x}a_0}{a_x \left(1 - \frac{1 - C_c}{h} z\right)} - \frac{\dot{x}b(w - \dot{x}a_0)}{a_x^2 \left(1 - \frac{1 - C_c}{h} z\right)}. \quad (2.22.14)$$

Integrating 2.22.14 we find

$$\begin{aligned} & \frac{\dot{w} - \ddot{x}a_0}{a_x} \int_0^h \frac{1}{\left(1 - \frac{1 - C_c}{h} z\right)} dz + \\ & - \frac{\dot{x}b(w - \dot{x}a_0)}{a_x^2} \int_0^h \frac{1}{\left(1 - \frac{1 - C_c}{h} z\right)} dz = \\ & = \frac{(\dot{w} - \ddot{x}a_0)h \ln C_c}{a_x(C_c - 1)} - \frac{\dot{x}(w - \dot{x}a_0)bh \ln C_c}{a_x^2(C_c - 1)}. \end{aligned} \quad (2.22.15)$$

Substituting eq. (2.22.15) in (2.22.1) we find

$$\begin{aligned} p_x - p_c = \rho \left\{ \frac{w^2}{2C_c^2 a_x^2} - \frac{w\dot{x}(a_0 + a_x)}{C_c^2 a_x^2} + \frac{\dot{x}^2(a_0 + a_x)^2}{2C_c^2 a_x^2} + \right. \\ \left. + \frac{(\dot{w} - \ddot{x}a_0)h \ln C_c}{a_x(C_c - 1)} - \frac{\dot{x}(w - \dot{x}a_0)bh \ln C_c}{a_x^2(C_c - 1)} \right\}. \end{aligned} \quad (2.22.16)$$

As bh signifies the increase in area of the tube over the distance

which will be much smaller than a_0 and $C_c \approx 0.6$, the last term in eq. (2.22.16) can be neglected in comparison with the second and third ones.

$$p_x - p_c = \rho \left\{ \frac{w^2}{2 C_c^2 a_x^2} - \frac{w\dot{x}(a_0 + a_x)}{C_c^2 a_x^2} + \frac{\dot{x}^2 (a_0 + a_x)^2}{2 C_c^2 a_x^2} + \frac{(\dot{w} - \ddot{x}a_0) h \ln C_c}{a_x (C_c - 1)} \right\}. \quad (2.22.17)$$

Combining eq. (2.22.17) and (2.22.3) we find the equation of motion (2.22.4, 2.22.5), without accounting for the float body.

To account for the float body the streamline pattern has to be idealized in another way (fig. 2.22.3).

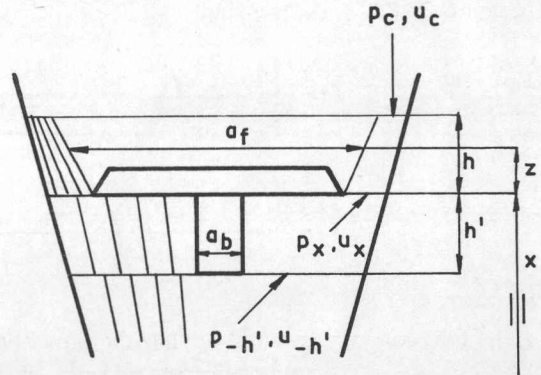


Fig. 2.22.3
The idealized flow pattern
for a float with a body.

The flow now has to pass two restrictions, in each of which the flow can be idealized as described in sec. 2.21. The cross section of the float body is called a_b ; the length of the float body is h' ; the pressure in the jet at the vena contracta is p_c ; the pressure just beneath the float edge p_x ; and the pressure just beneath the float body $p_{-h'}$. Similarly the velocities in the jet, just beneath the float edge and just beneath the float body are called u_c , u_x and $u_{-h'}$ respectively. The force on the float caused by the pressure difference will be equal to

$$F = a_b (p_{-h'} - p_c) + (a_0 - a_b)(p_x - p_c). \quad (2.22.18)$$

Now with Bernoulli's equation applied to the two successive restrictions we find

$$p_x - p_c = \frac{1}{2} \rho (u_c^2 - u_x^2) + \rho \int_0^h \left(\frac{dv}{dt} \right)_{\dot{x}} dz \quad (2.22.19)$$

and

$$p_{-h'} - p_c = \frac{1}{2} \rho (u_c^2 - u_{-h'}^2) + \rho \int_{-h'}^h \left(\frac{dv}{dt} \right)_{\dot{x}} dz. \quad (2.22.20)$$

The force acting on the float can be written by substituting these two equations in (2.22.18)

$$F = \frac{1}{2} \rho \left\{ a_0 u_c^2 - a_b u_{-h'}^2 - (a_0 - a_b) u_x^2 \right\} + \rho (a_0 - a_b) \int_0^h \left(\frac{dv}{dt} \right)_{\dot{x}} dz + \rho a_b \int_{-h'}^h \left(\frac{dv}{dt} \right)_{\dot{x}} dz. \quad (2.22.21)$$

For the considered floats and tubes the velocity in the narrowest part of the jet is much higher than the velocity next to the float body, so

$$F \approx \frac{1}{2} \rho a_0 u_c^2 + \rho a_0 \int_0^h \left(\frac{dv}{dt} \right)_{\dot{x}} dz + \rho a_b \int_{-h'}^0 \left(\frac{dv}{dt} \right)_{\dot{x}} dz. \quad (2.22.22)$$

It is possible to prove that the error which is made by the last approximation is smaller than 10% when $\frac{a_x}{a_0} < 0.5$. In practice $\frac{a_x}{a_0}$ will always be smaller. Thus the only effect of the float body is a change of the term $\int \left(\frac{dv}{dt} \right)_{\dot{x}} dz$. To evaluate the integral $\int_{-h'}^0 \left(\frac{dv}{dt} \right)_{\dot{x}} dz$,

the velocity next to the float body can, from eq. (2.21.3), be written as

$$v = \frac{w - \dot{x} a_b}{a_0 + a_x - a_b}, \quad (2.22.23)$$

neglecting the taper of the tube over the length of the float body.

$$\left(\frac{dv}{dt} \right)_{\dot{x}} = \frac{\dot{w} - \ddot{x} a_b}{a_0 + a_x - a_b} - \frac{w - \dot{x} a_b}{(a_0 + a_x - a_b)^2} b \dot{x}. \quad (2.22.24)$$

Integration of this equation gives

$$\int_{-h'}^0 \left(\frac{dv}{dt} \right)_{\dot{x}} dz = \frac{\dot{w} - \ddot{x} a_b}{a_0 + a_x - a_b} h' - \frac{\dot{x}(w - \dot{x} a_b)}{(a_0 + a_x - a_b)^2} b h' . \quad (2.22.25)$$

The maximum value of eq. (2.22.25) occurs for $a_x = 0$. Then eq. (2.22.25) becomes

$$\int_{-h'}^0 \left(\frac{dv}{dt} \right)_{\dot{x}} dz = \frac{\dot{w} - \ddot{x} a_b}{a_0 - a_b} h' - \frac{\dot{x}(w - \dot{x} a_b)}{(a_0 - a_b)^2} b h' . \quad (2.22.26)$$

The symbol b is, as stated before, a small quantity and when $a_0 - a_b$ is not too small the second term in (2.22.26) can again be neglected in comparison with the second and third term of eq. (2.22.17). The term with \ddot{x} can be neglected compared with the term in the equation of motion for the float. When derived with the float body taken into account, the equation of motion remains the same, except for a correction on the term E

$$E = 2h a_x C_c^2 \frac{\ln C_c}{C_c - 1} + \frac{2h' C_c^2 a_x^2 a_b}{(a_0 + a_x - a_b) a_0} = e_1 x + e_2 x^2 . \quad (2.22.27)$$

3. APPROXIMATE SOLUTIONS OF THE EQUATION OF MOTION FOR SMALL SINUSOIDAL PULSATIONS.

Consider a volumetric fluid flow w with mean value w_0 and pulsations Δw , with Δw a periodic function. The mean position the float assumes with pulsating flow is called x_0 . Eq. (2.22.4) can be rewritten by substituting $w = w_0 + (\Delta w)$ and $x = x_0 + (\Delta x)$

$$w_0^2 + 2w_0 (\Delta w) + (\Delta w)^2 - C(w_0 + \Delta w)(\Delta'x) + D(\Delta'x)^2 + E(\Delta'w) + F(\Delta''x) - g_2 x_0^2 - 2g_2 x_0 (\Delta x) - g_2 (\Delta x)^2 = 0 \quad (3.1.1)$$

where C , D , E and F still contain terms with x_0 and Δx .

In this equation $\frac{d(\Delta x)}{dt}$ is written as $(\Delta'x)$ and $\frac{d^2(\Delta x)}{dt^2}$ as $(\Delta''x)$.

The difference between stationary and dynamic conditions is of interest. For this reason consider also a stationary flow with the same input w_0 . Under these conditions the value of x is called x_{0w} . For stationary flow it can be written:

$$w_0^2 = g_2 x_{0w}^2 \quad (3.1.2)$$

By substituting (3.1.2) in (3.1.1) we find:

$$g_2 (x_0^2 - x_{0w}^2) = 2w_0 (\Delta w) + (\Delta w)^2 - C(w_0 + \Delta w)(\Delta'x) + D(\Delta'x)^2 + E(\Delta'w) - F(\Delta''x) - 2g_2 x_0 (\Delta x) - g_2 (\Delta x)^2, \quad (3.1.3)$$

where

$$\left. \begin{aligned} C &= c_0 + c_1 (x_0 + \Delta x), \\ D &= d_0 + d_1 (x_0 + \Delta x) + d_2 (x_0 + \Delta x)^2, \\ E &= e_1 (x_0 + \Delta x) + e_2 (x_0 + \Delta x)^2 \\ \text{and } F &= f_1 (x_0 + \Delta x) + f_2 (x_0 + \Delta x)^2. \end{aligned} \right\} \quad (3.1.4)$$

Eq. (3.1.3) describes the deviation of the mean value indicated by the float from the true mean value.

Putting $\Delta w = \hat{w} \cos \omega t$ it is found that

$$\Delta x = \sum_{k=1}^{\infty} \hat{x}_k \cos (k \omega t + \varphi_k). \quad (3.1.5)$$

Assuming the terms with frequencies $2\omega, 3\omega, \dots$ to be much

smaller than the terms containing the frequency ω and substituting $\Delta x = \hat{x} \cos(\omega t + \varphi)$ and $\Delta w = \hat{w} \cos \omega t$ in eq. (3.1.3) and (3.1.4), an equation is found which contains time dependent parts and time independent parts. This equation has to be valid for both kinds of terms, and in particular, for the time dependent terms containing the frequency ω .

The equation for the time dependent terms which contains terms with the frequency ω is

$$\begin{aligned}
 & 2w_0 (\Delta w) - w_0 (c_0 + c_1 x_0) (\Delta \dot{x}) + (e_1 x_0 + e_2 x_0^2) (\Delta \dot{w}) - (f_1 x_0 + f_2 x_0^2) (\Delta \ddot{x}) \\
 & - 2 g_2 x_0 (\Delta x) + \left\{ - f_2 (\Delta x)^2 (\Delta \ddot{x}) + d_1 (\Delta x) (\Delta \dot{x})^2 + \right. \\
 & \left. - c_1 (\Delta x) (\Delta \dot{x}) (\Delta w) \right\} = 0.
 \end{aligned} \tag{3.1.6}$$

For small amplitudes the term between brackets can be neglected, and using complex variables the response of the system can be written as

$$\begin{aligned}
 \bar{A} &= \frac{\overline{\Delta x}}{r \overline{\Delta w}} = \frac{1 + j\omega q}{1 + j\omega s + (j\omega)^2 t}, \\
 \text{with } r &= \frac{w_0}{g_2 x_0} \approx \frac{1}{\sqrt{g_2}}, \\
 q &= \frac{e_1 x_0 + e_2 x_0^2}{2w_0} \approx \frac{e_1 + e_2 x_0}{2\sqrt{g_2}}, \\
 s &= \frac{w_0 (c_0 + c_1 x_0)}{2 g_2 x_0} \approx \frac{c_0 + c_1 x_0}{2\sqrt{g_2}}, \\
 t &= \frac{f_1 + f_2 x_0}{2 g_2}.
 \end{aligned} \tag{3.1.7}$$

The last approximations are based on the fact that

$$w_0 \approx \sqrt{g_2} x_0 \tag{3.1.8}$$

for small deviations of the mean value.

For the terms independent of time we can write

$$g_2 (x_o^2 - x_{ow}^2) = \frac{\hat{w}^2}{2} - \frac{\hat{x}^2}{2} g_2 + \omega^2 (d_o + d_1 x_o + d_2 x_o^2 + f_1 + 2f_2 x_o) \frac{\hat{x}^2}{2} + \frac{\hat{w}\hat{x}}{2} \omega \sin \varphi (c_o + c_1 x_o + e_1 + 2e_2 x_o). \quad (3.1.9)$$

Substitution of $\hat{x} = \frac{|\bar{A}| \hat{w}}{\sqrt{g_2}}$ gives

$$\frac{g_2 (x_o^2 - x_{ow}^2)}{\hat{w}^2} = \frac{1}{2} \left\{ 1 - |\bar{A}|^2 + \alpha \omega^2 |\bar{A}|^2 + \beta \omega |\bar{A}| \sin \varphi \right\} = M, \quad (3.1.10)$$

with

$$\alpha = \frac{d_o + d_1 x_o + d_2 x_o^2 + f_1 + 2f_2 x_o}{g_2} \quad \left. \vphantom{\alpha} \right\} \quad (3.1.11)$$

and

$$\beta = \frac{c_o + c_1 x_o + e_1 + 2e_2 x_o}{\sqrt{g_2}}.$$

In the following we will use M to describe the deviation of the mean value.

For

$$M = \frac{g_2 (x_o^2 - x_{ow}^2)}{\hat{w}^2}$$

we can write

$$M = \frac{w_{oi}^2 - w_o^2}{\hat{w}^2} \quad (3.1.12)$$

where w_{oi} is the w_o indicated, and w_o the true value of the mean input. For small deviations of the mean this can be written as

$$M = \frac{(w_{oi} - w_o) 2w_o}{\hat{w}^2} \quad (3.1.13)$$

For the relative error we find

$$\frac{w_{oi} - w_o}{w_o} = \frac{\hat{w}^2}{2w_o^2} M. \quad (3.1.14)$$

Eq. (3.1.10) for M can be written in a form which is more convenient to handle

$$M = \frac{1}{2} \operatorname{Re} \left\{ 1 - |\bar{A}|^2 + \alpha \omega^2 |\bar{A}|^2 - j\beta \omega \bar{A} \right\}. \quad (3.1.15)$$

For α we now consider the case in which

$$d_0 + d_1 x_0 + d_2 x_0^2 \gg f_1 + 2f_2 x_0.$$

This turns out to be true in most instances where the density of fluid and float do not differ very much, as in the case when measuring flow of incompressible fluid. In most cases $e_1 + 2e_2 x_0$ can also be neglected in comparison with $c_0 + c_1 x_0$. With these approximations we find with eq. (2.22.5) and (3.1.7)

$$\left. \begin{aligned} \alpha &= \frac{d_0 + d_1 x_0 + d_2 x_0^2}{g_2} = \frac{(c_0 + c_1 x_0)^2}{4 g_2} = s^2 \\ \text{and} \\ \beta &= \frac{c_0 + c_1 x_0}{\sqrt{g_2}} = 2 s. \end{aligned} \right\} \quad (3.1.16)$$

Substituting eq. (3.1.16) and (3.1.7) in (3.1.15) it is found that

$$M = \frac{1}{2} \frac{\omega^4 (qs - t)^2 + 2 \omega^2 (qs - t) - \omega^2 q^2}{(1 - \omega^2 t)^2 + \omega^2 s^2}. \quad (3.1.17)$$

Inspecting (3.1.17) we see that as $\omega \rightarrow \infty$

$$M = \frac{1}{2} \left\{ \frac{qs}{t} - 1 \right\}^2. \quad (3.1.18)$$

The term $\frac{qs}{t}$ governs the value of M for high frequencies and it seems useful to inspect this term further.

From (3.1.7) it is concluded that

$$\frac{qs}{t} = \frac{(e_1 + e_2 x_0) (c_0 + c_1 x_0)}{f_1 + f_2 x_0}. \quad (3.1.19)$$

For most rotameters this can be approximated by

$$\frac{qs}{t} = \frac{e_1 (c_0 + c_1 x_0)}{f_2 x_0} = \frac{2 \ln C_c}{(C_c - 1)} \frac{(a_0 + a_x) a_0 \rho h}{V_{fl} \rho_{fl} a_x}. \quad (3.1.20)$$

Making this term as nearly as possible equal to one reduces the error for high frequencies.

It is necessary to investigate the agreement between theory and measurements of the neglect of the higher harmonics of Δx . For small amplitudes the above assumption will certainly hold, because all terms containing frequencies higher than ω have coefficients with at least the square of the amplitude or the product of two amplitudes.

4. MEASUREMENTS FOR INCOMPRESSIBLE FLUID FLOW.

4.1 THE TEST SET-UP.

The test set-up is shown schematically in fig. 4.1.1 ~~±~~ From a reservoir the water is conducted to cock I, which is used to adjust the mean value of the flow. A pulsator with a metal bellow

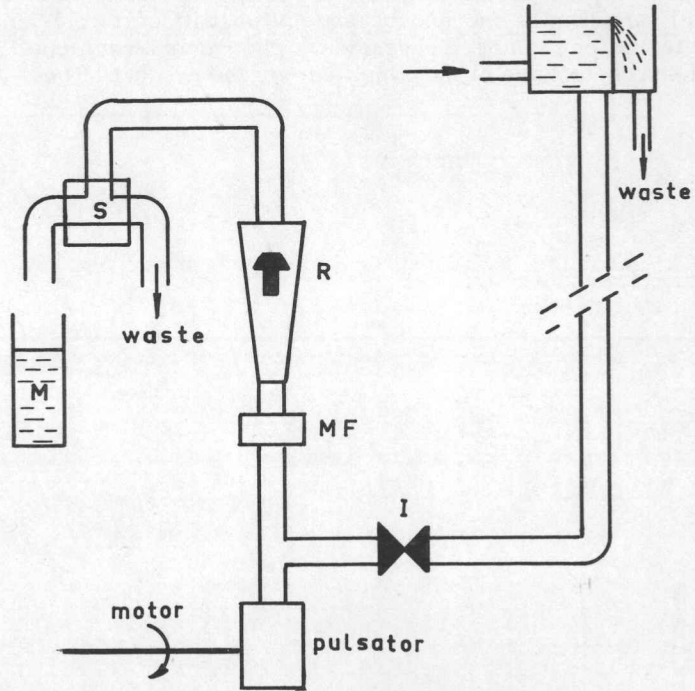


Fig. 4.1.1
Test apparatus for measuring sinusoidal varying flow of an incompressible fluid.

generates sinusoidal variations. The pulsations are measured with a magnetic flowmeter MF, which is connected to the rotameter R. The switch S connects the flow during a certain interval to a measuring vessel. This time interval is measured by means of an electronic counter, which counts a 1000 c/s voltage generated by a tuning fork oscillator.

4.11 The water circuit.

To obtain a flow independent of external circumstances, the water

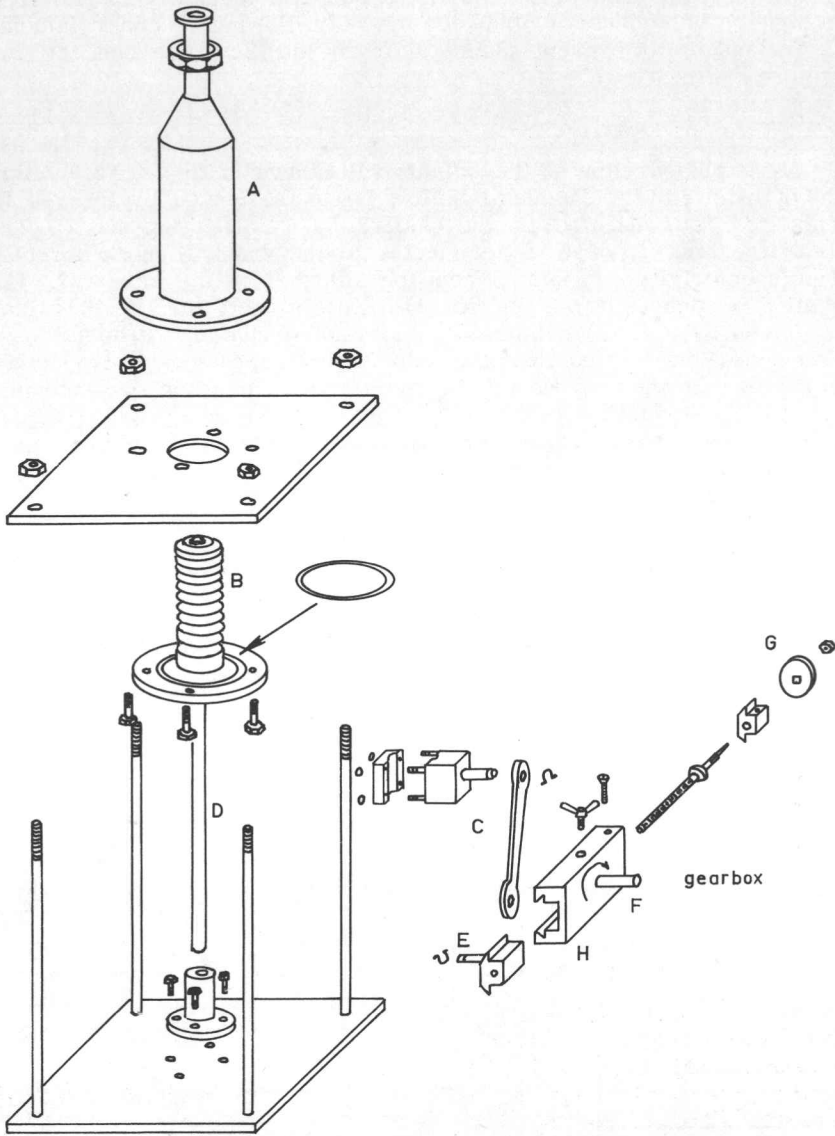


Fig. 4.12.1
 Pulsator for generating sinusoidal varying flow for an incompressible fluid.

is drawn from a reservoir having a constant level situated about 8 m higher. The connection between magnetic flowmeter and rotameter is inelastic, to prevent phase shift in the flow between the two meters.

4.12 The pulsator.

An exploded view of the pulsator is drawn in fig. 4.12.1. A is the cylinder in which a metal bellow B can be moved by the rod D. This rod is connected to the shaft F by a connecting rod C. The lower bearing E of C is connected to the crank H by a dovetail. The eccentricity of point E can be adjusted by the screw G. The shaft F is connected to a gearbox with ratio's 1 : 1; to 1 : 16, which is driven by a D.C. compound motor, 1400 rpm, 0.75 hp. The motorspeed is continuously adjustable by means of a resistance in series with the armature. The maximum volumetric displacement caused by the bellow is 50 cm³. This pulsator can produce sinusoidal pulsations in the magnetic flowmeter with a maximum amplitude of about 50.10⁻⁶m³/s, from 1 c/s to 25 c/s.

4.13 The magnetic flowmeter.

The magnetic flowmeter is used to measure the instantaneous value of the flow. It consists of an electromagnet which generates a magnetic field perpendicular to the direction of the flow (fig. 4.13.1). Assuming a uniform field and a uniform distribution of the flow in the pipe, an electromotive force V is induced between the electrodes a and b which is equal to

$$V = B v d. \quad (4.13.1)$$

In eq. (4.13.1) B is the magnetic induction, v the velocity of the fluid and d the diameter of the pipe. It can be proved¹⁴ that eq.

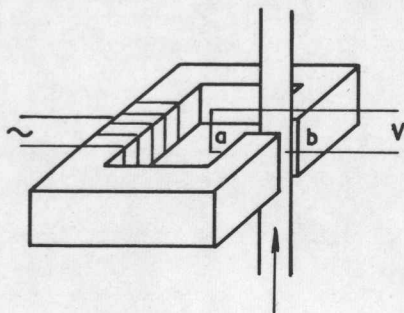


Fig. 4.13.1
The magnetic flowmeter.

(4.13.1) holds for axially symmetrical flow, regardless of the velocity distribution, when v is the mean velocity in the tube. In general,

In general, electromagnetic flowmeters are designed for the power supply frequency. This frequency however, was too low for our purposes. The present meter is designed for a frequency of 1000 c/s. Using this frequency, even the highest frequencies occurring in the flow rate can be measured. The 1000 c/s voltage is generated by a tuning fork oscillator and fed to a circuit providing automatic gain control to obtain a constant amplitude supply. Power amplification is provided by a class B power amplifier. The magnetic circuit is tuned by some capacitors in a series resonant circuit to suppress harmonics in the circuit and to get a reasonable matching to the power amplifier. The magnetic field in the air gap is approximately 0.06 Wb/m^2 .

The signal generated by the meter is fed to an amplifying and compensating circuit. The compensating voltage can be varied in amplitude and phase to cancel the spurious signal induced in the pick-up circuit. The signal is fed to a bandpass filter with a center frequency of 1000 c/s and a bandwidth of 80 c/s, and can be observed on an oscilloscope.

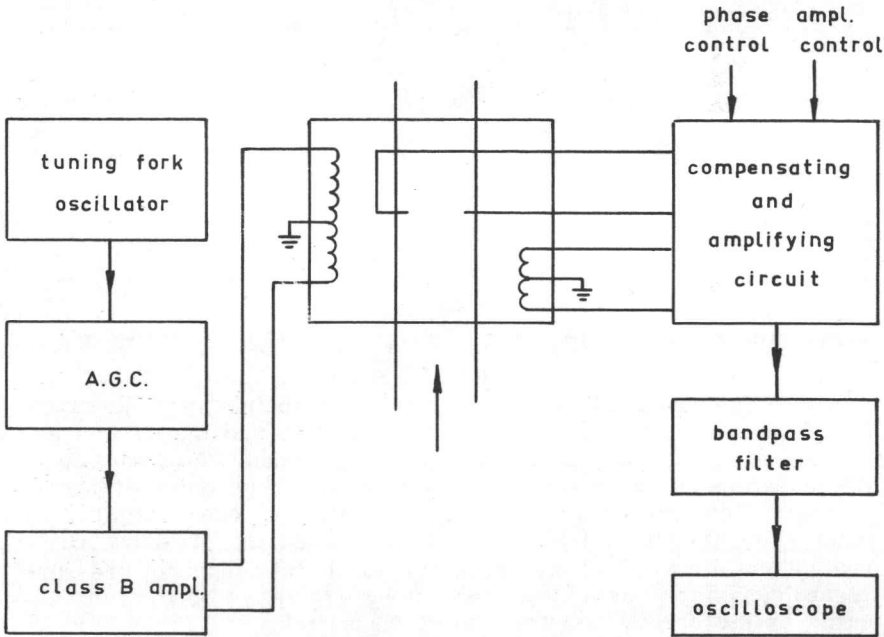


Fig. 4.13.2

Block diagram of the magnetic flowmeter and its auxiliary equipment.

The phase shift of the m-derived, constant k filter is linear within at least 60 c/s. The time delay of this filter is about 3.5 ms. The total gain of the electronic system is approximately 10^5 . The band-passfilter output at a flow rate of $50 \cdot 10^{-6} \text{ m}^3/\text{s}$ is approximately 10 V. The drift of the system in 30 minutes is less than 1% of this value. Because the magnetic flowmeter is only used for short times and its compensation is regularly checked, this amount of drift is tolerable.

The block diagram of the system is given in fig. 4.13.2.

Fig. 4.13.3 shows a picture taken from the oscilloscope, which displays a sinusoidal pulsating flow. The pulsations appear as an amplitude modulation of the 1000 c/s voltage.

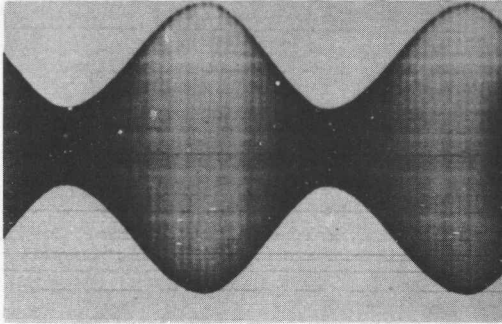


Fig. 4.13.3
Output signal of the
magnetic flowmeter
with pulsating flow.

4.14 The switch.)¹

The switch is used in order to measure the mean flow volumetrically. Its construction was guided by the principle that the switch had to have no influence at all on the flow rate and that it was necessary to be able to measure during a whole number of periods of the pulsation. Furthermore the switching had to be quick enough to measure time intervals accurately. The first object is attained by making the fluid flow freely into the switch so the pressure at the end of the line will always be equal to the atmospheric pressure regardless of the position of the switch. The other objects are secured by the special construction of the switch.

)¹ The switch was designed and constructed by H. v. d. Biggelaar.

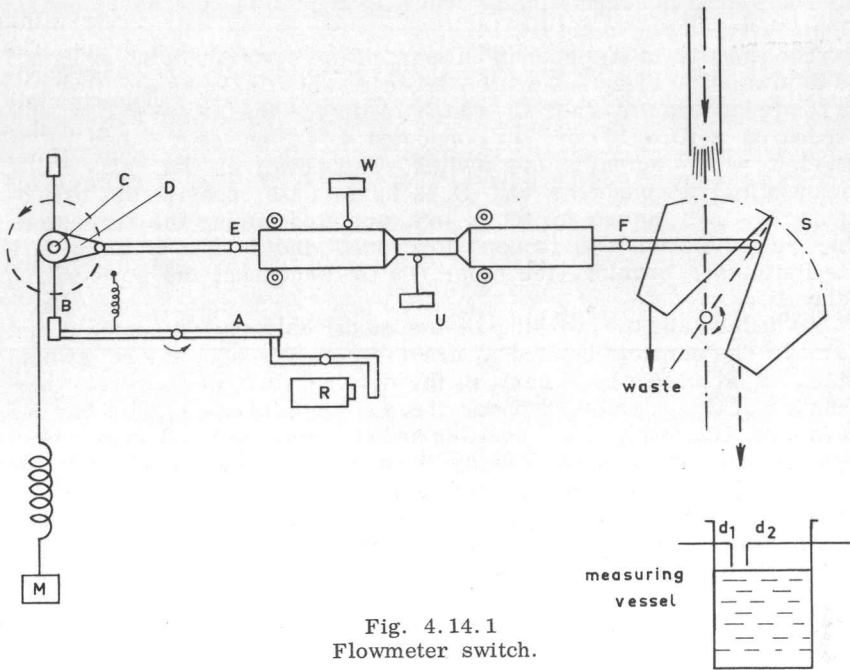


Fig. 4.14.1
Flowmeter switch.

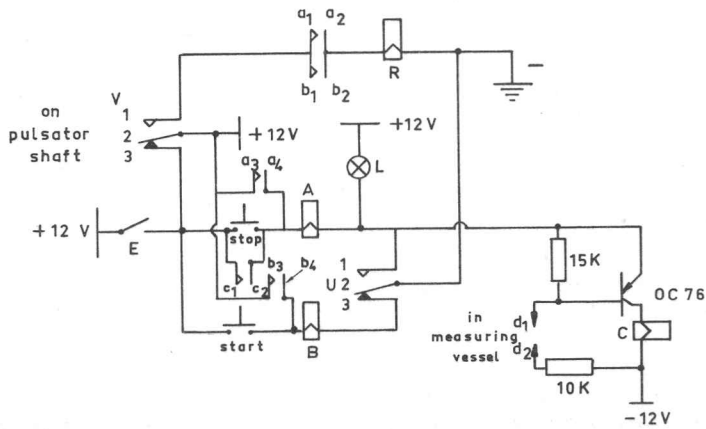


Fig. 4.14.2
Electrical system for flowmeter switch.

The switch is schematically drawn in fig. 4.14.1. The electrical diagram is shown in fig. 4.14.2.

The working of the mechanical part of the system can be explained as follows. The relay R actuates lever A which unlocks B. B starts to rotate around its shaft C, which is driven by the weight M suspended on a rope. Crank D, connected to C, moves the bar EF to the left which actuates the switch. The power on the relay R is, meanwhile, disconnected and B is held in its opposite position by lever A. Two micro switches are actuated during the transition. One micro switch (W) is used to connect the 1000 c/s tuning fork oscillator to a counter, the other (U) to disconnect the power from relay R.

To understand the working of the electrical scheme consider fig. 4.14.2. The contacts labeled V are the contacts of a micro switch, which is actuated by a cam on the driving shaft of the crank mechanism of the pulsator. Suppose the switch E is open. The bar EF is in its greatest righthand position and the contacts U 23 are closed. Pushing the start button, relay B can only be energized when the cam on the pulsator is in such a position that contacts V 23 are closed. Relay B holds itself through contacts $b_3 b_4$, so the start button can be released. As soon as the cam on the pulsator actuates contacts V to close contacts V 12, coil R will be energized because contacts $b_1 b_2$ are closed. The bar EF will move to the left and consequently micro switch contacts U 23 will be disconnected and coils B and R will be deenergized.

As soon as the measuring vessel is filled to the point where the contacts $d_1 d_2$ are closed, the transistor starts to conduct and relay C will become energized. When switch U 12 and contacts V 23 are closed, coil A will be energized through contacts $c_1 c_2$. It will hold itself through contacts $a_3 a_4$ and close through contacts $a_1 a_2$. Transition of switch V from contacts V 23 to V 12 will energize coil R, and bar EF will move to the left. Actuating the stop button results in the same action as closing the contacts $d_1 d_2$. The switching action only takes place at the moment of transition from contacts V 23 to V 12, and is always at the same position of the shaft of the pulsator. By closing the switch E and fixing contacts V in the upper position (V 12 closed), we can actuate the switch directly by the start- and stop-buttons. The switching action occurs in a time interval of less than 50 ms.

4.15 The measuring vessel.

The measuring vessel is a cylindrical tube of perspex. For most measurements only the linearity of a small portion of this tube is important. The vessel is always filled up to approximately the same level, where the electrodes d_1 and d_2 of the switch (sec. 4.14) are located. An exact reading of the level is obtained by lowering a needle by means of a screw into the vessel until it reaches the water-level. The position of the screw with needle is indicated on

a ruler. The screw and needle mechanism, is fixed to the measuring vessel, the measuring vessel which is always left in the same position, can be drained by means of a tap mounted in the bottom. The water-level can be measured within 0.2 mm. The height of the measuring vessel is about 25 cm and its volume is approximately 2 dm³.

4.16 Measuring the frequency of pulsation.

The number of rotations of the shaft, which drives the pulsator is counted during a measuring interval with an electric counter. On the shaft a disc with ten holes is mounted. On one side of the disc a small incandescent lamp is mounted and on the other side is a phototransistor. The incandescent lamp L (fig. 4.14.2) is only lighted when the flow is connected to the measuring vessel (contacts U 12 closed). When lamp L is lighted and the shaft of the pulsator turns, pulses are generated by the phototransistor which are fed to an electronic counter. From the measured time interval (with micro switch W, sec. 4.14) and the number of rotations we can compute the frequency of pulsation.

4.17 Measuring the phase of the float.

The phase of the float is measured with a light beam and photodiode. In fig. 4.17.1 horizontal and vertical cross sections of the

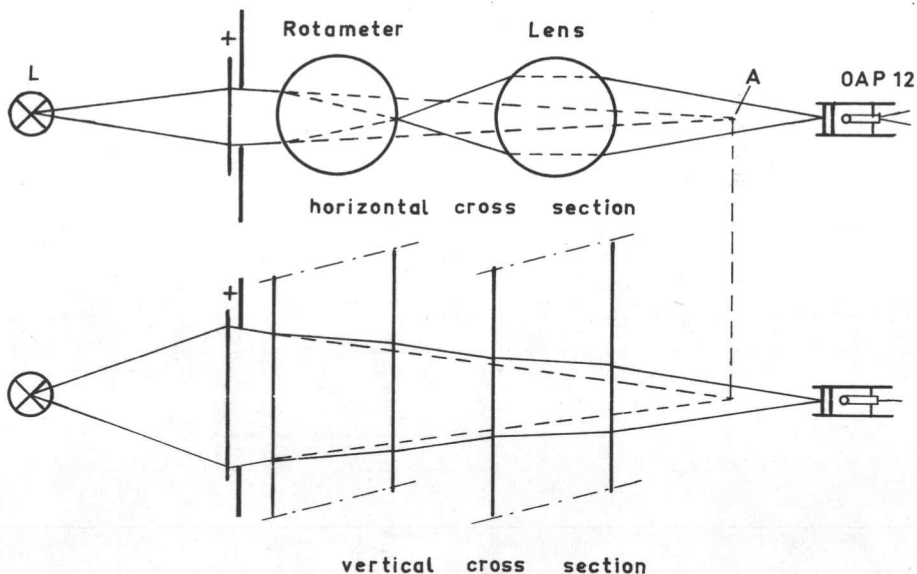


Fig. 4.17.1
Optical phase measuring system.

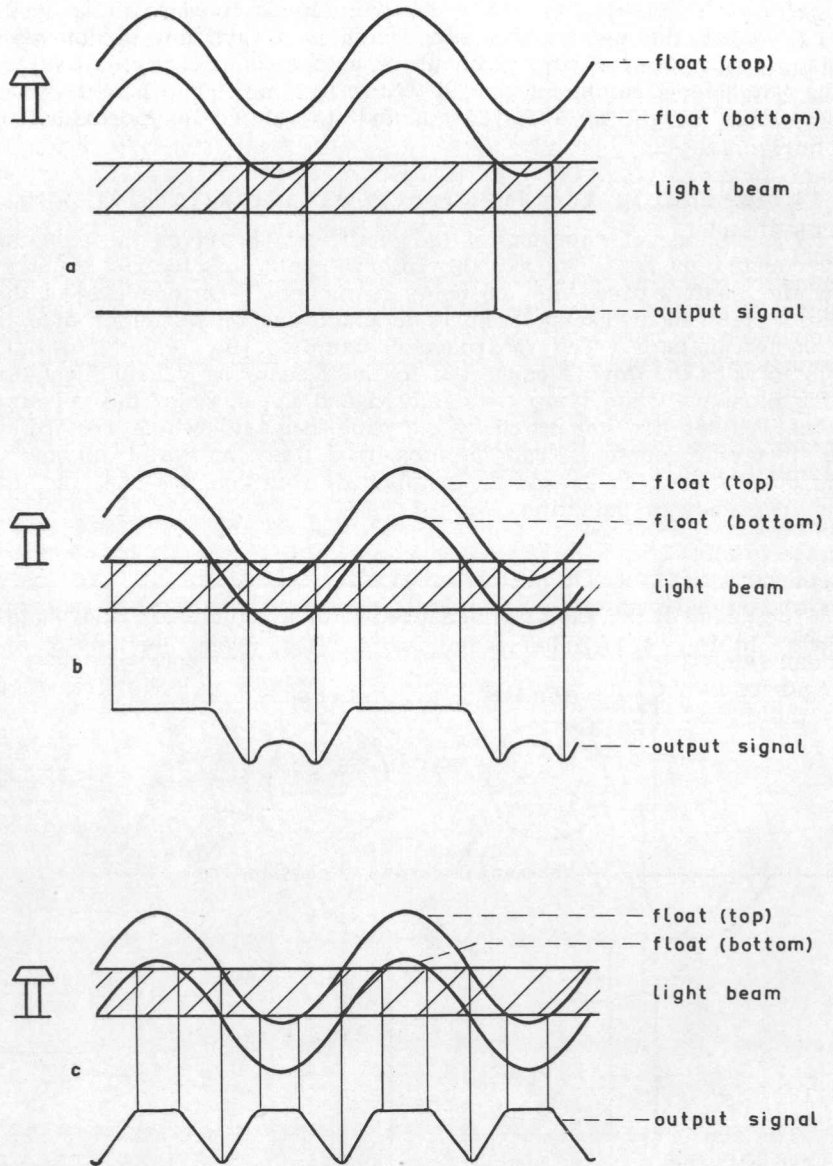


Fig. 4.17.2

The float intercepting the light beam and the output signal of the photo diode at different mean float positions relative to the light beam.

apparatus are shown. The 20W, 6V incandescent lamp is designated as L. A lens mounted in front of a rectangular slit focuses the light in point A. The length and width of the slit are a little smaller than the height and diameter of the float. In a vertical plane the light beams are only slightly influenced by the tube of the flowmeter. In a horizontal plane, the tube acts as a cylindrical lens. To focus the light another cylindrical lens (a piece of perspex) is used.

As the float intercepts the light beam, a signal can be obtained from the photodiode which is approximately linearly dependent on the float position for small amplitudes. For small amplitudes we can measure the amplitude as well as the phase by displaying both the signal of the magnetic flowmeter and the signal of the photodiode on a double beam oscilloscope. For large amplitudes one of the signals as indicated in fig. 4.17.2 is obtained. The signal that appears depends on the mean position of the float relative to the light beam.

The phase measurements are the least accurate of all measurements. This is due to the fact that even for slightly distorted wave forms it makes a large difference where the time interval between the two signals is measured. It would have been possible to obtain more accurate phase measurements by using other techniques but these would have taken considerably more time. To increase the accuracy of the measurements for small amplitudes, the time intervals are measured at four different places. These are the positive peak value, the negative peak value, and both intersections at the mean value (fig. 4.17.3). The mean value of these measurements is regarded as the time shift, correction being made for the time delay in the filter.

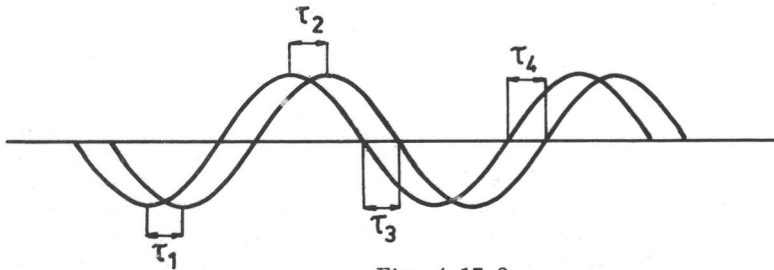


Fig. 4.17.3
The four places where the phase is measured.

4.18 The measuring procedure.

The static characteristic of each tube-float combination is measured with the aid of the measuring vessel. The cock I (fig. 4.1.1) is adjusted to make the float take a certain position in the tube. For this position a line on the scale of the rotameter tube is chosen. This results in a low spread of the measurement errors. For samples of 10 measurements at maximum flow a spread $s = 0.035 \%$

the value of the flow rate was found. This consistency could not be maintained with pulsating flow, because of the difficulty in the reading of the float position, which varied on the order of 0.5 mm. The values of s obtained for stationary conditions give, however, an impression of the accuracy of the switch and counting procedure.

The measurements with pulsating flow are performed as follows: First the pulsator is geared to the desired speed. To obtain a flow $w = w_0 + \hat{w} \cos \omega t$ the crank of the pulsator must be adjusted to its correct position. The impedance of the water system is frequency dependent so the eccentricity of the crank has to be readjusted for each frequency. To obtain the correct position of the crank first the rotameter is set to the value corresponding to $w = \bar{w}_0 - \hat{w}$ by varying cock I. Then the compensation signal of the magnetic flowmeter is adjusted so as to get zero signal. The flow is increased to raise the float to the position corresponding to w_0 . After starting the motor the screen of the oscilloscope is observed. Three displays are possible (fig. 4.18.1).

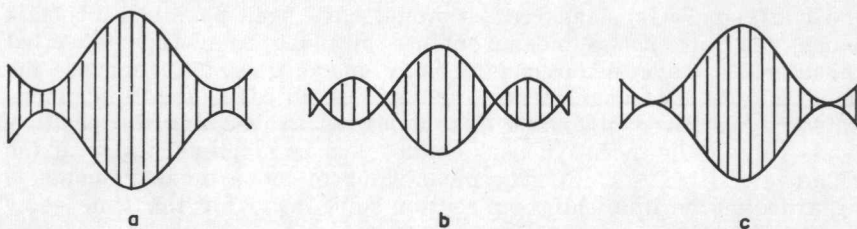


Fig. 4.18.1

Three possible displays of the signal of the magnetic flowmeter;
a: \hat{w} too small, b: \hat{w} too large, c: \hat{w} correct.

In a, \hat{w} is too small; in b it is too large. Only when the modulation is exactly 100% as in c, is the crank in the correct position. This method of positioning the crank proves to be satisfactory and \hat{w} can be adjusted to within $0.5 \cdot 10^{-6} \text{ m}^3/\text{s}$.

Having adjusted \hat{w} , the frequency of pulsation and the mean flow rate is measured with the aid of the measuring vessel and counters. The mean float position and float amplitude are measured by eye. The mean float position is measured from the maximum and minimum height of the float and the phase with the instruments described in sec. 4.17.

To obtain the value of M (sec. 3.1) the measured mean float position is converted into w_{oi} (the mean flow indicated) by means of the steady flow calibration data. From this value and the measured value of the mean flow w_0 , we can deduce

$$M = \frac{w_{oi}^2 - w_0^2}{\hat{w}^2}$$

Although the accuracy of these measurements is within 1%, the accuracy of the value of M is far less, because M is made up of the difference of two almost equal values. Supposing a possible error of 0.5% existed in w_{oi} . Neglecting the error in w_o , it is found that the maximum possible error in M for $w_{oi} \approx w_o \approx \hat{w}$ is about 0.01. To increase the accuracy most measurements were performed 10 times so that a mean value of M could be computed. For every measurement the value of \hat{w} was checked. In table 4.18.1 an example of a series of measurements of M is given.

n	t	Q	\bar{x}	Q/t	M
rotations, dimension- less	time, s	height in measuring vessel, cm	float position, divisions	mean flow	error, dimension- less
653	59.65	23.12	92.4	0.3875	0.0234
652	59.60	23.07	"	0.3870	0.0260
650	59.48	23.02	"	0.3870	0.0266
648	59.00	23.00	"	0.3900	0.0119
642	59.02	22.99	"	0.3895	0.0134
648	59.23	22.98	"	0.3880	0.0213
647	59.12	22.90	"	0.3875	0.0249
647	59.14	22.91	"	0.3875	0.0249
648	59.02	22.88	"	0.3880	0.0244
646	59.08	22.90	"	0.3875	0.0228

$$s = 0.0005$$

$$w_{oi} = 0.392 \pm 0.002$$

$$s_M = 0.005$$

$$\bar{M} = 0.022 \pm 0.002$$

Table 4.18.1
Example of a series of measurements
of M.

In this table n is the number of rotations, t the time in seconds, Q the height to which the measuring vessel was filled in cm and \bar{x} the mean position of the float. From the steady calibration data and \bar{x} , w_{oi} was computed, and from eq. (3.1.12)

$$M = \frac{w_{oi}^2 - w_o^2}{\hat{w}^2}$$

M was computed.

As can be seen from table 4.18.1, the spread in the measurements of M is on the same order of magnitude as the maximum possible error in M computed before. For small values of M it is necessary to increase the accuracy by taking 10 measurements. As it was not known beforehand whether the value of M would be large or small, a series of 10 measurements for each point was made. The consistency of the measurements is, of course, better for large values of M than for small values. Repeatability is influenced by temperature, contamination, viscosity and wear of the float. As an example, measurements of M made at different days are listed in fig. 4.4.1.

4.2 TUBES AND FLOATS.

Measurements were carried out with several tubes and floats. All tubes were commercially available types of Fischer & Porter. Most of the floats were made at the workshop according to the geometrical specifications of original Fischer & Porter floats but with different materials. In table 4.2.1. the four principal combinations are mentioned.

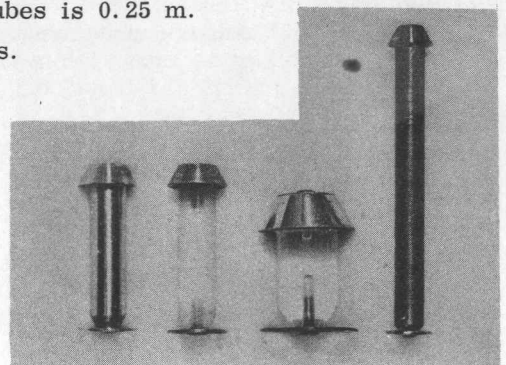
	I	II	III	IV
tube	B-4-21-10	B 4-21-10	B 5-27-25/70	B 3-27-10/70
float model	BSVT 44	BSVT 44	BSVT 54	
materials of float	stainless steel	aluminium and perspex	aluminium and perspex	stainless steel and lead
mass of float, kg	$14.3 \cdot 10^{-3}$	$5.4 \cdot 10^{-3}$	$7.25 \cdot 10^{-3}$	$19.3 \cdot 10^{-3}$
mean density of float, kg/m ³	8020	3030	2090	10690

Table 4.2.1
Float dimensions.

The scale length of all the tubes is 0.25 m.

Fig 4.2.1 shows the floats.

Fig. 4.2.1
The four floats.



The floats were designed in accordance with the capacity of the measuring system. To get a float with a certain weight with the same dimensions as the original float, different materials had to be used. The float edge has to be made of a material able to withstand wear during the measuring period.

The coefficients of the differential equations were computed from the float and tube data with eq. (2.22.5). A value of 0.64 was assumed for the contraction coefficient. For all tube-float combinations h was assumed to be 5 mm. The values of q resulting from this assumption give a reasonable agreement between measured and calculated phase shifts at high frequencies. Comparing the results of experiments with the dynamic eq. (2.22.4) with $\dot{w} = \dot{x} = 0$, we found a slight difference. In practice the flow needed to attain a certain value of x , is a little larger than that computed. For example, the value of w at maximum scale was 1.084 times larger than the computed value for combination II. This can be attributed to several factors. First of all the contraction coefficient might be different from the assumed value. Second it is possible that the pressure difference over the float is not exactly equal to the pressure difference between the points x and c of the mathematical model. Third, no account has been made for turbulence nor for viscosity in the theory. A correction factor ϵ may be applied to help compensate for the foregoing inadequacies in the theory.

$$p_x - p_c = \frac{\epsilon}{2} \rho (u_c^2 - u_x^2). \quad (4.2.1)$$

The value of ϵ can easily be determined from calibration with stationary flow. From eq. (2.22.2)

$$p_x - p_c = B' w^2 - C' w \dot{x} + D' \dot{x}^2 + E' \dot{w} - F' \ddot{x},$$

and remembering that B' , C' and D' are the terms corresponding with $(u_c^2 - u_x^2)$, eq. (4.2.1) results in

$$p_x - p_c = \epsilon (B' w^2 - C' w \dot{x} + D' \dot{x}^2) + E' \dot{w} - F' \ddot{x}. \quad (4.2.2)$$

Combining eq. (4.2.2) with eq. (2.22.3) and dividing by B'

$$\epsilon (w^2 - C w \dot{x} + D \dot{x}^2) + E \dot{w} - F \ddot{x} = G, \quad (4.2.3)$$

$$\text{from which} \quad w^2 - C w \dot{x} + D \dot{x}^2 + \frac{E}{\epsilon} \dot{w} - \frac{F}{\epsilon} \ddot{x} = \frac{G}{\epsilon}. \quad (4.2.4)$$

There is no reason to treat the coefficients resulting from $\int \left(\frac{dy}{dt} \right) dx$ in the same way as the terms C and D , ~~of~~ the integral resulting from another different mechanism. This does not imply that these factors are exact. They also result from a rather crude model.

The corrected coefficients of the differential equation for the different combinations are listed in table 4.2.2.

	I	II	III	IV	V
c_0	2.6	2.6	6.5	1.4	$\cdot 10^{-4} \text{ m}^2$
c_1	0.043	0.043	0.155	0.034	$\cdot 10^{-2} \text{ m}$
d_0	1.7	1.7	10.5	0.50	$\cdot 10^{-8} \text{ m}^4$
d_1	0.56	0.56	5.2	0.24	$\cdot 10^{-7} \text{ m}^3$
d_2	0.47	0.47	6.0	0.29	$\cdot 10^{-7} \text{ m}^2$
e_1	1.3	1.3	3.9	0.45	$\cdot 10^{-6} \text{ m}^2$
e_2	4	4	9	21	$\cdot 10^{-8} \text{ m}$
f_1	0.17	0.17	1.3	0.032	$\cdot 10^{-7} \text{ m}^4$
f_2	0.55	0.22	1.25	0.51	$\cdot 10^{-8} \text{ m}^3$
g_2	4.28	1.24	5.56	4.55	$\cdot 10^{-8} \text{ m}^4/\text{s}^2$

Table 4.2.2

The corrected coefficients of the differential equation, computed for the four floats.

With these constants x and w are expressed in m and m^3/s . The values of e_2 given in this table are computed for $x = 0.2 \text{ m}$.

Apart from g_2 these constants are the result of measurements and a crude model, so it is difficult to give an approximate value of their accuracy. The value of g_2 is given in three decimals because it can be measured with steady flow. The other factors cannot be measured directly, so the number of decimals given in the table is more or less a reflection of the authors faith in the accuracy of the model.

For the time constants used in sec. 3.1 we find the values listed in table 4.2.3., for $x_0 = 0.2 \text{ m}$ as before.

	I	II	III	IV	
q	$0.51 \cdot 10^{-2}$	$1.0 \cdot 10^{-2}$	$1.2 \cdot 10^{-2}$	$0.16 \cdot 10^{-2}$	s
s	0.84	1.6	2.0	0.49	s
t	$1.2 \cdot 10^{-2}$	$2.7 \cdot 10^{-2}$	$3.4 \cdot 10^{-2}$	$1.16 \cdot 10^{-2}$	s^2

Table 4.2.3
The float time constants.

4.3 AMPLITUDE AND PHASE MEASUREMENTS.

As a first check on the theory, measurements about amplitude and phase of the float movement were carried out. As a typical example the characteristics of I and II are reproduced in fig. 4.3.1 and 4.3.2. The lines indicate the values computed with eq. (3.1.7). The amplitude curve for I was measured for two values of $\frac{\dot{w}}{w_0}$,

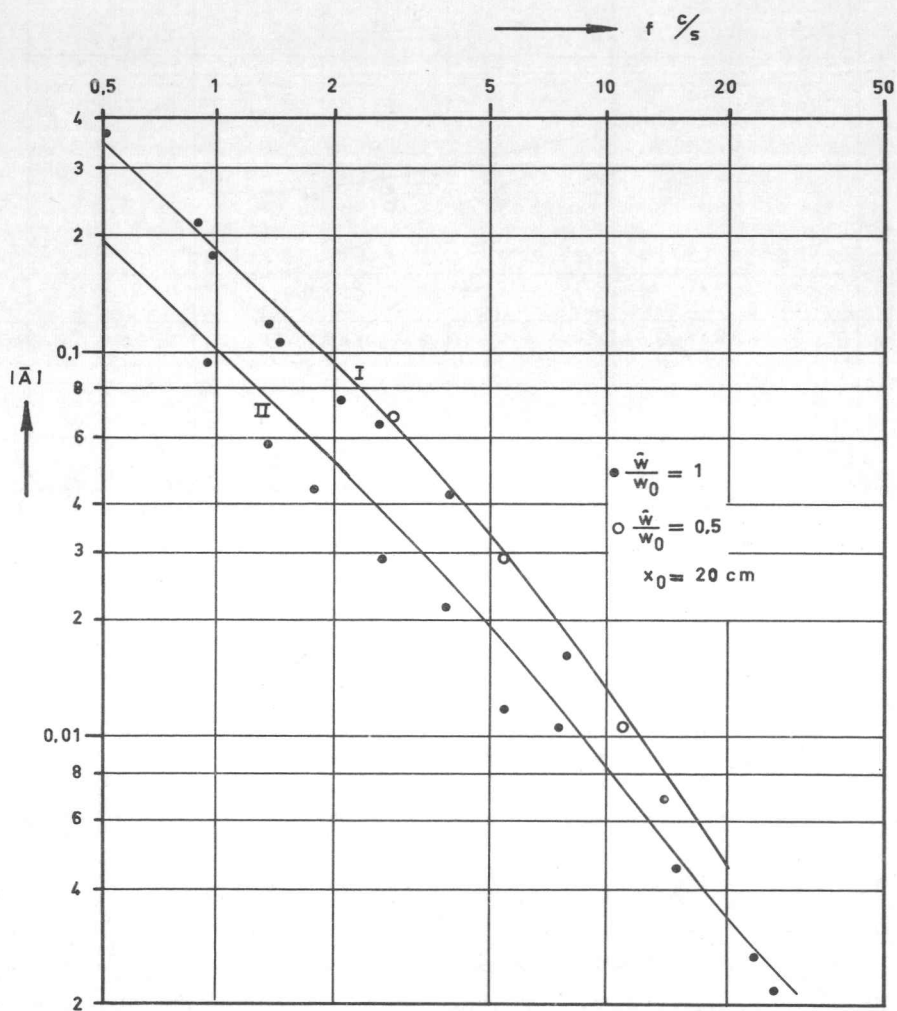


Fig. 4.3.1
 The amplitude characteristic for float tube combinations I and II.
 The solid lines indicate the theoretically derived characteristics.

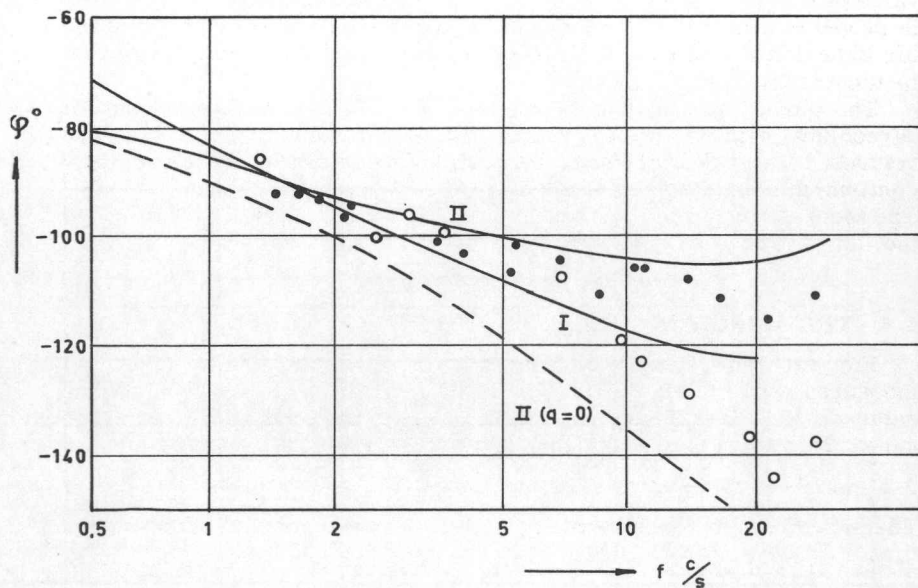


Fig. 4.3.2

The phase shift for float tube combinations I and II.

o: measurements for I; o measurements for II; $\frac{\hat{w}}{w_0} = 1$ and $x_0 = 20$ cm for all measurements.

The solid lines indicate the theoretically derived characteristics.

The dotted line indicates the theoretical phase shift for $q = 0$.

$$\frac{\hat{w}}{w_0} = 1 \text{ and } \frac{\hat{w}}{w_0} = 0.5.$$

Inspecting fig. 4.3.1 we see that the measurements for $\frac{\hat{w}}{w_0} = 1$ and $\frac{\hat{w}}{w_0} = 0.5$ give about the same result, indicating that the restriction of eq. (3.1.7) to small amplitudes is, at least in this case, not so severe. The fact that the gain of the system is almost independent of amplitude indicates that at least for these measurements the system acts as a linear one. Although measurements and theory do not agree completely, there is a reasonable correspondence in spite of the number of approximations made in the derivation of eq. (3.1.7). Especially for the combination II we see that the computed

value of the gain is somewhat higher than the measured value. This is probably a result of the fact that viscosity has a greater influence for light floats and that the effects of viscosity have been neglected in the theory.

The phase measurements of fig. 4.3.2 show also a reasonable agreement with theory. For high frequencies the theoretical curve returns to -90° . At least for combination II, the measurements confirm this to a useful accuracy.

The theoretical curves were computed from eq. (3.1.7). For $q = 0$ the dotted curve of fig. 4.3.2 is found for II.

4.4 THE ERROR IN THE INDICATED MEAN VALUE.

For all four floats, the error of the indicated mean value was measured as a function of frequency. From these measurements the value of M (3.1.12) was computed. As a typical example the measured M values for I are reproduced in fig. 4.4.1, again for $x = 0.2$ m. The measurements are made with $\frac{\hat{w}}{w_0} = 1$ and $\frac{\hat{w}}{w_0} = 0.5$. The measurements made with $\frac{\hat{w}}{w_0} = 0.5$ tend to give a larger value of M than the measurements with $\frac{\hat{w}}{w_0} = 1$. This is probably due to the fact that the approximations used in sec. 3.1 are only valid for small pulsations. The considerable spread in the measurements can be attributed to several factors. The overall accuracy of the measurements is strongly reduced by the fact that a difference between two almost equal values has to be measured. Furthermore, the amplitude of the pulsations is known only with limited accuracy. For high frequencies it is not always possible to get exact sinusoidal pulsations.

We can also compute a theoretical value for M based on eq. (3.1.15) with the values listed in table 4.2.3. Doing so we find the dotted curve of fig. 4.4.1. Although this curve does not fit at all to the measurements, there is a definite resemblance. By computation it turns out that eq. (3.1.15) is made up of the difference of nearly equal parts. This leads us to investigate a change in the coefficients α and β that would result in a curve that better suits the measurements. This seems to be the more a justified approach as the constants of table 4.2.2 are merely the result of a mathematical model with only a correction made for the stationary case.

For the dotted curve in fig. 4.4.1 α and β are 31.4 and 12.2 respectively. Changing these values to 39.7 and 12.6 leads to the solid curve of fig. 4.4.1, that fits the data quite well.

A further check on the theory developed in sec. 3.1 was performed by measuring the dependence of M on the value of $\frac{qs}{t}$. For high frequencies M is approximately given by eq. (3.1.18)

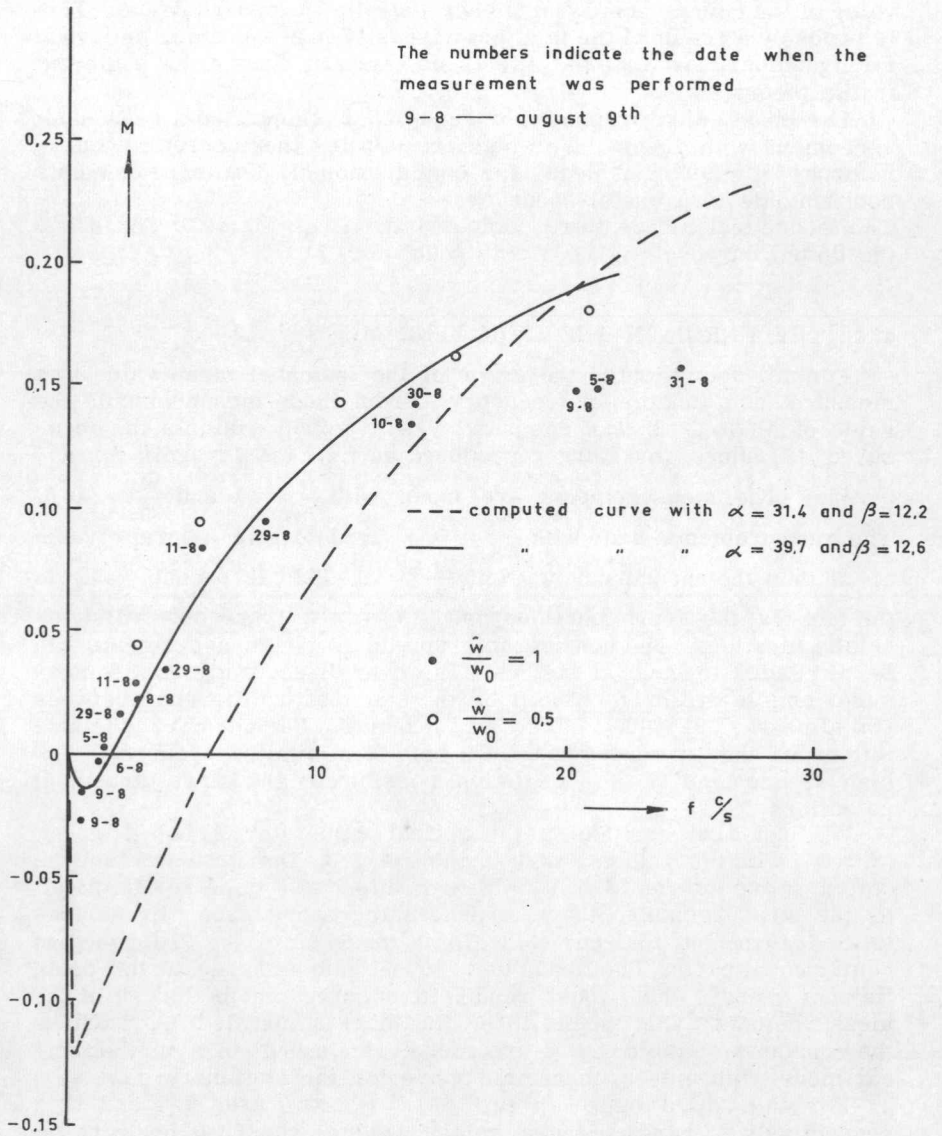


Fig. 4.4.1
 The value of M as a function of frequency.

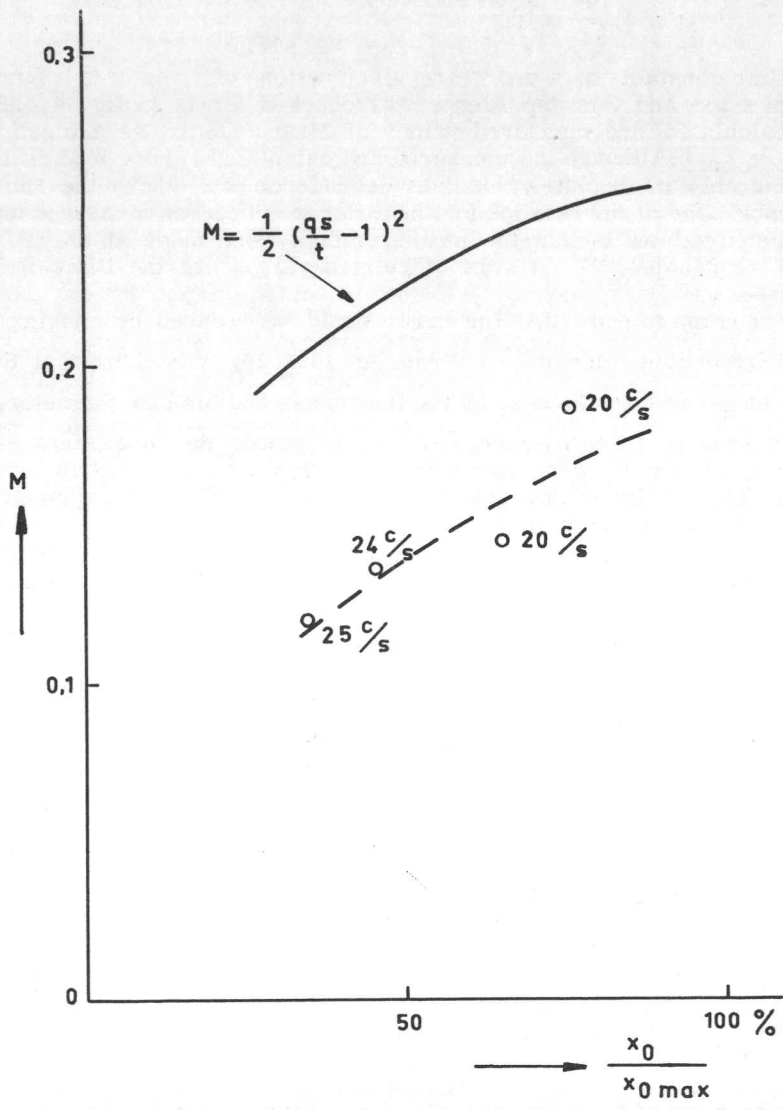


Fig. 4.4.2
 The value of M as a function of the mean float position.
 The solid curve indicates the theoretical value for $\omega \rightarrow \infty$.

$$M = \frac{1}{2} \left(\frac{qs}{t} - 1 \right)^2.$$

The time constants q , s and t are all functions of x , so M is a function of x too and this dependence was checked for I. In fig. 4.4.2, the calculated and measured values of M are plotted as a function of $x_0/x_{0 \max}$. Although the measured and calculated values of M differ considerably in absolute value their dependence of x_0 shows the same tendency. One of the reasons for the difference between measured and calculated values is that the measurements were made at the indicated frequencies, whereas the calculated values are the limit of M for $\omega \rightarrow \infty$.

It remains to show that the error could be reduced by choosing a more favourable value of $\frac{qs}{t}$. From eq. (3.1.20) it is found that the value of $\frac{qs}{t}$ can be influenced by the float mass and the tube diameter.

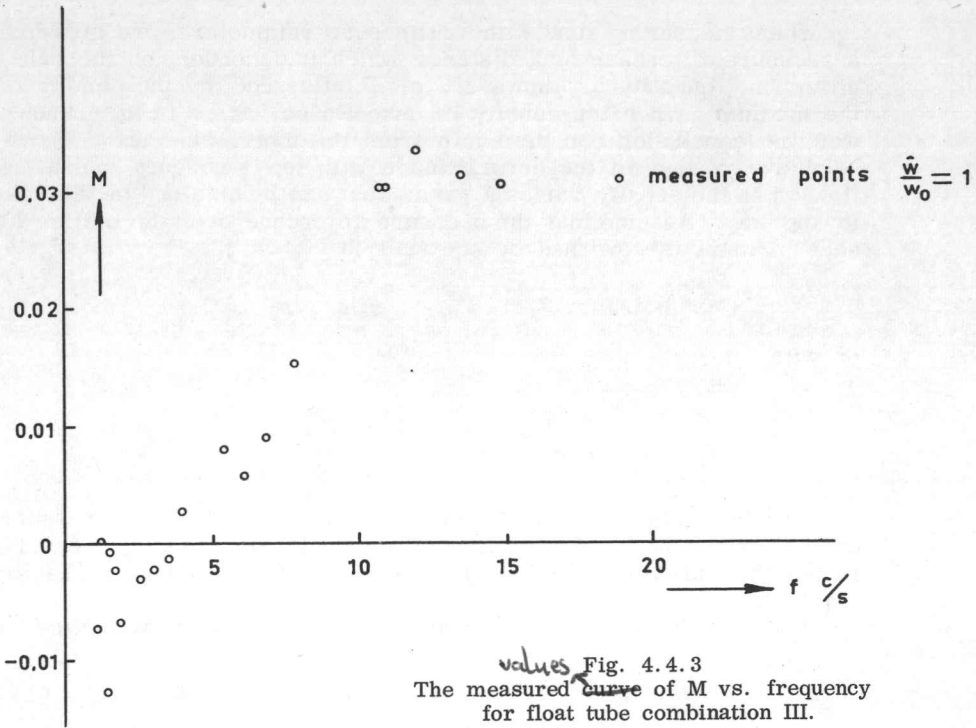
To get an idea if improvement could be obtained, the three arrangements I, III and IV were compared. The results are listed in table 4.4.1. The maximum flow rate capacities of all three arrangements are of the same order of magnitude.

Tube-float arrangement	I	III	IV
$w_{0 \max} 10^{-6} \text{ m}^3/\text{s}$	52.0	61.1	53.3
$\frac{qs}{t}$ calculated for $x_0/x_{0 \max} = 80\%$	0.29 0.21	0.71	0.067
M_{\max} calculated	0.18 0.24	0.042	0.43
M_{\max} measured	0.22	0.04	0.42
relative error $\frac{w_{oi} - w_o}{w_o}$ for			
$\frac{\hat{w}}{w_o} = 1$	10%	2%	20%

Table 4.4.1
Comparison of the errors resulting from pulsating flow for the ~~four~~ three rotameters.

The values M_{\max} measured, mentioned in table 4.4.1 are the estimated asymptotic values from the measured curves. See for example fig. 4.4.1 and 4.4.3.

The measurements of M vs. frequency for III are plotted in fig. 4.4.3. The measurements show that it is possible to reduce the error by choosing suitable dimensions for tube and float.



4.5 CONCLUSION.

Although there is no absolute agreement between calculated and measured values we can conclude that the approximations made in sec. 3 of the differential equation derived in sec. 2 agree to a large extent with the actual behaviour of the rotameter. In particular it has been shown that the error in the indicated mean value due to pulsating flow can be reduced by choosing suitable values for float weight and tube diameter.

The difference between calculated and measured values of this error can be attributed to measuring faults and in part to the following cause: The theoretical model will only give a rough approximation of the actual process. The constants used in the differential equation are, therefore, only approximations of their true value. This is important because the error consists of the difference of nearly equal quantities.

5. FLOWMETERS FOR COMPRESSIBLE MEDIA.

5.1 FIXED ORIFICES.

When measuring flow with orifices or rotameters, we measure a pressure difference or a distance which is dependent on the velocity. This quantity is, however, also influenced by the density of the medium. When the density is unknown or varies in an unknown way, no conclusion can be drawn from the meter reading.

A rough idea of the errors made with low frequency pulsating flow when the density varies a great deal can be obtained in the following way. Assume that the pressure difference over the orifice at each moment is governed by eq. (2.1.2)

$$w = K \sqrt{p_1 - p_2} \quad ,$$

or with

$$K = \frac{1}{\sqrt{K' \rho}}$$

$$p_1 - p_2 = K' \rho w^2 \quad .$$

As will be shown later on, this equation holds when the pressure drop over the orifice is small compared with the absolute pressure in the fluid and the pressure drop due to acceleration is negligible (eq. 5.1.8).

Consider the mean density in the instrument to vary according to

$$\rho = \rho_0 + \hat{\rho} \sin \omega t$$

and the volumetric flow according to

$$w = w_0 + \hat{w} \sin(\omega t + \varphi) \quad .$$

When the pressure difference is measured with a damped manometer, the reading of the instrument can be computed from

$$\begin{aligned} \overline{p_1 - p_2} &= \overline{K' \rho w^2} = \\ &= \frac{K'}{2\pi} \int_0^{2\pi} (\rho_0 + \hat{\rho} \sin \omega t) \left\{ w_0 + \hat{w} \sin(\omega t + \varphi) \right\}^2 d\omega t = \\ &= K' \rho_0 w_0^2 \left\{ 1 + \frac{\hat{\rho} \hat{w}}{\rho_0 w_0} \cos \varphi + \frac{1}{2} \left(\frac{\hat{w}}{w_0} \right)^2 \right\} \quad . \end{aligned}$$

For the pathological case in which

$$\frac{\hat{p}}{\rho_0} = 1, \frac{\hat{w}}{w_0} = 1, \text{ and } \cos \varphi = 1$$

an erroneous reading in the pressure is found, which is 2.5 times the pressure for stationary flow with the same mean value. Of course

$$\frac{\hat{p}}{\rho_0} = 1 \text{ is not a condition likely to occur, and apart from this,}$$

the condition that the pressure drop over the orifice is small compared with the absolute pressure in the gas will not be fulfilled. Even though the factor 2.5 has little meaning, it can be seen that

$$\text{with } \frac{\hat{w}}{w_0} = 1, \cos \varphi = 1 \text{ and } \frac{\hat{p}}{\rho_0} = \frac{1}{2}, \text{ (a condition which does not necessarily disagree with the assumption that the pressure difference over the orifice is small compared with the absolute pressure) the error will be a factor 2 in the pressure difference. For incompressible flow the error will only amount to 1.5 times the stationary value. In this chapter only cases are considered in which the change of the density as a function of time is small compared with the mean density.}$$

It will be assumed that the flow in the neighbourhood of the orifice is adiabatic. As will be shown at the end of this section, the equation of Bernoulli becomes

$$\frac{k}{k-1} \left(\frac{p_1}{\rho_1} - \frac{p_2}{\rho_2} \right) = \frac{1}{2} (v_2^2 - v_1^2), \quad (5.1.1)$$

where the specific heat ratio is $k = \frac{c_p}{c_v}$

Analogous to the case of incompressible flow, a term must be added to account for the acceleration of the medium

$$\frac{k}{k-1} \left(\frac{p_1}{\rho_1} - \frac{p_2}{\rho_2} \right) = \frac{1}{2} (v_2^2 - v_1^2) + \int_1^2 \frac{\partial v}{\partial t} \cdot dl. \quad (5.1.2)$$

For adiabatic flow the equation

$$\frac{p_1}{\rho_1^k} = \frac{p_2}{\rho_2^k} = \text{constant is valid.} \quad (5.1.3)$$

With this equation it is found that

$$\frac{k}{k-1} \left(\frac{p_1}{\rho_1} - \frac{p_2}{\rho_2} \right) = \frac{k}{k-1} \left(\frac{p_1}{\rho_1} \right) \left\{ 1 - \left(\frac{p_2}{p_1} \right)^{\frac{k-1}{k}} \right\} =$$

$$= \frac{k}{k-1} \frac{p_1 - p_2}{\rho_1} \frac{1 - (p_2/p_1)^{\frac{k-1}{k}}}{1 - p_2/p_1} \quad (5.1.4)$$

The continuity equation is

$$\rho_1 v_1 a_1 = \rho_2 v_2 a_2 + \frac{d(\rho V)}{dt}$$

where V is the considered volume and ρ the mean density in this volume. Together with eq. (5.1.2) this equation describes the flow in the orifice when the streamline pattern is known. These equations are very difficult to handle and some approximations are used to derive the equation for the pressure difference.

Considering a small volume, the region of the orifice, the continuity equation can be written as

$$\rho_1 v_1 a_1 = \rho_2 v_2 a_2 \quad (5.1.5)$$

because the increase of the mass can be neglected.

The first term on the right of eq. (5.1.2) can then be written as

$$\begin{aligned} (v_2^2 - v_1^2) &= v_1^2 \left\{ \frac{v_2^2}{v_1^2} - 1 \right\} = v_1^2 \left\{ \left(\frac{\rho_1 a_1}{\rho_2 a_2} \right)^2 - 1 \right\} = \\ &= v_1^2 \left\{ \left(\frac{p_1}{p_2} \right)^{2/k} \left(\frac{a_1}{a_2} \right)^{2-1} \right\} \end{aligned} \quad (5.1.6)$$

Substituting eq. (5.1.4) and (5.1.6) into eq. (5.1.2) we find

$$\begin{aligned} \frac{k}{k-1} \frac{(p_1 - p_2)}{\rho_1} \left\{ \frac{1 - (p_2/p_1)^{\frac{k-1}{k}}}{1 - (p_2/p_1)} \right\} &= \frac{1}{2} v_1^2 \left\{ \left(\frac{p_1}{p_2} \right)^{2/k} \left(\frac{a_1}{a_2} \right)^{2-1} \right\} + \\ + \int_1^2 \frac{\partial v}{\partial t} \cdot dl. \end{aligned} \quad (5.1.7)$$

Although (5.1.7) is easier to handle, it is still far from simple. A further approximation which can be made is $p_1 - p_2 \ll p_1, p_2$, so that

$$\frac{1 - (P_2/P_1)^{\frac{k-1}{k}}}{1 - (P_2/P_1)} \approx \frac{k-1}{k} + \frac{1}{k} \left(\frac{k-1}{k}\right) \left(1 - \frac{P_2}{P_1}\right) \approx \frac{k-1}{k}$$

and $\left(\frac{P_1}{P_2}\right)^{2/k} \approx 1$, which results in

$$\frac{P_1 - P_2}{\rho_1} = \frac{1}{2} v_1^2 \left\{ \left(\frac{a_1}{a_2}\right)^2 - 1 \right\} + \int_1^2 \frac{\partial v}{\partial t} \cdot dl. \quad (5.1.8)$$

This is the same equation as the one found in sec. 2.1, eq. (2.1.9) for incompressible flow. Indeed the approximation that the pressure drop over the orifice is small compared with the absolute pressure is in fact equivalent to the assumption of incompressible flow in the region of the orifice. Considering the case of small volumes and pulsations not resulting in large pressure differences it can be concluded that the same equation holds as for incompressible fluids. We will restrict the scope of this thesis to cases where these conditions are met.

Eq. (5.1.1) can be derived from eq. (2.1.8) in the following way: For a perfect gas undergoing an isentropic process, the equation $\rho = C p^{1/k}$ is applicable.

$$\text{Hence } p \nabla \frac{1}{\rho} = \frac{p}{C} \nabla p^{-1/k} = \frac{-p}{kC} \nabla p = -\frac{1}{k\rho} \nabla p. \quad (5.1.9)$$

Substituting eq. (5.1.9) into

$$\nabla \left(\frac{p}{\rho}\right) = \frac{1}{\rho} \nabla p + p \nabla \frac{1}{\rho}$$

$$\text{gives } \frac{1}{\rho} \left(1 - \frac{1}{k}\right) \nabla p = \nabla \frac{p}{\rho}, \text{ so}$$

$$\frac{1}{\rho} \nabla p = \frac{k}{k-1} \nabla \frac{p}{\rho}. \quad (5.1.10)$$

This leads by integration to the left side of eq. (5.1.1.).

5.2 ROTAMETERS.

5.21 Approximations for sinusoidal pulsations.

When the condition that $p_1 - p_2 \ll p$ mentioned in section 5.1 is fulfilled, it can be shown that the equation of motion for the float in a rotameter has the same form as the one derived for incompressible flow.

The volumetric flow w is, however, defined in sec. 2 as the volumetric flow at $x = 0$, the lower end of the tube. This value is used to derive the velocity of the fluid at the float edge. For compressible fluids the flow at the lower end of the tube will not necessarily be equal to the flow some distance higher, due to the capacitive behaviour of the gas. In other words, the volume is too large to make eq. (5.1.5) applicable.

In the equations for incompressible flow, w is independent of the place in the circuit where it is measured. The same results would have been obtained if the reference point for the definition of w had been chosen a short distance beneath the float. If this reference point is assumed for compressible flow the capacitive effect of the volume upstream of the float can be taken into account separately. With this modification the equation of motion is the same as for incompressible flow.

However, as the range in the densities is considerably larger than with incompressible fluids, the approximations made for incompressible fluids do not always hold. In particular when the density of the gas is very much smaller than the density of the float, other approximations have to be made. In the following this case will be treated.

The same approximations as were made in sec. 3.1 up to eq. (3.1.15) for the gain and phase characteristics can be used and also

$$M = \frac{w_{oi}^2 - w_o^2}{\hat{w}^2} = \frac{1}{2} \operatorname{Re} \left\{ 1 - |\bar{A}|^2 + \alpha \omega^2 |\bar{A}|^2 - j\beta \omega \bar{A} \right\} \quad (3.1.15)$$

holds. However the approximation

$$\alpha = s^2$$

(eq. 3.1.16) is not valid.

As can be seen from eq. (3.1.11),

$$\alpha = \frac{d_o + d_1 x_o + d_2 x_o^2 + f_1 + 2f_2 x_o}{g_2}$$

It turns out that for gases

$$2f_2 x_0 \gg f_1 + d_0 + d_1 x_0 + d_2 x_0^2$$

for values of x_0 not too low and $\rho_{fl} \gg \rho$.

From eq. (3.1.7) it follows that to a first approximation

$$\alpha = 4t$$

$$\text{and } \beta = 2s.$$

(5.21.1)

These values for α and β substituted in eq. (3.1.15) with (3.1.7) lead to

$$M = \frac{1}{2} \frac{(\omega^4 t^2 + 2\omega^2 t - \omega^2 s^2) + 2\omega^2 q (s - \frac{1}{2}q + 2\omega^2 q t - \omega^2 s t)}{(1 - \omega^2 t)^2 + \omega^2 s^2} \quad (5.21.2)$$

For $\omega \rightarrow \infty$ this equation becomes

$$M = \frac{1}{2} \left(1 - \frac{2qs}{t} + \frac{4q^2}{t} \right) \approx \frac{1}{2} \left(1 - \frac{2qs}{t} \right) \quad (5.21.3)$$

as $q \ll s$.

Making $\frac{qs}{t}$ as closely as possible equal to $\frac{1}{2}$ would result in a low value for the error. For several float-tube combinations the value of $\frac{qs}{t}$ was estimated for air at atmospheric pressure and room temperature, and even for light floats values of about 10^{-2} at $x = 10$ cm were found because q is small. From eq. (3.1.20) it is found that

$$\frac{qs}{t} : : \frac{(a_0 + a_x) a_0 \rho h}{V_{fl} \rho_{fl} a_x}$$

To multiply $\frac{qs}{t}$ by a factor 10^2 by decreasing the float mass is almost impossible. Even if it were possible the sensitivity $\frac{x}{w}$ of the instrument would increase with a factor 10 and so the maximum flow rate will decrease with a factor 10. To multiply $\frac{qs}{t}$ by a factor 10^2 by increasing the tube diameter leads to unreasonably large tubes. As the volume of the float is proportional to at least the square of the tube diameter, the tube diameter would have to be at least 10 times larger.

For normal float-tube combinations, used for air at atmospheric pressure, q can safely be neglected when considering the error of the mean value.

For $q = 0$ eq. (5.21.2) becomes

$$M = \frac{1}{2} \left\{ \frac{\omega^4 t^2 + 2 \omega^2 t - \omega^2 s^2}{(1 - \omega^2 t)^2 + \omega^2 s^2} \right\}, \quad (5.21.4)$$

which as $\omega \rightarrow \infty$ results in

$$M = \frac{1}{2}.$$

For the phase and amplitude response, the frequency where q becomes important is on the order of 1000 c/s. As the tests performed with these flowmeters hardly ever reach 30 c/s, q can also be neglected for these characteristics.

The amplitude and phase characteristics for floats under these conditions are given by

$$\bar{A} = \frac{1}{1 + j \omega s + (j \omega)^2 t}, \quad (5.21.5)$$

where s and t are given by eq. (3.1.7)

$$s = \frac{c_0 + c_1 x_0}{2 \sqrt{g_2}}$$

and

$$t = \frac{f_1 + f_2 x_0}{2 g_2} \approx \frac{f_2 x_0}{2 g_2}.$$

The resonant frequency of this system is given by

$$\omega_0 = \frac{1}{\sqrt{t}} \quad (5.21.6)$$

and the quality factor by

$$Q = \frac{\sqrt{t}}{s}. \quad (5.21.7)$$

Substituting eq. (3.1.7) and (2.22.5) in eq. (5.21.6) it is found that neglecting ρ in comparison with ρ_{fl} and $f_1 x$ in comparison with $f_2 x^2$,

$$\omega_0 = \sqrt{\frac{2g}{x_0}}. \quad (5.21.8)$$

Thus, the resonance frequency is to the first approximation given solely by the acceleration of gravity and the mean position of the float.

5.22 The impedance of the float and the rotameter tube.

Although for compressible flow the same equation of motion holds as for incompressible flow, a rotameter used with a compressible, low density medium may show an effect which is absent for high density incompressible fluids.

The mentioned effect is known as bouncing, a spontaneous oscillating movement of the float without any forced pulsation of the flow. As the effect of bouncing is strongly influenced by the pipes connected to the meter, we will consider the ratio of the variations of pressure difference and flow rate, the impedance of the float, together with the elements attached to it. This gives all the necessary information about the stability of the system. If there is a closed loop in the system containing a source of energy having a loop impedance with a negative real part it will be unstable.

As dashpots are frequently used to prevent float bouncing, the impedance will be computed for a float having an external damping mechanism attached to it. Only the lower end of the frequency band will be considered, where wavelengths are large compared with the dimensions of the system. For such a rotameter the force on the float can be expressed as

$$(p_x - p_c) a_o = \rho_{fl} V_{fl} g + \rho_{fl} V_{fl} \ddot{x} + \gamma \dot{x}, \quad (5.22.1)$$

where γ signifies the damping of the dashpot. From (3.1.7) it can be found by neglecting q , that

$$\bar{A} = \frac{\overline{\Delta x}}{\overline{\Delta w}} \sqrt{g_2} = \frac{1}{1 + j\omega s + (j\omega)^2 t} \quad (5.22.2)$$

Where the reference level for Δw is chosen just beneath the float. Considering small harmonic variations $\overline{\Delta x}$, $\overline{\Delta p_x}$ and $\overline{\Delta p_c}$ in x , p_x and p_c , eq. (5.22.1) can, by substitution of complex variables, be written as

$$(\overline{\Delta p_x} - \overline{\Delta p_c}) a_o = (j\omega)^2 \rho_{fl} V_{fl} \overline{\Delta x} + j\omega \gamma \overline{\Delta x}. \quad (5.22.3)$$

Eliminating $\overline{\Delta x}$ from (5.22.3) and (5.22.2) leads to

$$\begin{aligned} \frac{(\overline{\Delta p_x} - \overline{\Delta p_c})}{\overline{\Delta w}} &= \bar{Z}_f = \frac{j\omega \gamma + (j\omega)^2 \rho_{fl} V_{fl}}{a_o \sqrt{g_2} \{1 + j\omega s + (j\omega)^2 t\}} = \\ &= \frac{b'_1 j\omega + b'_2 (j\omega)^2}{b_o + b_1 j\omega + b_2 (j\omega)^2} \end{aligned} \quad (5.22.4)$$

The polar diagram of \bar{Z}_f is drawn in fig. 5.22.1.

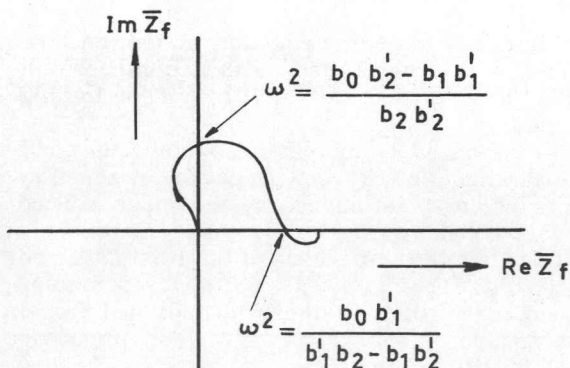


Fig. 5.22.1
Polar diagram of the impedance \bar{Z}_f .

When the real part of \bar{Z}_f is negative the float can start to bounce, if the impedances in the rest of the circuit are unfavourably chosen. With eq. (3.1.7) and (2.22.5) we find for

$$\left. \begin{aligned}
 b'_1 &= \gamma \\
 b'_2 &= \rho_{fl} V_{fl} \\
 b_0 &= a_0 \sqrt{g_2} = \frac{C_c a_x}{x} \sqrt{\frac{2a_0 g \rho_{fl} V_{fl}}{\rho}} \\
 b_1 &= a_0 s \sqrt{g_2} = \frac{a_0 (c_0 + c_1 x_0)}{2} = a_0 (a_0 + a_x) \\
 b_2 &= a_0 t \sqrt{g_2} = \frac{a_0 f_2 x_0}{2 \sqrt{g_2}} = \frac{1}{2} C_c a_x a_0 \sqrt{\frac{2 \rho_{fl} V_{fl}}{g \rho a_0}}
 \end{aligned} \right\} (5.22.5)$$

Eq. (5.22.4), however, does not give the desired impedance of the rotameter but the impedance of the float.

For the impedance of the rotameter, the capacitance of the volume upstream and downstream of the float must be taken into account. The capacitance C of a volume is defined from

$$w_{in} - w_{out} = C \frac{dp}{dt}, \quad (5.22.6)$$

where p is the pressure in the volume, w_{in} the flow entering and w_{out} the flow leaving the volume. The capacitance C can be written, assuming adiabatic conditions,

$$C = \frac{V}{kp} \quad (5.22.7)$$

when the variations in p are small compared with the mean value of p . Eq. (5.22.7) can be easily derived from the continuity equation

$$\frac{d \rho V}{dt} = \rho(w_{in} - w_{out}) \quad (5.22.8)$$

With $\frac{p}{\rho k} = \text{constant}$, it is found that

$$d \rho = \frac{\rho}{kp} dp.$$

Substitution of the last equation in (5.22.8) and assuming a constant volume results in

$$w_{in} - w_{out} = \frac{V}{kp} \frac{dp}{dt}, \quad (5.22.9)$$

from which (5.22.6) and (5.22.7) follow.

With the complex variables $\overline{\Delta w}$ and $\overline{\Delta p}$, eq. (5.22.9) can be written as

$$\overline{\Delta w}_{in} - \overline{\Delta w}_{out} = j \omega C \overline{\Delta p}. \quad (5.22.10)$$

The volume upstream of the float is to a first approximation equal to $a_0 x$. The capacitance of this volume can be derived from

$$\rho(w_{in} - w_{out}) = \frac{d \rho V}{dt} = V \frac{d \rho}{dt} + \rho \frac{dV}{dt} = \frac{\rho a_0 x_0}{kp} \dot{p} + \rho a_0 \dot{x}. \quad (5.22.11)$$

The last term signifies the mass flow due to the movement of the float. For small variations in the float position, however, the reference level for the definition of w can be chosen such that the float never passes this level. For small amplitudes of the float the volume between reference level and float will be nevertheless small enough to apply eq. (5.1.5). The capacitance upstream from the float now remains fixed, because the reference level is fixed.

The capacitance upstream the float is thus equal to

$$C_u = \frac{a_0 x_0}{kp}. \quad (5.22.13)$$

5.23 The stability of the float.

The stability of the float can be determined by considering the impedance of the closed loop of the electrical analogue circuit of fig. 5.23.1.

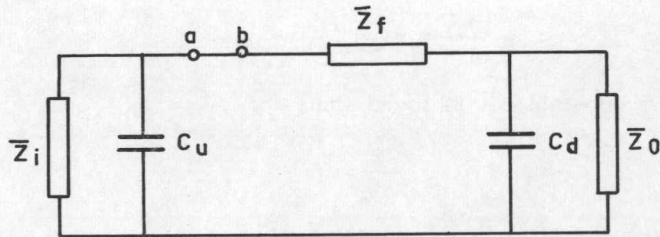


Fig. 5.23.1
Electrical analogue of a circuit with a rotameter.

The impedance \bar{Z}_i is the impedance of the circuit upstream of the rotameter and \bar{Z}_o the impedance downstream of the rotameter. Computing the impedance between the points a and b, the relation can be found between $\Delta \bar{w}$ and $\Delta \bar{p}_a - \Delta \bar{p}_b$;

$$\frac{\Delta \bar{p}_a - \Delta \bar{p}_b}{\Delta \bar{w}} = \frac{P_1(j\omega)}{P_2(j\omega)}, \quad (5.23.1)$$

where $P_1(j\omega)$ and $P_2(j\omega)$ are polynomials in $(j\omega)$.

From eq. (5.23.1) it is found that

$$(\Delta \bar{p}_a - \Delta \bar{p}_b) P_2(j\omega) = \Delta \bar{w} P_1(j\omega). \quad (5.23.2)$$

As all the relations between pressure and flow variations are supposed to be linear, $j\omega$ in (5.23.2) can be substituted by $\frac{d}{dt}$ and a differential equation relating $\Delta \bar{p}_a - \Delta \bar{p}_b$ and $\Delta \bar{w}$ is found. Closing the circuit at points a, b signifies that $\Delta \bar{p}_a = \Delta \bar{p}_b$. The stability of the system can now be investigated by considering the roots of the differential equation for $\Delta \bar{w}$. For stability the polynomial P_1 has to satisfy the criterion of Hurwitz or Routh.

Another way to investigate the stability of the system is to plot the impedance of the loop in a polar diagram. The system will be stable when the impedance is situated completely in the right hand part of the diagram.

As an application of the theory some special cases will be treated.

An interesting question is, what value of the damping coefficient γ has to be chosen to prevent bouncing for every possible circuit with an impedance without a negative real part attached in series with the float.

From eq. (5.22.4) the real part of \bar{Z}_f can be computed:

$$\text{Re } \bar{Z}_f = \frac{(b_2 b'_2 \omega^2 - b_0 b'_2 + b_1 b'_1)}{D}, \quad (5.23.3)$$

where the denominator D is positive for every ω .

From eq. (5.23.3) it follows that $\text{Re } \bar{Z}_f$ can never be negative when

$$b_0 b'_2 < b_1 b'_1 \quad (5.23.4)$$

By substituting the values from eq. (5.22.5) this equation leads to

$$\gamma > \frac{\rho_{fl} V_{fl}}{(a_o + a_x)} \sqrt{g_2}. \quad (5.23.5)$$

The minimum value of a_x being zero, it is found that no bouncing will be possible when

$$\gamma > \frac{\rho_{fl} V_{fl}}{a_o} \sqrt{g_2}. \quad (5.23.6)$$

Another method often used to prevent bouncing is to place a restriction immediately upstream of the rotameter. First the effect of a very high resistance will be treated. Now the impedance $\bar{Z}_i = R$. For simplicity the impedance \bar{Z}_0 and the impedance of the capacity C_d are omitted. The air is flowing freely into the atmosphere at the end of the rotameter tube. The analogue circuit is given in fig. 5.23.2.

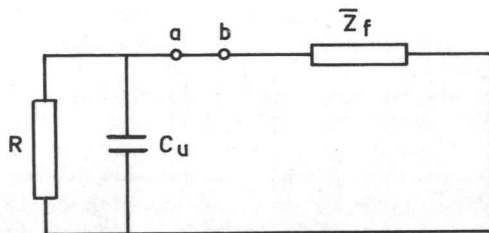


Fig. 5.23.2
Analogue of a rotameter with a restriction upstream of the float.

Computing the impedance between the points a and b, the following expression is found.

$$\bar{Z}_{ab} = \frac{b_0 + b_1 j \omega + (b_2 + b'_1 C_u) (j \omega)^2 + b'_2 C_u (j \omega)^3}{\left\{ b_0 + b_1 j \omega + b_2 (j \omega)^2 \right\} j \omega C_u}, \quad (5.23.7)$$

when $R \rightarrow \infty$.

The Hurwitz stability conditions for the polynomial of the numerator lead to

$$\left. \begin{aligned} b_0 > 0 \\ b_1 > 0 \\ b'_2 C_u > 0 \\ b_1 (b_2 + b'_1 C_u) > b_0 b'_2 C_u \end{aligned} \right\} \quad (5.23.8)$$

as a condition for stability.

For simplicity the external damping will now be considered to be zero, so $b'_1 = 0$ and

$$C_u < \frac{b_1 b_2}{b_0 b'_2}. \quad (5.23.9)$$

With eq. (5.22.5) and eq. (5.22.13)

$$\frac{a_0 + a_x}{g \rho_{fl} V_{fl}} > \frac{2}{kp}. \quad (5.23.10)$$

From the last equation it can be seen that bouncing is most likely to occur for low float positions.

Considering the stability of a float with a finite restriction upstream of the rotameter, it is thus justified to consider only the very low float positions where C_u can be neglected. The impedances \bar{Z}_i and \bar{Z}_o can also be neglected if the lowest possible value of R to prevent bouncing for any circuit is investigated. The resistive parts of \bar{Z}_i and \bar{Z}_o could only make the real part of the impedance of the circuit larger than R whereas the reactive parts have no influence on the real part of the loop impedance. Of course this is only true when the rest of the circuit contains only elements with impedances with positive real parts. For simplicity the external damping will be neglected. The real part of the impedance of the float can be computed from eq. (5.23.3) with $b'_1 = 0$.

$$\operatorname{Re} \bar{Z}_f = \frac{-\omega^2 b_2' (b_0 - \omega^2 b_2)}{(b_0 - \omega^2 b_2)^2 + \omega^2 b_1^2} \quad (5.23.11)$$

The minimum value of $\operatorname{Re} \bar{Z}_f$ exists when

$$\omega^2 = \frac{b_0^2}{b_0 b_2 + \sqrt{b_0 b_1^2 b_2}} \quad (5.23.12)$$

Substituting this value of ω^2 in (5.23.11) the minimum value $\operatorname{Re} \bar{Z}_f$ can ever assume is found

$$\operatorname{Re} \bar{Z}_{f \min} = \frac{-b_0 b_2'}{b_1^2 + 2b_1 \sqrt{b_0 b_2}} \quad (5.23.13)$$

With eq. (5.22.5) it is found that

$$\operatorname{Re} \bar{Z}_{f \min} = \frac{-\rho_{fl} V_{fl} \sqrt{g_2}}{a_0 (a_0 + a_x) \left\{ a_0 + a_x + 2\sqrt{g_2} \sqrt{\frac{x_0}{2g}} \right\}} \quad (5.23.14)$$

Considered as a function of x , $\operatorname{Re} \bar{Z}_{f \min}$ has a minimum for $x_0 = 0$, which is equal to

$$\frac{-\rho_{fl} V_{fl} \sqrt{g_2}}{a_0^3} \quad (5.23.15)$$

To prevent bouncing for every circuit in which the rotameter is mounted it is necessary to put a restriction upstream of the rotameter which has a resistance

$$R \geq \frac{\rho_{fl} V_{fl} \sqrt{g_2}}{a_0^3} \quad (5.23.16)$$

Notice that the compressibility is not present in the equations derived in this chapter and therefore it is not an essential parameter for bouncing to exist. However, the probability of bouncing is greater for a gas because of the capacitance added to the system and lower densities (high values of g_2) of the medium.

6. MEASUREMENTS FOR COMPRESSIBLE FLOW.

6.1 THE MEASURING CIRCUITS.

Measurements were made with two different circuits, one for maximum flow rates of about $0.03 \text{ m}^3/\text{s}$, the other for maximum flow rates of about $0.5 \cdot 10^{-3} \text{ m}^3/\text{s}$. We will refer to the two circuits as the one for high and the other for low flow rates. For all measurements the pressure in the rotameter is approximately equal to the atmospheric pressure and the medium used is air.

6.11 The measuring circuit ¹⁾ for high flow rates.

The flow is generated by a ventilator V with a maximum pressure of 3000 N/m^2 ($0.3 \text{ m H}_2\text{O}$). Sinusoidal variations are generated by a generator G. The air is fed to the rotameter by a pipe 1.5 m long and internal diameter 50 mm in which fins are inserted to suppress helical motion.

A hot wire anemometer H serves to measure both actual mean flow and the amplitude of flow pulsations.

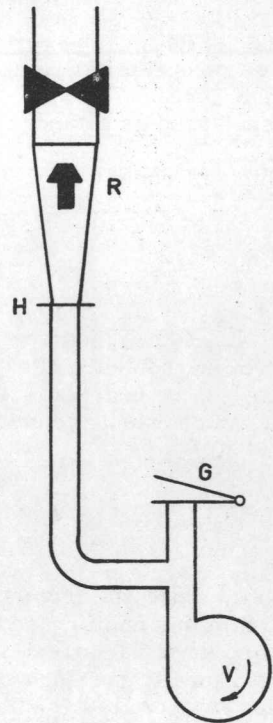


Fig. 6.11.1
The measuring circuit for high flow rates.

¹⁾This measuring circuit was build by J.de Groot.

The aperture on top of the rotameter can be varied to regulate the mean flow.

6.111 The ventilator.

The ventilator is equipped with an 1.2 Hp, 2800 rpm electric motor. Its rotor has 8 blades, which give some small high frequency fluctuations in the flow. Its pressure (3000 N/m^2) varies 15% when the flow rate changes from zero to $0.03 \text{ m}^3/\text{s}$.

6.112 The sine generator.

The design of a generator capable of generating sinusoidal pulsations was guided by trial and error. A satisfactory solution turned out to be the one indicated in fig. 6.112.1.

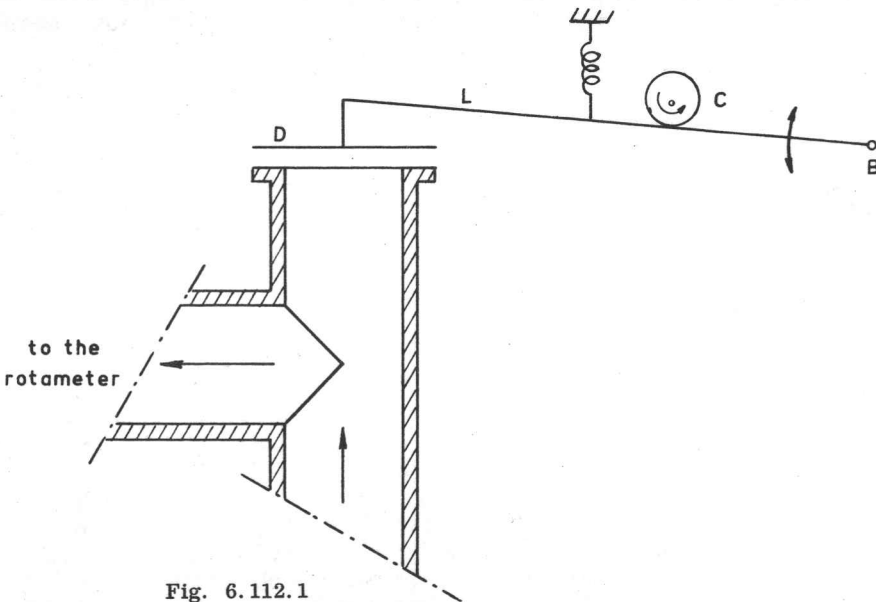


Fig. 6.112.1

The sine generator for high flow rates.

The lever L is moved around its bearing B by an eccentrically mounted cylinder C. The disc D, attached to lever L, periodically opens and closes the pipe end. The shaft of the cylinder C is driven by a small electric motor with a variator. The frequency can be varied from 0 - 11 c/s. The amplitude produced is approximately 25% of the maximum flow capacity of the rotameter. The waveform of the pulsation is shown in fig. 6.112.2.

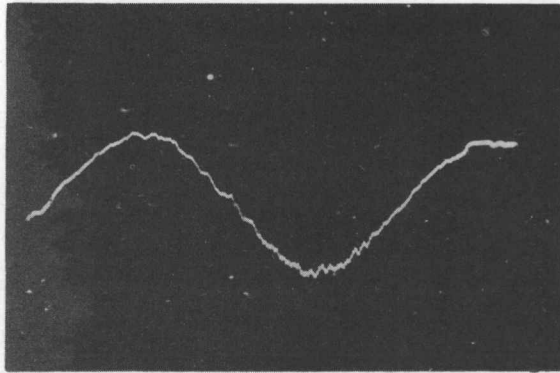


Fig. 6.112.2

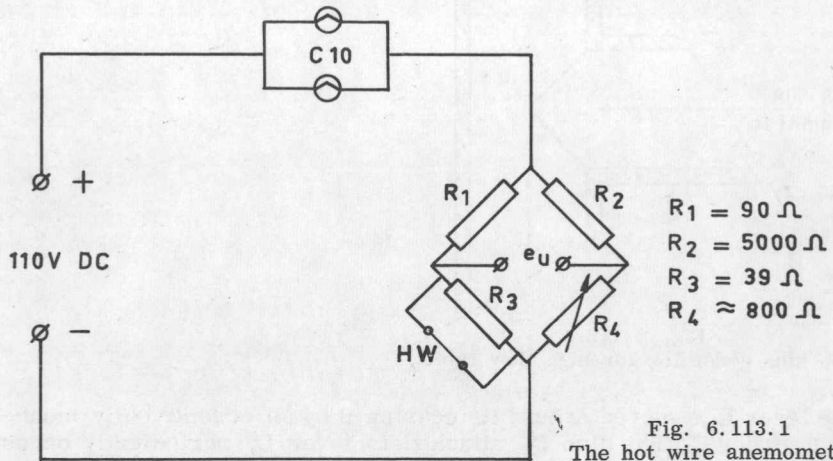
The flow pulsations as measured with the hot wire anemometer.

$$f = 0.25 \text{ c/s}, \quad \frac{w}{w_0} = 0.5.$$

6.113 The hot wire anemometer.

The hot wire is made of platinum + 10% iridium and has a diameter of $20 \mu\text{m}$ and a length of 5 cm. Its resistance at room temperature is 15Ω

The hot wire is mounted in a bridge circuit (fig. 6.113.1)



which has the advantage that by adjusting R_4 the level of the output voltage of the bridge can easily be varied. The bridge current is taken from a 110 V DC source which is fed to the bridge by two

current stabilizing tubes C 10. These tubes keep the current through the bridge almost constant at 408 mA. The resistance R_3 is used to make the current through the hot wire equal to the desired value of 260 mA. The resistors R_1 and R_3 are both immersed in petroleum to stabilize their temperatures.

To get some information about the drift of the system, the output voltage was measured during one hour while, the flow was constant. The output voltage varied 2 mV out of 362 mV which gives an error of about 0.5% of the maximum flow rate. This fluctuation is partly due to variations in the flow.

The response of the hot wire is measured by applying a step current to the hot wire. The current is made to step between 260 and 225 mA by connecting a resistor parallel to the hot wire. By observing the voltage over the bridge on an oscilloscope it can be seen that the hot wire behaves in first approximation as a first order system having a time constant of 0.017 s.

The output voltage is not linearly related to the flow. To be able to measure the mean flow the output voltage had to be linearized. This was performed by the circuit shown in fig. 6.113.2.

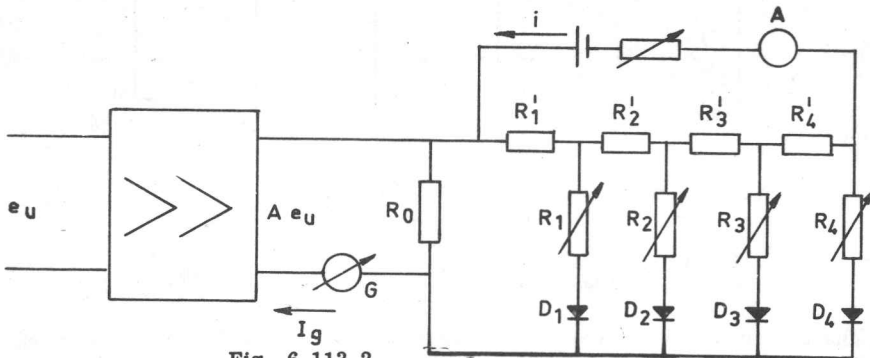


Fig. 6.113.2

The linearising circuit for the hot wire anemometer.

The output of the bridge, e_u , is first amplified by a DC amplifier of amplification A and then measured by a galvanometer G with a high series resistance R_0 .

The series resistance of the galvanometer is shunted by a diode network. When Ae_u is small, no diode is conducting. When Ae_u increases, first D_1 , then D_2 , etc., begin to conduct which means that the galvanometer current increases more rapidly. The resistances R_1, R_2, R_3, R_4 define together with the current i the voltages where the diodes D_1, D_2, D_3, D_4 start to conduct. The variable resistors R_1, R_2, R_3, R_4 can be varied to obtain the desired correction of the slope of the curve e_u vs. w .

The curves e_u vs. $\frac{w}{w_{max}}$ and I_g vs. $\frac{w}{w_{max}}$ are drawn in fig.

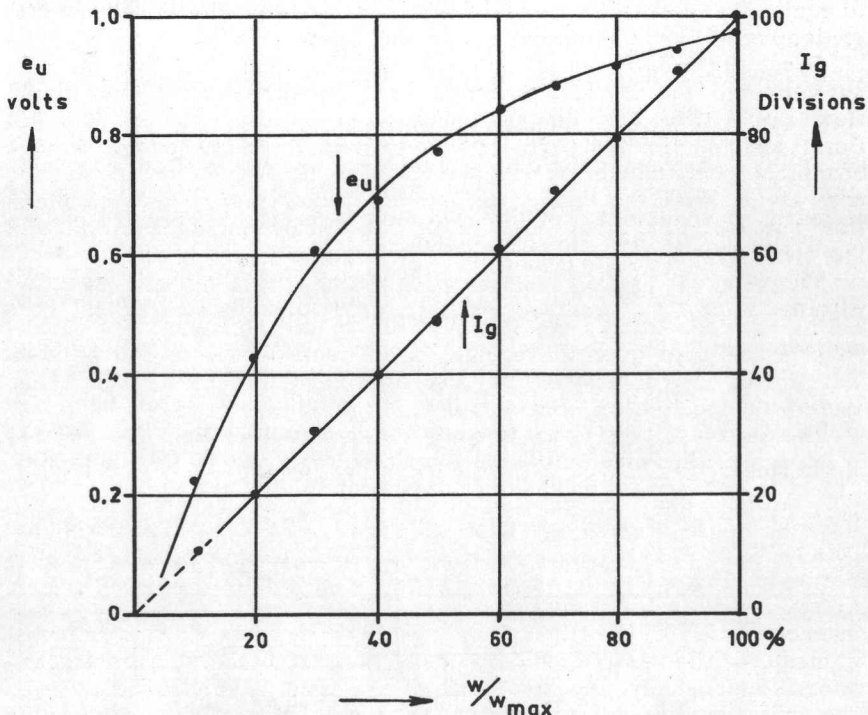


Fig. 6.113.3

The output e_u of the bridge circuit and the reading of the galvanometer I_g as functions of the flow rate w/w_{max} .

The rotameter was used as a reference to obtain the curves of fig. 6.113.3 (see sec. 6.114). With pulsating flow the galvanometer can be damped by attaching a large condenser in parallel to measure the mean flow.

The dynamic behaviour of the flow can be observed by replacing the galvanometer by a resistor and connecting an oscilloscope to this resistor.

6.114 The measuring procedure.

As a positive displacement meter to measure the large mean flow rates accurately was not at our disposal, the rotameter itself served as a standard. The rotameter is a Fischer & Porter B 9-27-10 equipped with a float BSX 944.

A special lightweight float is used for most measurements in the rotameter to prevent the flow from being determined by the float instead of by the generator G. With a heavy float the pulsations tend

to excite the float in its natural frequency, and the flow is then partly determined by the movement of the float.

First, the rotameter is equipped with the light float and the output voltage of the hot wire anemometer is measured at the maximum flow rate. Then the float is substituted by the original BSX 944 float, and the flow is varied so as to give the same output voltage of the hot wire anemometer as before. The reading of the rotameter now gives, with the data given by the manufacturer, the maximum flow rate with the light float. With this measurement the value of the coefficient $\sqrt{g_2}$ (eq. 2.22.5) is determined.

The rotameter which is, according to the specifications, accurate within 2% of its maximum scale serves to calibrate the hot wire anemometer. At $\frac{w}{w_{\max}} = 0.1$ the galvanometer is made to indicate

10 divisions of its scale by adjusting the resistance R_4 of the bridge of fig. 6.113.1. Then subsequently the resistances R_1, R_2, R_3, R_4 of the linearizing circuit are adjusted at values of $\frac{w}{w_{\max}} = 0.2; 0.4;$

0.6 and 0.8 to give meter readings of 20, 40, 60 and 80 divisions. This calibration is regularly checked. The linearity of the galvanometer reading as a function of the flow rate indicated by the rotameter, is within 1% of the full scale. When measuring the amplitude characteristic of the light float the desired mean flow is adjusted by means of the restriction on top of the rotameter. The sine generator is started and the amplitude of the float is measured by eye. The galvanometer is substituted by a resistance of the same value and the voltage across this resistance is displayed on a Tektronix oscilloscope, type 543; plug in unit E. From the displayed picture the amplitude of the flow pulsations is measured.

With this circuit no phase measurements were made.

The error in the mean value is measured in the following way: With pulsating flow the restriction on top of the rotameter is varied to make the float pulsate around a certain mean value.

The galvanometer is damped by a large capacitance, and the mean galvanometer reading is noted. Immediately after this measurement a measurement with stationary flow is performed. The flow is adjusted to make the galvanometer indicate the same value as with pulsating flow. From these two measurements the value of M is computed.

The accuracy of the amplitude measurements of the float is about 0.5% of full scale. The accuracy of the amplitude measurements of the flow is about 5%. For the measurement of the mean value of the float position the accuracy is dependent on the amplitude of the float motion. For small amplitudes it is about 0.5% of the full scale, for large amplitudes about 1%. As the amplitude of the pulsations is 25% of the maximum flow, a maximum possible error in M of about 0.2 to 0.4 can occur.

6.12 The measuring circuit ¹⁾ for low flow rates.

The circuit is shown in fig. 6.12.1.

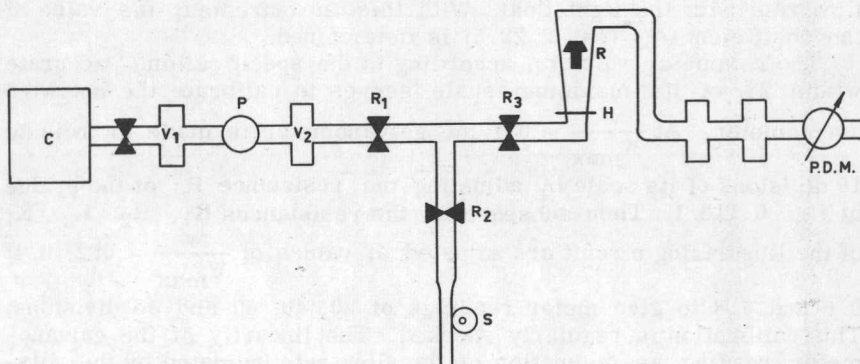


Fig. 6.12.1
The measuring circuit for low flow rates.

The compressor C is connected to a volume V_1 . A pressure controller P keeps the pressure in the volume V_2 at a constant value. A very high restriction R_1 maintains the flow into the rest of the circuit constant. The resistances R_2 and R_3 are small compared with R_1 but large compared with the impedance of the rotameter and following equipment. The flow is divided in two branches. One branch leads to the rotameter; the other to the sine generator S , which is in fact a restriction with a sinusoidal varying resistance. By adjusting R_2 and R_3 the division of the flow over the two branches and the amplitude of the flow pulsations in the rotameter can be adjusted.

The mean flow is measured by a positive displacement meter of the wet gasmeter type. Between the rotameter and the gasmeter two vessels of about 2.5 dm^3 each are inserted to give some damping of the pulsations.

The amplitude and phase of the pulsations are measured with a hot wire anemometer H .

¹⁾ The measuring circuit was build by F. Koopmans who also made the measurements.

6.121 The sine generator.

The sine generator consists of a piece of rubber tube with some foam plastic inserted in it.

It is shown schematically in fig. 6.121.1.

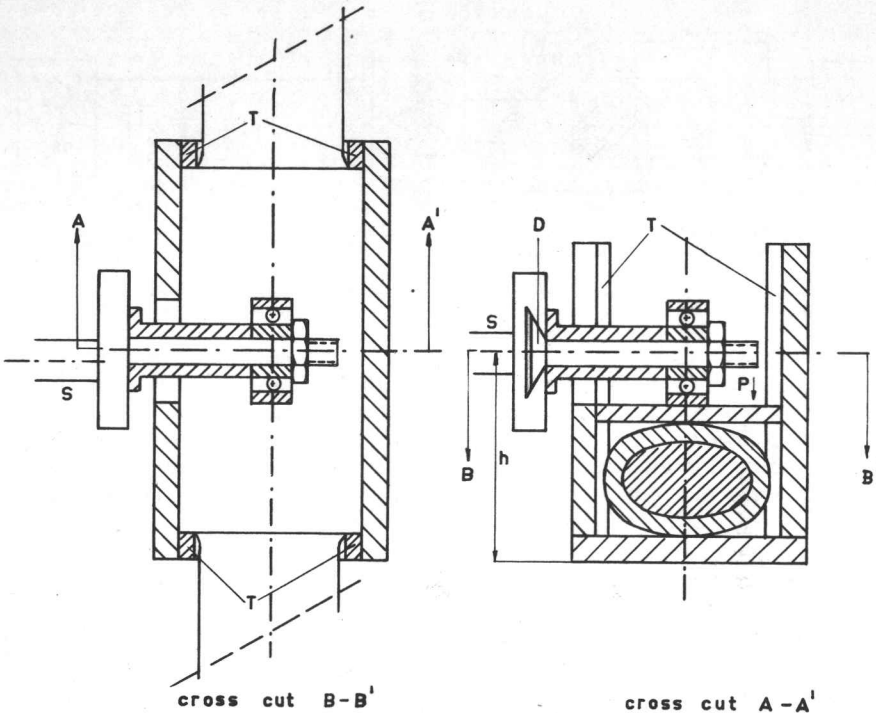


Fig. 6.121.1
The sine generator for low flow rates.

A ball bearing is eccentrically attached to the shaft *S*, which rotates when driven by a motor and gearbox. The eccentricity of the ball bearing can be altered by adjusting a dove tail mechanism *D*. The ball bearing pushes the plate *P* downward and thus pinches the rubber tube. The plate *P* is prevented from being displaced in the direction of the tube by the four small beams *T*. When the restriction is varied, a pulsating flow is obtained. The mean resistance can be varied by altering the distance *h* in fig. 6.121.1. With this

generator and the circuit of fig. 6.12.1 it is possible to obtain sinusoidal pulsations from 0.7 - 40 c/s without appreciable change in amplitude.

6.122 The hot wire anemometer ¹⁾.

The hot wire is inserted in a Wheatstone bridge which is fed by an oscillator with a frequency of 10 kc/s. The output voltage is amplified and detected. The detected signal is displayed on an oscilloscope.

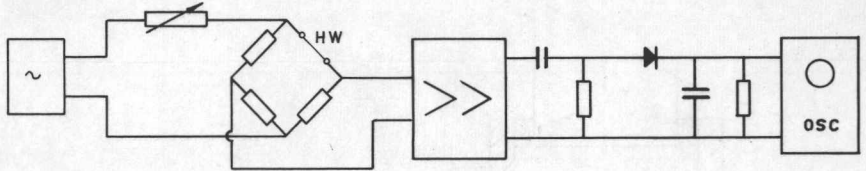


Fig. 6.122.1
The circuit used for the hot wire anemometer.

Because the mean flow for these flow rates is measured with a positive displacement meter, the hot wire anemometer is only used to measure the amplitude and phase of the pulsations. The length of the hot wire is 10 mm, its diameter $7 \mu\text{m}$ and its cold resistance is 14Ω . The heating current of the wire is 70 mA. The frequency response of the hot wire is measured with the circuit of fig. 6.122.2. The heater current is supplied to the bridge from a DC source.

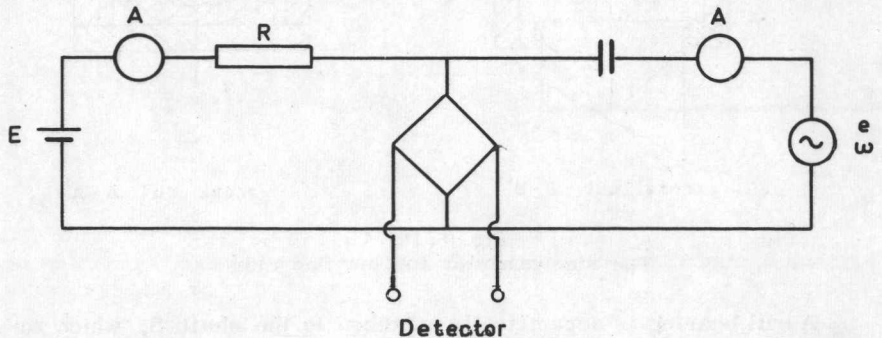


Fig. 6.122.2
Circuit for measuring the frequency response of the hot wire.

¹⁾ The hot wire anemometer used for the low flow rates is different from the one used for high flow rates. Both circuits were developed simultaneously, so both were used.

The resistance R in fig. 6.122.2 is large in comparison with the bridge resistance. A small AC current of 2mA is also fed to the bridge. Observing the output of the detector as a function of the frequency of the AC current, the amplitude response of the hot wire is found. The measured amplitude characteristic is drawn in fig. 6.122.3, from which a time constant of $2.7 \text{ ms} \pm 0.2 \text{ ms}$ follows. As the hot wire acts very closely as a first order system, the phase characteristic can be deduced from the measured time constant.

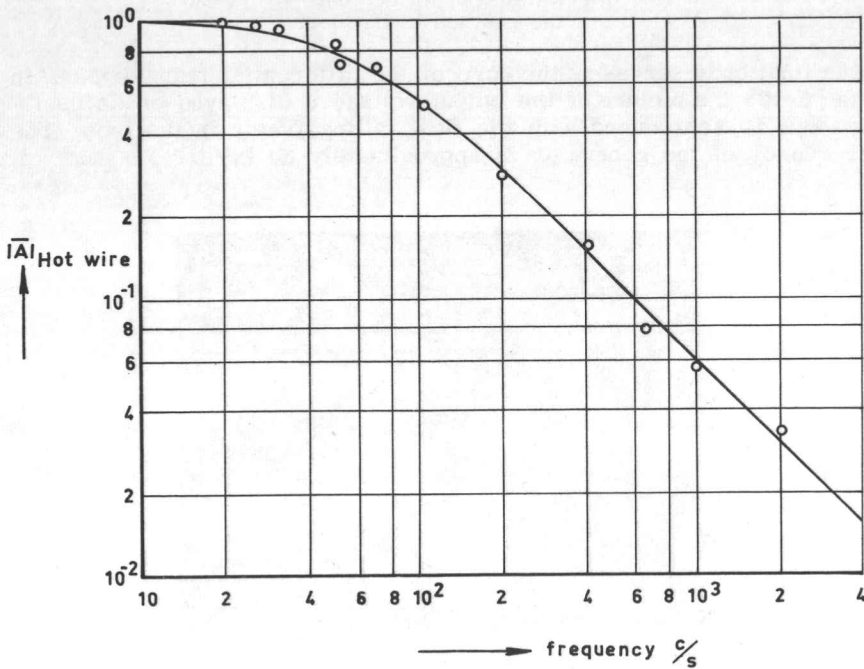


Fig. 6.122.3
The amplitude characteristic of the hot wire.

6.123 Measurement of the float movement.

The float movement is measured by eye for large amplitudes and with the aid of a differential transformer for small amplitudes. The differential transformer is also used to measure the phase of the float for all amplitudes. The differential transformer consists of one primary and two secondary windings, ratio 2 : 1 : 1, wound on a body which fits close over the tube of the rotameter. The length of each secondary is equal to the float length and the length of the primary is twice the float length (fig. 6.123.1).

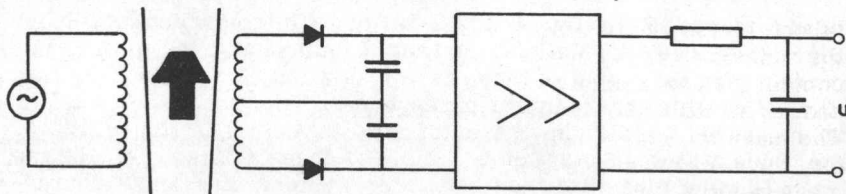


Fig. 6.123.1
The differential transformer used to measure the position of the float.

The float body serves as the core of the differential transformer. In fig. 6.123.2 a picture of the output voltage u displayed on an oscilloscope is reproduced with the float falling freely in the tube. The frequency of the generator is approximately 30 kc/s.

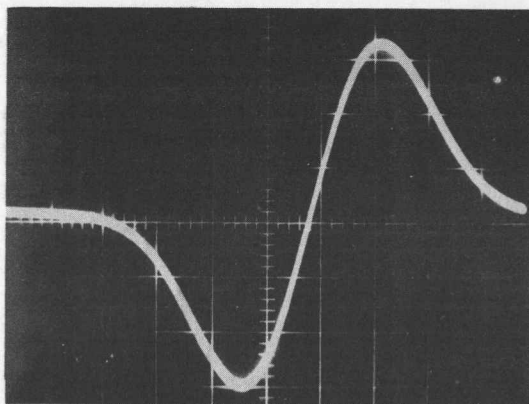


Fig. 6.123.2
The output voltage of the float position indicator with the float falling freely in the tube.

The numbers of turns are: primary 300, secondary 2×150 .

When the float amplitudes are less than half the float length, the characteristic of the instrument is linear. The instrument can then be used to measure the mean position of the float by measuring the output voltage with a damped voltmeter.

6.124 The positive displacement meter.

This wet gasmeter serves to measure the mean flow. Its sensitivity is one revolution for 1.00 dm^3 air. At the lowest frequencies

(about 1 c/s) one chamber receives about 2 pulsations. As long as the waterlevel in the instrument does not vary, every chamber will contain the same amount of gas. The waterlevel could be observed, and even with the lowest frequencies no change in it was noticed. The mean flow is measured by measuring the time interval necessary for three revolutions with a stopwatch. The repeatability of this measurement is $\frac{1}{2}\%$.

6.125 The measuring procedure.

The rotameter, Fischer & Porter B 2-18-127/70, is calibrated for stationary flow with the aid of the positive displacement meter. The output of the differential transformer, which is used for measuring the position of the float, is also calibrated with this meter; and so the relation between this quantity and the rotameter reading is established.

Most points of the amplitude characteristic are measured from pictures made from the screen of a double beam oscilloscope displaying both the signals of the differential transformer and the hot wire anemometer. The phase characteristic is also measured from these pictures. For large amplitudes the differential transformer is removed and the float amplitude is measured by eye.

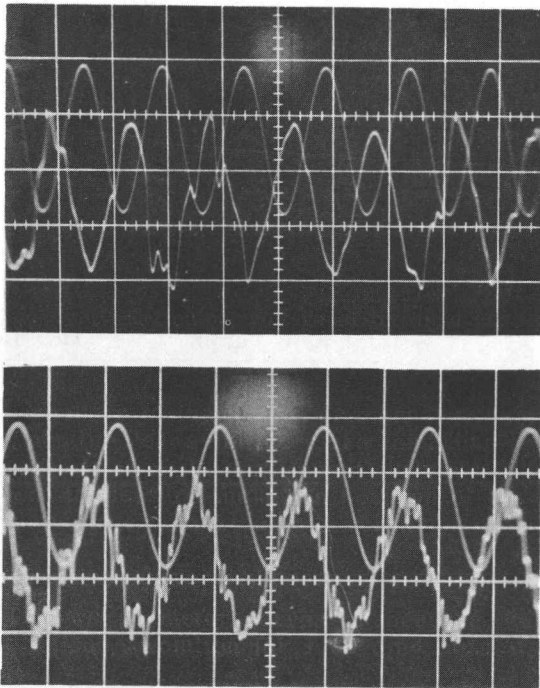


Fig. 6.125.1

The float position (upper trace) and the flow (lower trace) measured at $f = 20$ c/s (a) and $f = 2.8$ c/s (b).

Most points of the amplitude characteristic are measured from pictures made from the screen of a double beam oscilloscope displaying both the signals of the differential transformer and the hot wire anemometer. The phase characteristic is also measured from these pictures. For large amplitudes the differential transformer is removed and the float amplitude is measured by eye.

Some pictures are reproduced in fig. 6.125.1. As can be seen from these pictures, fluctuations due to turbulence make the interpretation of the pictures difficult. Three pictures are taken for each measurement. From these three pictures about ten values for amplitude and phase are obtained. The spread in the phase measurements is about 10° . For high frequencies a systematic error is introduced by the uncertainty in the correction made for the frequency response of the hot wire which is equal to $+2^\circ$ at 20c/s. The accuracy of the phase measurements is influenced by distortion of the flow pulsations and the noise due to turbulence. The spread in the measured points of the amplitude characteristic is about 10%, the accuracy is also influenced by distortion and noise. The influence of noise is largest for high frequencies.

The mean value of the float position, measured by eye for the large amplitudes and with the differential transformer for small amplitudes, is compared with the result of the measurement made with the wet gasmeter. The accuracy of this measurement is about 0.5 mm which results in a possible error of about 1 in M for a mean float position of 6 cm and $\frac{\bar{w}}{w_0} = 12\%$.

6.2 TUBES AND FLOATS.

Measurements are carried out with several tubes and floats. All tubes were commercially available types of Fischer & Porter. The floats are made at the workshop to satisfy the conditions imposed on the floats by the measuring circuits.

The principal combinations used are mentioned in table 6.2.1.

	I (high flow rates)	II (low flow rates)	
tube	B 9 - 27 - 10	B 2 - 18 - 127/70	
scale length of tube	0.25	0.125	m
mass of float	$37.8 \cdot 10^{-3}$	$1.2 \cdot 10^{-3}$	kg
area of float	$20.7 \cdot 10^{-4}$	$0.33 \cdot 10^{-4}$	m ²

Table 6.2.1

The tubes and floats used for the experiments.

Float I is made of aluminium to obtain a light float and has a very slender body which reduces the factor e_2 to a neglectible quantity.

Float II is made of steel to be able to use it as the core of a differential transformer. The coefficients of the differential equation are listed in table 6.2.2.

float-tube combination	I	II
c_0	$0.41 \cdot 10^{-2}$	$0.66 \cdot 10^{-4} \text{ m}^2$
c_1	$1.0 \cdot 10^{-2}$	$0.22 \cdot 10^{-3} \text{ m}$
d_0	$4.4 \cdot 10^{-6}$	$0.11 \cdot 10^{-8} \text{ m}^4$
d_1	$2.1 \cdot 10^{-5}$	$0.72 \cdot 10^{-8} \text{ m}^3$
d_2	$2.5 \cdot 10^{-5}$	$0.12 \cdot 10^{-8} \text{ m}^2$
e_1	$0.5 \cdot 10^{-4}$	$0.3 \cdot 10^{-6} \text{ m}^2$
e_2	-----	$0.4 \cdot 10^{-6} \text{ m}$
f_1	$0.1 \cdot 10^{-7}$	$0.1 \cdot 10^{-11} \text{ m}^4$
f_2	$0.32 \cdot 10^{-3}$	$0.37 \cdot 10^{-6} \text{ m}^3$
g_2	$0.31 \cdot 10^{-2}$	$0.36 \cdot 10^{-5} \text{ m}^4/\text{s}^2$

Table 6.2.2
The coefficients of the differential equation.

The values of s and t can be computed from this table, but it is easier to compute these parameter in another way.

From eq. (3.1.7) it is found that

$$\left. \begin{aligned}
 t &= \frac{f_1 + f_2 x_0}{\sqrt{2g_2}} \approx \frac{f_2 x_0}{2g_2} \\
 s &= \frac{c_0 + c_1 x_0}{2 \sqrt{g_2}}
 \end{aligned} \right\} \quad (6.2.1)$$

by neglecting f_1 . Substituting eq. (2.22.5) in eq. (6.2.1)

$$\left. \begin{aligned}
 t &= \frac{x_0}{2g} = t_1 x_0 \\
 s &= \frac{a_0 + a_x}{\sqrt{g_2}} = s_0 + s_1 x_0,
 \end{aligned} \right\} \quad (6.2.2)$$

is found.

With (6.2.2) the coefficients of s can be easily computed from float and tube area and the measured value of $\sqrt{g_2}$, whereas t is independent from the dimensions of the rotameter.

The values of s and t computed from eq. (6.2.2) are listed in table 6.2.3.

rotameter	I	II
s_0	$3.7 \cdot 10^{-2}$	$1.7 \cdot 10^{-2} \text{ s}$
s_1	$9.0 \cdot 10^{-2}$	$5.7 \cdot 10^{-2} \text{ s/m}$
t_1	$5.1 \cdot 10^{-2}$	$5.1 \cdot 10^{-2} \text{ s}^2/\text{m}$

Table 6.2.3
The coefficients of s and t for the rotameters.

6.3 AMPLITUDE AND PHASE MEASUREMENTS.

In fig. 6.3.1 the measured amplitude characteristic for the float-tube combination I is reproduced. The dotted line indicates the amplitude characteristic computed with eq. (5.21.5) and the values of s and t from table 6.2.3 with $x_0 = 17 \text{ cm}$. The computed values of Q and f_0 , which are 1.8 and 1.7 c/s respectively, differ somewhat from the measured values $Q = 1.3$ and $f_0 = 1.6 \text{ c/s}$. The amplitude of the pulsations is 25% of the maximum capacity of the rotameter.

The measured amplitude characteristic of II is reproduced in fig. 6.3.2.

In this case the measured value of Q is 4.2 and the computed value is 2.8. The measured and computed value of f_0 are both $f_0 = 2.8 \text{ c/s}$. The mean float position for this measurement is 6.35 cm and the amplitudes of pulsation $\frac{\bar{w}}{w_0}$ range from 10% at the resonant frequency of the float to 70% at high frequencies. The measured phase characteristic of II is indicated in fig. 6.3.3.

For the last rotameter the agreement of theory and measurements is not so good, especially for high frequencies. The discrepancy in the amplitude characteristic cannot be accounted for by the neglect of q in eq. (3.1.7). Assumption of a value of q so as to make the curves of fig. 6.3.3 fit close, leads to an unreasonable large value of q . The tendency of the float to "stick" indicates a large influence of the wall friction. It is, however, also very unlikely that this effect is responsible for the observed differences between measured and calculated values, because friction tends to give larger phase shifts. The measurements agree at least fairly good up to the resonant frequency and the computed value of the resonant frequency almost coincides with the measured value.

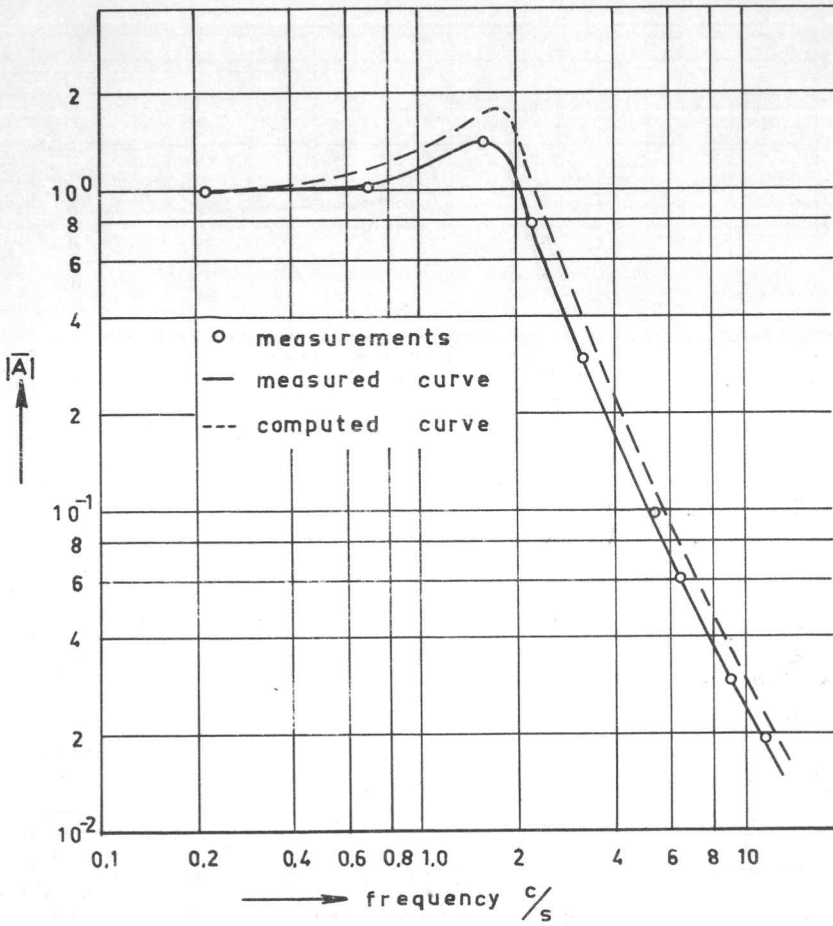


Fig. 6.3.1
 The amplitude characteristic of rotameter I.
 ($x_0 = 17$ cm)

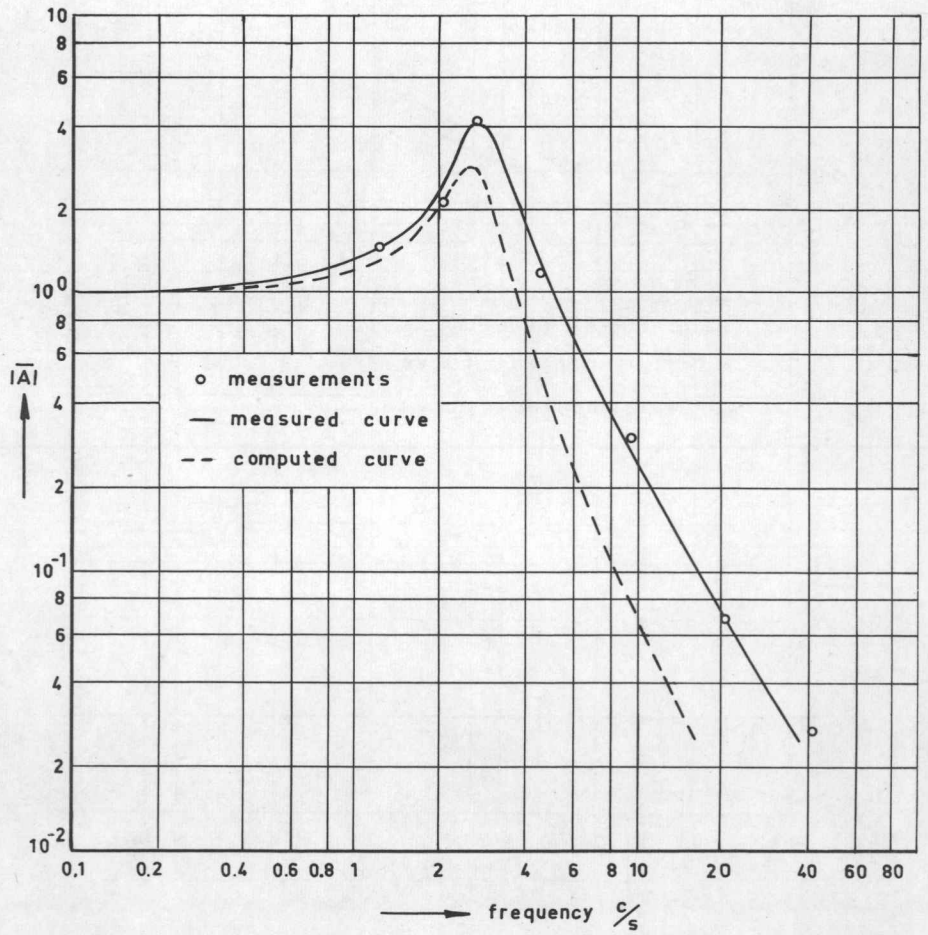


Fig. 6.3.2
 The amplitude characteristic of rotameter II.
 ($x_0 = 6.35$ cm)

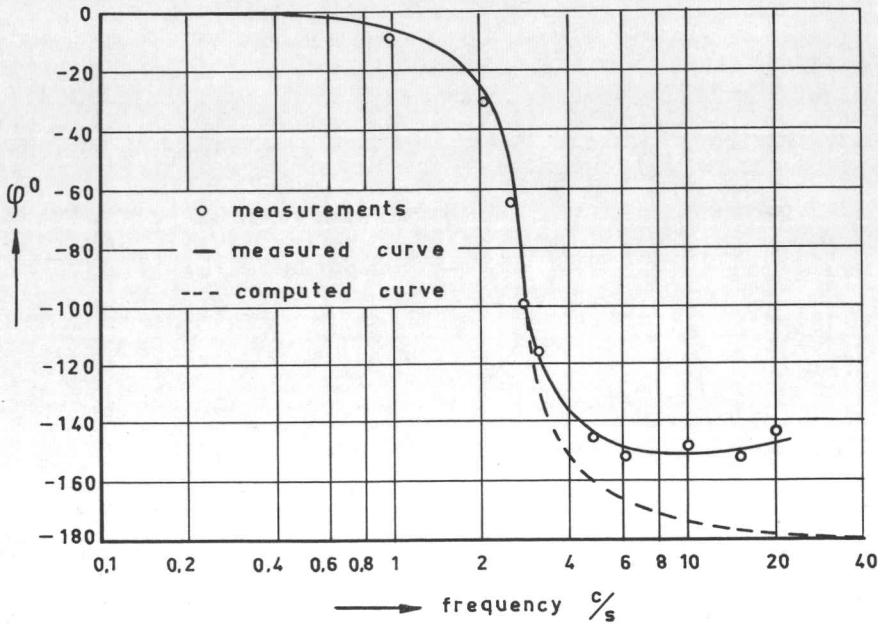


Fig. 6.3.3
The phase characteristic of rotameter II.
($x_0 = 6.35$ cm)

6.4 THE ERROR IN THE INDICATED MEAN VALUE.

For the float-tube combination mentioned in sec. 6.2 the error of the indicated mean value is measured as a function of frequency. The deviation of the mean value M (eq. 3.1.12) is computed from these measurements. The measured values of M together with a line indicating the computed value of M are reproduced in fig. 6.4.1 and 6.4.2. The theoretical value of M is computed from eq. (5.21.4). The values of s and t in this equation are derived from the measured values of Q and f_0 .

The theoretically derived curve, and the measurements agree fairly good. Especially the behaviour in the neighbourhood of the resonant frequency is very closely predicted. For high frequencies the spread in the measurements is relatively large. The theoretical value of $\frac{1}{2}$ for M at high frequencies is reasonably well assumed, when taking into account the possible error of 0.2 to 0.4 for I and 1 for II in M .

Fig. 6.4.1
The value of M as a function of frequency for rotameter I.

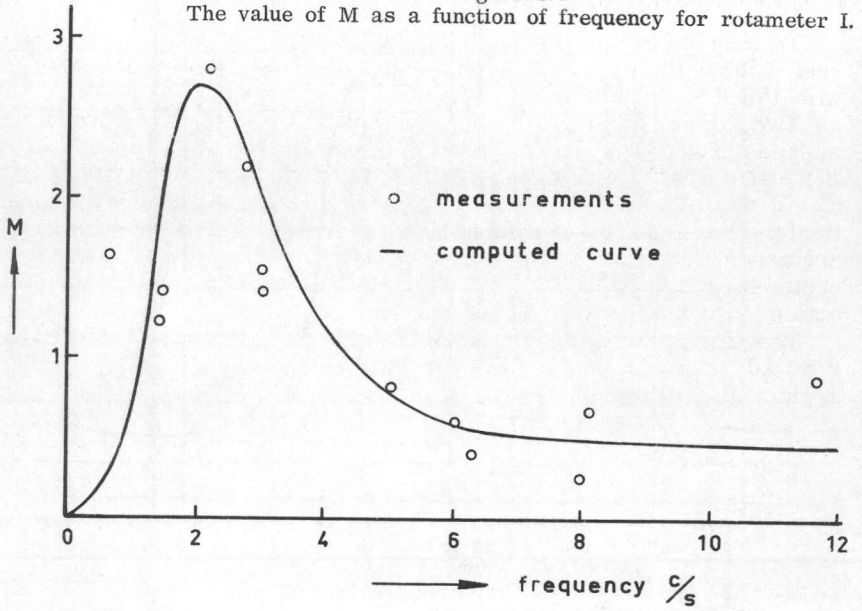
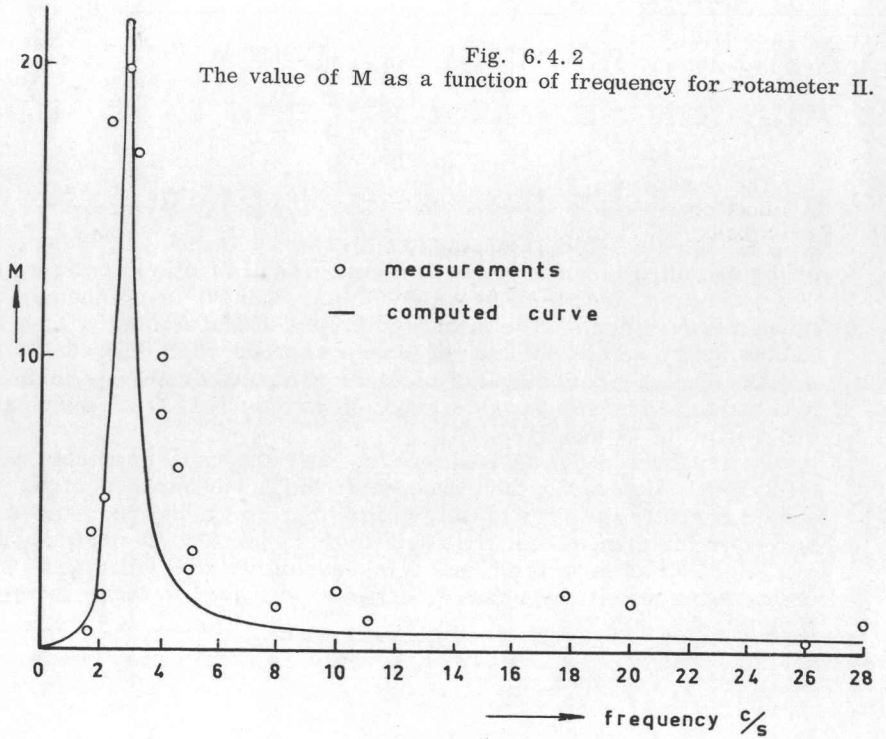


Fig. 6.4.2
The value of M as a function of frequency for rotameter II.



6.5 MEASUREMENTS ABOUT BOUNCING.

To investigate if, and how far the theory which is developed in sec. 5.22 holds for practical rotameters, some tests are performed with three tubes and several floats.

Two of the tubes of the beaded glass type with three beads are manufactured by Fischer & Porter. The following types are used: B 1 - 14 - 250/70 with $a_0 = 24.5 \cdot 10^{-6} \text{ m}^2$ and B 3 - 27 - 10/70 with $a_0 = 0.69 \cdot 10^{-4} \text{ m}^2$. The floats used with these tubes are schematically drawn in fig. 6.5.1. As can be seen from this figure the floats are assembled from three different parts. The head and tail are connected by a bolt. One or both of the body parts may be inserted to obtain different float weights.

The third tube is manufactured by Rota, type 32978/54 with $a_0 = 2.80 \cdot 10^{-4} \text{ m}^2$. It is, in contrast with the Fischer & Porter tubes, a plain glass tube. A float is drawn in fig. 6.5.2.

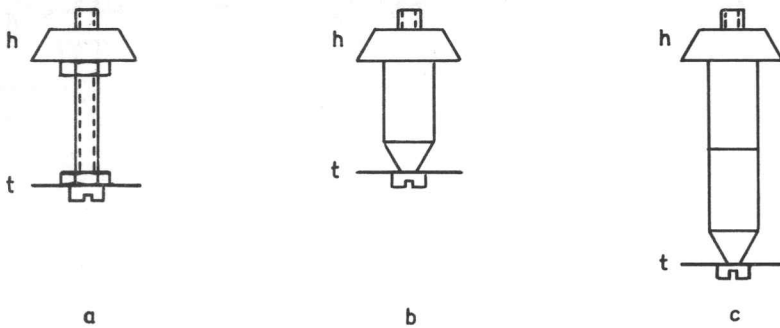


Fig. 6.5.1

The construction of the floats for the bouncing experiments. The float consists of the head *h* and the tail *t* which are connected by a bolt (fig. a). One (fig. b) or two (fig. c) body pieces may be inserted to obtain different float weights.

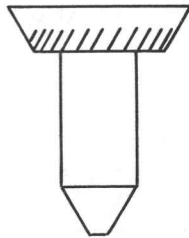


Fig. 6.5.2
The float for the tube manufactured by Rota.

The test circuit is shown in fig. 6.5.3. The flow is conducted to a vessel with volume V by a restriction S . The effective volume of the vessel can be varied by filling the vessel to different levels. The rotameter R is connected to the volume V by mounting it directly on the cork of the vessel.

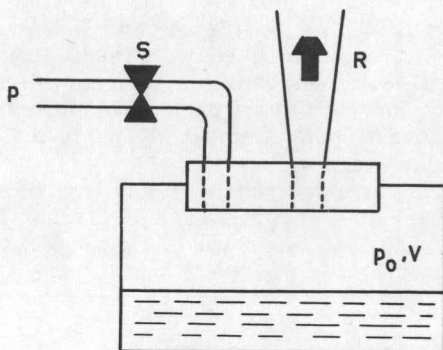


Fig. 6.5.3
The measuring circuit for the bouncing experiments.

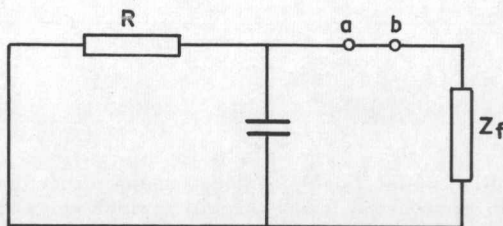


Fig. 6.5.4
The electrical analogue of the circuit of fig. 6.5.3.

The electrical analogue of the circuit is drawn in figure 6.5.4. In this circuit R is the resistance of the restriction S , C the capacity of the volume V , and Z_f the impedance of the float. The capacitance of the rotameter tube is neglected.

Investigating the stability of the float in the way mentioned in sec. 5.23, the impedance between the points a and b of fig. 6.5.4 is computed. The resistance R is very high ($p - p_0 \approx 10^5 \text{ N/m}^2$ for maximum flow), so its influence can be neglected.

With eq. (5.23.2), considering a float without external damping, it is found that

$$Z_{ab} = \frac{b_0 + b_1 j \omega + b_2 (j \omega)^2 + b_2' C (j \omega)^3}{\left\{ b_0 + b_1 j \omega + b_2 (j \omega)^2 \right\} j \omega C} \quad (6.5.1)$$

The stability of the system can now be investigated by considering the Hurwitz conditions for

$$P_1(j \omega) = b_0 + b_1 j \omega + b_2 (j \omega)^2 + b_2' C (j \omega)^3 \quad (6.5.2)$$

$$\text{The conditions } b_0; b_1; b_2' C \geq 0 \quad (6.5.3)$$

$$\text{and } b_1 b_2 - b_0 b_2' C > 0 \quad (6.5.4)$$

have to be fulfilled for stability.

The condition (6.5.3) is fulfilled for every rotameter. For the condition (6.5.4) can be written, substituting eq. (5.22.5) and (5.22.7)

$$H = \frac{kp a_0 (a_0 + a_x) x_0}{2 g \rho_{fl} V_{fl} V} > 1 \quad (6.5.5)$$

$$\text{from which } \overset{\text{kleine } x}{X_0 \text{ critical}} = \overset{\text{kleine } x}{X_b} = \frac{2 g \rho_{fl} V_{fl} V}{kp a_0 (a_0 + a_x)} \quad (6.5.6)$$

The term on the left of eq. (6.5.5) is the stability governing factor, which will for brevity be designated as H.

The measurement is performed in the following way: The vessel V is filled to a certain level and the pressure p is adjusted to give maximum flow through the rotameter. Now the pressure upstream of the restriction is diminished, and so the float lowers. At a certain float position the float will start bouncing according to the theory. It turns out, however, that when using the Fischer & Porter beaded glass tubes, it is possible to make the float take every position without bouncing. This occurs when the pressure is diminished very slowly and care is taken that the float lowers gradually. If, however, a disturbance is introduced the float will start to bounce if in a favourable position.

To measure the highest value of x where bouncing is possible, a disturbance is introduced by temporarily lowering the float a few millimeters. This is done by slightly applying a fingertip to the end of the rotameter tube. Several situations may occur. When the float remains in the region where the damping is always positive the float will return to its initial position. If the float reaches the region where negative damping occurs, two actions may result. The net damping in a complete cycle can be negative or zero and bouncing will be started, or the net damping in this cycle is positive and the float will return to its initial position. In some experiments, especially if boun-

cing only occurred at low float positions, it was obvious that the float had to come down to a certain value to initiate bouncing. For the high positions however, a range of values could be found depending on the magnitude of the applied disturbance. For large disturbances higher values of the critical value of x are measured.

To get repeatable measurements the disturbance has to be specified. The measurements mentioned in this chapter are made with two disturbances, one which lowers the float 3mm, and the other which lowers the float 10 mm. For every disturbance two series of measurements are made. The total number of measurements at one point thus becomes four. The maximum difference between several measurements depends on the float position and ranges from 4 cm at float positions of about 15 cm to 0.5 cm at float positions of 1.5 cm. The spread in the values of H found in this way is about 0.1. The exact vertical position of the tube was found to be very important.

As an example three series of measurements are reproduced in table 6.5.1. The series I is made with disturbances of 3 mm, and the series II and III with disturbances of 10 mm. The float is indicated in fig. 6.5.1 b. For the I and II series it is used with the head in the indicated (BSVT) position. Series III is measured with the float head in the reversed (NSVT) position. As can be seen from table 6.5.1 the reversal of the float head does not seem to have a significant influence on H .

	Volume V	0.25	0.75	1.75	2.75	3.75	4.75	10^{-3} m^3
I	x_b	stable	2.0	6.0	7.2	11	11	10^{-2} m
	H		0.3	0.4	0.3	0.35	0.3	
II	x_b	stable	2.2	6.8	9.0	13	15.5	10^{-2} m
	H		0.3	0.45	0.4	0.45	0.45	
III	x_b	stable	3.0	8.2	11	11.5	14	10^{-2} m
	H		0.45	0.5	0.5	0.4	0.4	

Table 6.5.1

Measurement of the critical float position x_b (averaging over two measurements) and the stability factor H at different values of the upstream volume V . Tube B 3-27-10/70; float mass $3.25 \cdot 10^{-3}$ kg; float indicated in fig. 6.5.1 b.

I disturbance 3 mm, float head normal.

II disturbance 10 mm, float head normal.

III disturbance 10 mm, float head reversed.

The results of the measurements are listed in table 6.5.2.

tube	m (10^{-3} kg)	Volume V	0.25	0.75	1.75	2.75	3.75	4.75	10^{-3} m ³
B1 - 14 - 250/70	0.85	x_b calc	5	13	27	39	50	55	10^{-2} m
		x_b meas	stable	2	9	12	15	17	10^{-2} m
		H	-----	0.15	0.3	0.25	0.25	0.2	
	1.92	x_b calc	10	26	50	70	85	100	10^{-2} m
		x_b meas	stable	7	14	>25	>25	25	10^{-2} m
		H	-----	0.2	0.2	--	--	---	
	3.10	x_b calc	14	37	70	95	115	135	10^{-2} m
		x_b meas	2	11	22	>25	>25	25	10^{-2} m
		H	0.1	0.25	0.25	--	---	---	
B3 - 27 - 10/70	2.15	x_b calc	1.55	4.5	9	14	17	20	10^{-2} m
		x_b meas	stable	1	4	7	9	10	10^{-2} m
		H	-----	0.25	0.45	0.45	0.35	0.4	
	3.25	x_b calc	2.5	6	13	18	23	26	10^{-2} m
		x_b meas	stable	2	7	8	12	13	10^{-2} m
		H	-----	0.35	0.45	0.4	0.45	0.45	
	4.65	x_b calc	3.5	10	17	24	30	36	10^{-2} m
		x_b meas	stable	4	9	13	14	17	10^{-2} m
		H	-----	0.35	0.45	0.45	0.4	0.4	

Table 6.5.2

The float position x_b , where the float becomes unstable (measured and calculated values) and the stability factor H for several float masses and two different tubes.

By inspection of table 6.5.2 it can be seen that the stability factor H which is measured is always lower than the theoretical value which is equal to one. This is the result of the fact that the friction with the walls has been neglected in the theory. Furthermore the theory is only a rough approximation of the actual process.

The B 1 tube gives lower values of H than the B 3 tube which is probably a result of the fact that the float in the B 1 tube has a tendency to stick, which indicates a larger influence of the wall friction.

To verify whether the difference between the theoretical value and the measured value of x_b can be attributed to the wall friction some measurements are performed with a plain glass tube. With such a rotameter the wall friction will be smaller than with the beaded glass tubes. In the plain tube the float can only make contact with the wall at one point, whereas the float in a beaded tube can make contact with the three beads at more points, which increases the tendency to stick.

The measurements are carried out with the same test set up as mentioned before. It turns out that in contrast with the experiments already mentioned, no metastable positions of the float are found. The measurements are made with three different float weights.

At float positions somewhat above the critical value, the quality factor of the system is very high and noise due to turbulence makes the float behave unsteadily. This is particularly true at large values of x_b . As a result an accuracy of about 0.5 cm can be attained.

From eq. (6.5.6.) it is found that

$$x_{0 \text{ critical}} = x_b = \frac{2g \rho_{fl} V_{fl} V}{k_p a_o (a_o + a_x)}$$

Neglecting a_x in comparison with a_o , eq. (6.5.6) leads to

$$x_b = \frac{2g \rho_{fl} V_{fl} V}{k_p a_o^2} \quad (6.5.7)$$

The measured and calculated values of x_b are given in fig. 6.5.5. The solid line indicates the theoretical curve. The measured values are always lower than those calculated. This is partly due to the fact that at $x = 0$ the diameter of the tube is somewhat larger than the diameter of the float head. It turns out that the actual value of x where the diameter of the float is equal to the diameter of the tube is at $x = -1.1$ cm. The theoretical curve corrected for the zero shift is shown as a dotted line. This curve follows more closely the measurements but is perhaps a little too high. This last difference can at least partly be attributed to the wall friction.

6.6 CONCLUSION.

From the afore mentioned experiments it can be concluded that the theory which is developed in sec. 5 explains the behaviour of the float fairly good as far as its response and the error in the mean value are concerned.

The measurements about float bouncing show a very good agreement with the theory when the influence of the wall friction is negligible.

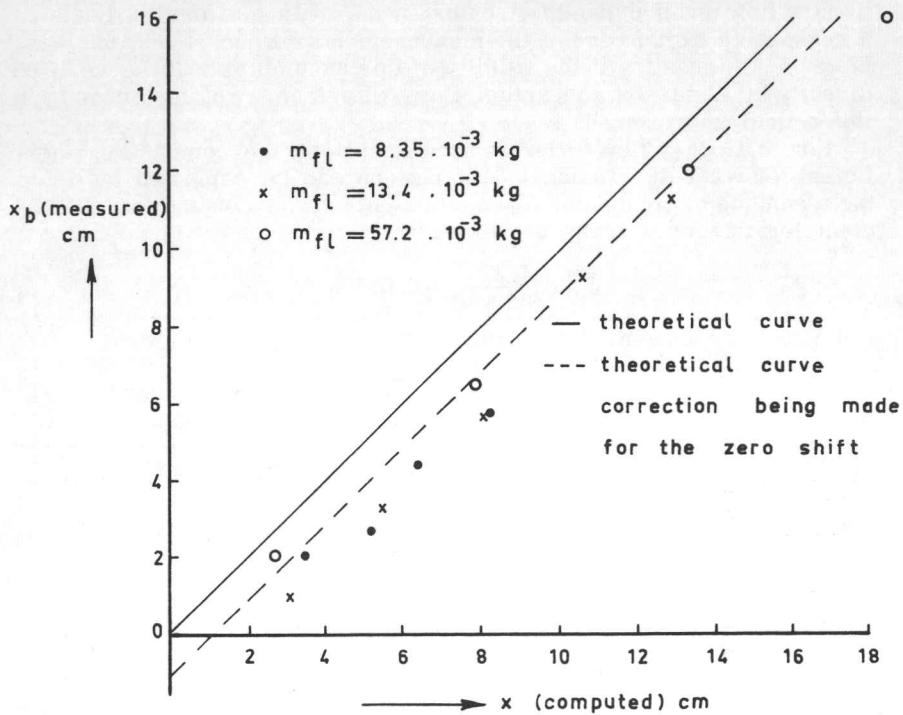


Fig. 6.5.5
 Measured and calculated values of the float position where the float becomes unstable for several float masses.

7. THE FLOW PATTERN IN A ROTAMETER.

7.1 THE CONTRACTION COEFFICIENT.

The contraction coefficient used in the equation of motion for the float is assumed to be constant and equal to the one used for stationary flow under dynamic circumstances. This assumption leads to a reasonable explanation of the measurements of sec. 4 and 6. It is, however, interesting if the validity of this assumption can be verified directly by observing the actual flow pattern in a rotameter or by a theoretical approach.

For stationary flow under certain conditions the contraction coefficient for a two-dimensional flow pattern can be computed by using the technique of conformal representation.*¹⁵ The contraction coefficient for this case turns out to be

$$C_c = \frac{\pi}{2 + \pi} = 0.611$$

and thus independent of the velocity.

In the calculations of sec. 4 and 6 a value of 0.64 is used, this value being the one commonly assumed for this type of rotameters.

For unstationary flow this theory does not hold because the velocity along a free streamline has to be a constant. A free streamline is the boundary between the moving liquid and the dead water zone, the condition at this boundary is the equality of the pressure on both sides. If two points A and B, on each side of the boundary are observed, eq. (2.1.8) gives for stationary flow

$$\nabla \left(\frac{p}{\rho} + \frac{1}{2} v^2 \right) = 0 \quad \left. \vphantom{\nabla} \right\} \quad (7.1.1)$$

$$\text{and } \frac{p_A}{\rho} + \frac{1}{2} v_A^2 = C_1 ,$$

$$\frac{p_B}{\rho} + \frac{1}{2} v_B^2 = C_2 . \quad \left. \vphantom{\frac{p_B}{\rho}} \right\} \quad (7.1.2)$$

Putting $v_A = 0$ and $p_A = p_B$, it is found that

$$v_B = \text{constant} \quad (7.1.3)$$

along a free streamline. In the approximated flow pattern of sec. 2 this condition is not fulfilled. The approximation, however, only influences the integral term of eq. (2.22.1).

Supposing free streamlines still exist eq. (2.1.8) leads to

$$\nabla \left(\frac{p}{\rho} + \frac{1}{2} v^2 + \frac{\partial \varphi}{\partial t} \right) = 0 \quad (7.1.4)$$

for unstationary curlfree flow by substitution of

$$\underline{v} = -\nabla\Phi . \quad (7.1.5)$$

Consequently

$$\left. \begin{aligned} \frac{p_A}{\rho} + \frac{1}{2} v_A^2 + \frac{\partial \varphi_A}{\partial t} &= C_1 \\ \text{and } \frac{p_B}{\rho} + \frac{1}{2} v_B^2 + \frac{\partial \varphi_B}{\partial t} &= C_2 , \end{aligned} \right\} \quad (7.1.6)$$

where C_1 and C_2 are functions of time. Substituting $v_A = 0$ and $\varphi_B = f(t)$ it is found that $p_A = p_B$ leads to

$$\frac{1}{2} v_B^2 + \frac{\partial \varphi_B}{\partial t} = C_3 , \quad (7.1.7)$$

where C_3 is a function of time again, so v_B will not in general be a constant. Hence, the analysis of the contraction coefficient for stationary flow is not valid for pulsating flow. A complete mathematical analysis of the behaviour of the contraction coefficient under dynamic conditions is very difficult and has as far as can be found never been made. A rough observation of the flow pattern with pulsating flow, however, is possible and will be described in the next sections.

7.2 THE APPARATUS¹⁾ FOR OBSERVING THE FLOW PATTERN IN A ROTAMETER WITH PULSATING FLOW.

The tests are performed with incompressible liquid flow and the rotameter III mentioned in sec. 4.2.

To make the flow pattern visible small air bubbles are used. These air bubbles are injected into the current by means of a siphon. Under normal circumstances the amount of air injected is far too large. When a restriction is put in the air inlet of the siphon, it turns out to be possible to generate a fair amount of satisfactory tiny bubbles like those in a glass of champagne. As the velocity of these bubbles due to the buoyant force is small compared with the fluid velocity, the paths of these bubbles indicate the streamlines to a good degree of accuracy.

To observe only a vertical cross-section of the streamline pattern a light beam, about 2 cm high and 1 mm wide is projected on the rotameter (fig. 7.2.1).

To prevent the light diffused by the bubbles from being reflected at the outer tube wall, the rotameter is immersed in a rectangular ves-

¹⁾ The apparatus has been build by F. Koopmans, who also made the pictures.

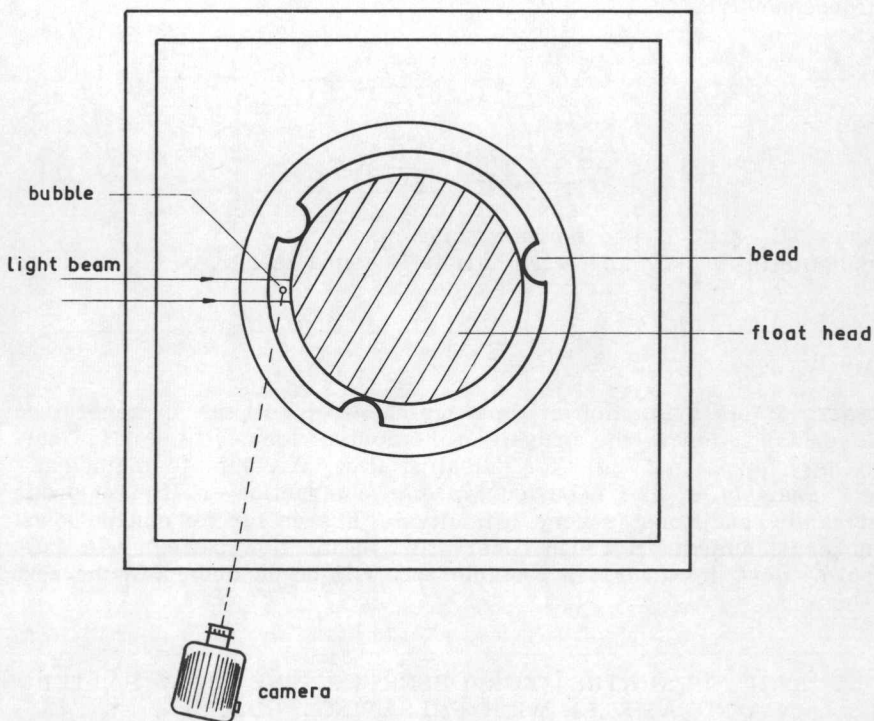


Fig. 7.2.1
The apparatus for observing the flow pattern.

sel with windows and filled with water. The float is painted black with camera paint.

The picture is distorted by the tube wall as it acts as a (bad) lens. In particular, the beads tend to distort the picture and cause spurious reflections.

Pulsations are generated by a generator similar to the one indicated in fig. 6.121.1, but without foam plastic inserted in the rubber tube.

The circuit is shown in fig. 7.2.2.

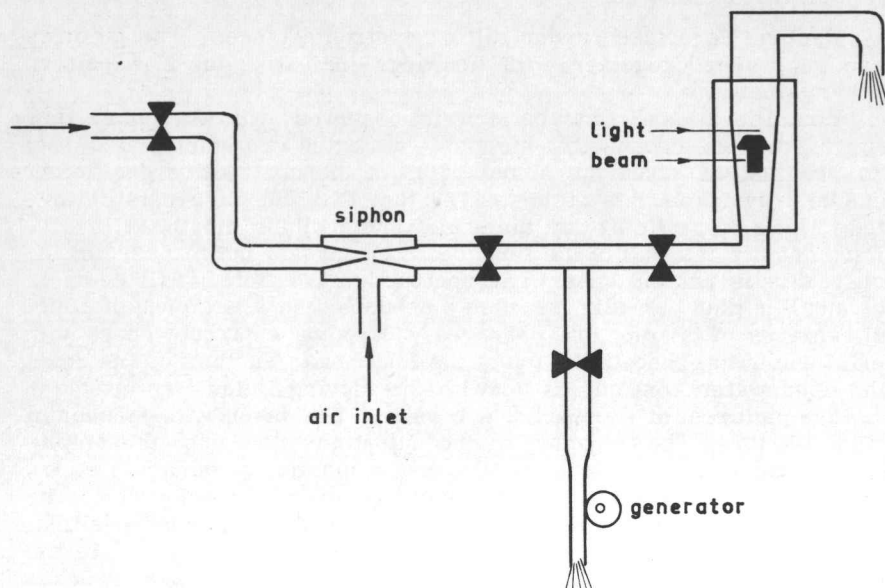


Fig. 7.2.2
The circuit used for observing the flow pattern.

The maximum frequency of the pulsations is 8.5 c/s. The amplitude of the flow pulsations can be estimated from the amplitude of the float and the measured amplitude characteristic of the rotameter. The maximum amplitude of the flow pulsations obtained is 40% of the maximum flow. The float amplitude is small.

Pictures of the streamline pattern are taken with an Alpa-reflex camera. As the quantity of light scattered by the bubbles is small, a large aperture should give the best results. This gives, however, faults that obscure the pictures. The time has to be taken long enough to give traces of a reasonable length on the picture. Finally, the combination $f\ 8, 1/25 - 1/100\ s$ when developed in strong developer proved to give satisfactory results.

7.3 MEASUREMENTS.

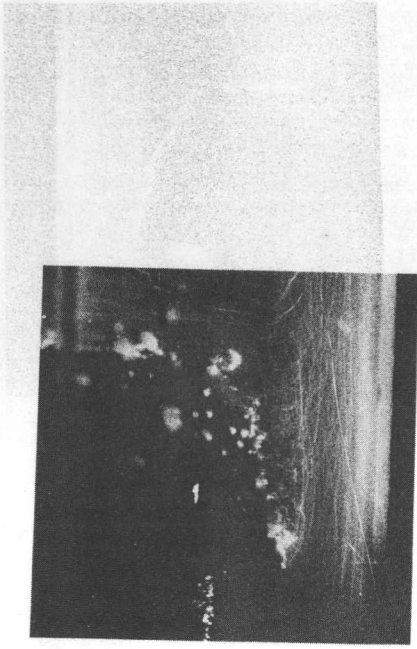
Pictures are taken under different circumstances. The pictures are reproduced together with drawings indicating the flow pattern schematically.

First of all the flow pattern is observed with stationary flow (fig. 7.3.1 a). Because the picture is distorted in a complicated way no conclusions about the actual value of the contraction coefficient can be drawn from this picture. The fact that the picture is distorted follows by realizing that the actual angle of the floathead is 45° . Furthermore the wall of the float head appears to be curved. In reality this is not the case. The contraction coefficient will seem to be smaller than in reality because the bubbles in a segment of finite dimensions of the tube are observed. The vena contracta appears to exist somewhat beneath the top of the float head. Further downstream the dead water zone mixes up with the moving fluid.

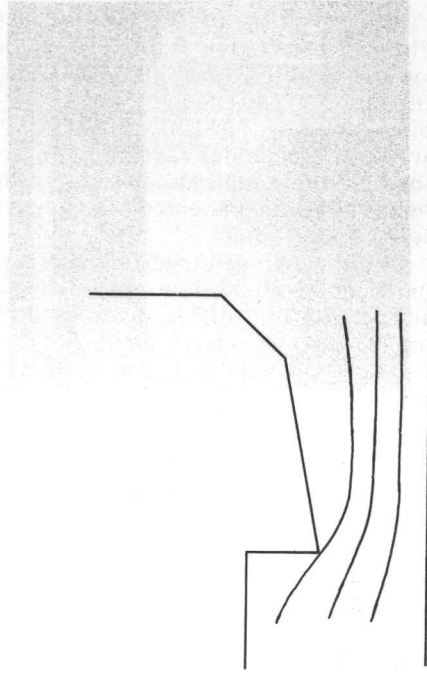
The pictures of fig. 7.3.2 a, b and c are taken with sinusoidal pulsating flow. The frequency of the pulsations is 6 c/s, the amplitude of the flow pulsations is 40% of the maximum value. The pictures a and b, are taken with the float in an extreme position. The picture c is taken when the float is about in its medium position. The flow pattern of fig. 7.3.2 a and b is approximately equal to the one drawn in fig. 7.3.1 b. The flow pattern of fig. 7.3.2 c is schematically drawn in fig. 7.3.2 d. In picture c the vena contracta appears to be closer to the float edge. This is probably the result of the dead water zone being filled up when the float is moving downward. The same effect can be seen in fig. 7.3.3 a and b which is made with a step function forced on the flow. The flow is suddenly decreased from maximum to zero and the flow is only due to the movement of the float. The picture is made about half-way in the tube. Again the vena contracta appears to be closer to the float edge, so the place of the contraction seems to vary with pulsating flow. As to the actual value of the contraction coefficient, no large variations in this quantity can be observed.

7.4 CONCLUSION.

The assumption made in the preceding sections about the contraction coefficient being constant with pulsating flow and equal to the contraction coefficient with stationary flow is not contradicted by the measurements.

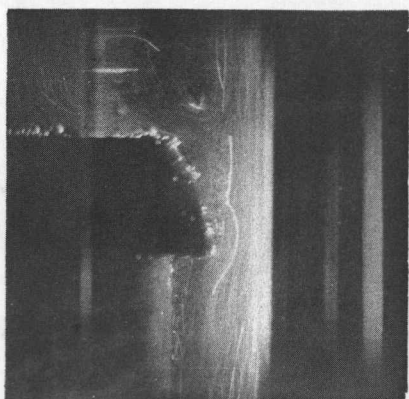


(a)

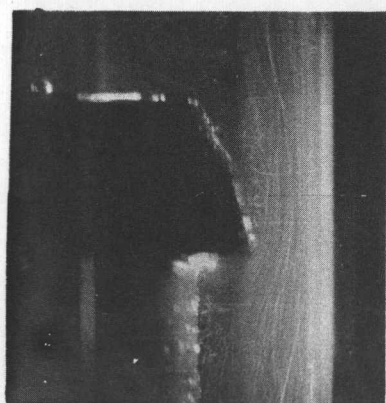


(b)

Fig. 7.3.1
The flow pattern with stationary flow.



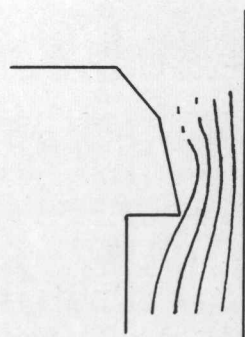
(a)



(b)



(c)



(d)

Fig. 7.3.2
The flow pattern with pulsating flow.

SUMMARY .

The equation of motion for a sharp edged float in a rotameter with incompressible fluid flow is derived from Euler's equation for flow of inviscid fluids (sec.2). Several assumptions mainly concerning the flow pattern are made. The equation of motion for the float, being strongly non-linear, is not solved but an approximate solution for small sinusoidal variations in the flow is given (sec. 3). Expressions for the amplitude and phase characteristics as well as for the deviation of the indicated mean value from the true mean value are given.

The measuring circuits and the measuring procedure used for incompressible fluid flow are discussed (sec.4). Measurements performed with four different float-tube combinations are given. A comparison is made between the actual measured and the theoretically derived amplitude and phase characteristics as well as between the measured and calculated deviation of the mean value. A reasonably good agreement between measurements and calculated values is found.

The circumstances under which the equation of motion derived for incompressible fluid flow remains valid for compressible fluid flow are discussed (sec.5). Again, a solution for small sinusoidal variations is given, the density of the gas now being neglected compared with that of the float. Apart from equations for amplitude and phase characteristics and the deviation of the mean value, an equation is given relating the variations in pressure difference over the float to the flow variations in the tube. This relation, the impedance of the float, together with the capacitance of the rotameter tube give the impedance of the rotameter. An inspection of the impedance equations shows that the float in a rotameter is liable to become unstable. This is the reason for the occurrence of the effect known in practice as "float bouncing". Several means for suppressing this instability are mentioned. A description of the circuits used for measuring the properties of rotameters used with air is given (sec.6). Measurements of the amplitude and phase characteristics as well as measurements of the deviation of the mean value are reproduced showing a reasonably good agreement with the theoretically derived behaviour. The theory of float bouncing is compared to measurements and shows a very good agreement in cases where wall friction is negligible.

To get some direct information as to whether some of the approximations about the streamline pattern hold, the streamline pattern is photographed (sec.7). Some pictures are reproduced. The streamline patterns seen in the photographs verify the presence of a flow pattern similar to that of stationary flow for the described dynamic cases.



SAMENVATTING.

De bewegingsvergelijking van een vlotter met scherpe rand in een rotameter voor onsamendrukbare vloeistoffen wordt afgeleid uit de hydrodynamische vergelijking van Euler (hoofdstuk 2); hierbij zijn verscheidene veronderstellingen o. a. over het stroomlijnprofiel gemaakt. De sterk niet-lineaire bewegingsvergelijking is niet opgelost, maar de oplossing werd benaderd voor kleine sinusvormige verstoringen (hoofdstuk 3). Er zijn uitdrukkingen afgeleid voor de amplitude- en fase-karakteristiek zowel als voor de afwijking van de aangewezen gemiddelde waarde van de werkelijke gemiddelde waarde van de stromen.

De meetopstellingen en de meetprocedure gebruikt voor het meten met onsamendrukbare vloeistofstromen komen vervolgens aan de orde. Metingen gedaan met vier verschillende buis- vlotter combinaties worden beschreven (hoofdstuk 4). De werkelijke gemeten en de theoretisch afgeleide amplitude- en fasekarakteristieken worden vergeleken, evenals de gemeten en de berekende afwijking van de gemiddelde waarde. Er blijkt een redelijk goede overeenstemming tussen gemeten en berekende waarden.

De voorwaarden waaronder de bewegingsvergelijking, zoals die afgeleid is voor onsamendrukbare vloeistofstromen, geldig blijft voor samendrukbare stromen worden vervolgens beschouwd (hoofdstuk 5). Wederom is een benaderde oplossing mogelijk voor kleine sinusvormige verstoringen. Nu is tevens de dichtheid van het gas verwaarloosd ten opzichte van die van de vlotter. Uit de benaderde oplossing volgen weer vergelijkingen voor de amplitude- en de fasekarakteristiek en de afwijking van de gemiddelde waarde. Bovendien wordt een verband afgeleid tussen de veranderingen van het drukverschil over de vlotter en de stroomvariatiën in de buis. Dit verband, de impedantie van de vlotter en de capaciteit van de rotameterbuis bepalen tesamen de impedantie van de rotameter. Uit een onderzoek van de vergelijkingen voor de impedantie blijkt dat de vlotter in een rotameter instabiel kan zijn. Dit is de reden van het optreden van het effect dat bekend is onder de naam "float bouncing". Dit verschijnsel blijkt op verschillende wijzen te onderdrukken.

De apparatuur die gebruikt werd voor het meten met luchtstromen wordt beschreven (hoofdstuk 6). Meetresultaten, zowel van amplitude- en fasekarakteristiek als van de afwijking van de gemiddelde waarde laten een redelijk goede overeenstemming zien met het theoretisch afgeleide gedrag. De theorie over de instabiliteit van de vlotter is aan de hand van metingen geverifieerd en blijkt een zeer goede verklaring van het werkelijke gedrag te geven wanneer de wrijving met de buiswand te verwaarlozen is.

Teneinde een directe controle te hebben of enige van de benaderingen over het stroomlijnprofiel met de werkelijkheid overeenstemmen, is het stroomlijnprofiel zichtbaar gemaakt (hoofdstuk 7). Enige foto's laten zien dat er geen reden is bij de beschreven dynamische metingen een stroomlijnprofiel aan te nemen dat afwijkt van dat bij stationaire stromen.



REFERENCES.

1. W. A. Wildhack: Review of some methods of flow measurement, *Science* 120 (1954), 191-197.
2. V. P. Head: A practical pulsation treshold for flowmeters, *Trans. ASME* 78 (1956), 1471-1479.
3. J. M. Zarek: Metering pulsating flow, *Engineering* 179 (1955), 17-19.
4. E. J. Lindahl: Pulsation and its effects on flowmeters, *Trans. ASME* 68 (1946), 883-887.
5. Unpublished laboratory report.
6. J. F. Ury: On the dynamic behaviour of a rotameter, *Bull. Res. Council. of Israël* 8C (1960), 119-127.
7. Unpublished laboratory report.
8. Unpublished laboratory report.
9. Unpublished laboratory report.
10. Unpublished laboratory report.
11. N. A. Hall: Orifice and flow coefficients in pulsating flow, *Trans. ASME* 74 (1952), 925-929.
12. C. J. D. M. Verhagen, A. M. Schneiders: Industriële volume- en stroommeting van gassen en vloeistoffen, Verslag van de leergang georganiseerd door de sectie regeltechniek van de afdeling Technische Wetenschappelijk Onderzoek van het Kon. Inst. van Ingenieurs, gehouden te Delft 20 en 21 sept. 1955.
13. Lao Tzu Li: New schemes for pulsating flow measurements with head type flowmeters, Paper no. 55 SA 79 of the ASME Jubilee annual meeting, june 19-23, 1955.
14. W. Engl: Relativistische Theorie des induktiven Durchfluszmessers, *Archiv für Electrotechnik* 46 (1961), 173-190.
15. L. M. Milne-Thomson: *Theoretical hydrodynamics*, MacMillan, London (1955).

STELLINGEN

1. De experimenteel door Harrison en Armstrong gevonden vergelijking voor de valsnelheid van een vlotter in een rechte cirkelcylindrische buis kan theoretisch verklaard worden. Hierbij blijkt dat de door hen gevonden "constante" bij de in rotameters gebruikelijke verhouding tussen buis- en vlotterdiameter varieert tussen de waarden 1 en 2.

G. S. Harrison, W. D. Armstrong: The frequency response of rotameters, Chem. Eng. Sci. 12 (1960), 253-259.

2. De bewering van Head dat voor rotameters het effect van pulserende stromen kleiner zou zijn dan voor meetflenzen is onjuist.

V. P. Head: A practical pulsation treshold for flowmeters. Trans. ASME 78 (1956), 1471-1476.

3. Isobe en Hattori houden geen rekening met het drukverschil veroorzaakt door de versnellingen van het medium bij hun theorie over de deelstroommethode.

Takashi Isobe, Hiroo Hattori: A new flowmeter for pulsating gasflow, ISA Journal 6 no. 12 (1959), 38-43.

4. Pulserende stromen kunnen ook bij turbinemeters aanleiding geven tot fouten in de aangegeven totale doorgestroomde hoeveelheid.

5. De indruk door Pio in de eerste hoofdstukken van zijn boek gewekt, dat de werking van de magnetische versterkers verklaard zal worden aan de hand van de theorie van Rozenblatt is niet juist.

E. Pio: Théorie simplifiée et calcul pratique des amplificateurs magnétiques, Dunod, Paris (1963).

6. De chopper frequentie van gelijkspanningsversterkers die uitgerust zijn met mechanische choppers, zou in sommige gevallen met voordeel lager gekozen kunnen worden.

7. Het verdient aanbeveling bij het met elektrische middelen verwezenlijken van binaire schakelsystemen, het verband tussen de schakelalgebraïsche niveau's en de spanningsniveau's zo te kiezen dat de schakelalgebraïsche "0" overeenkomt met spanning "0".

8. Bij het construeren van cyclische codes kan behalve van de gebruikelijke technieken zoals spiegelen, een weg uitstippelen in het Karnaugh diagram etc. met vrucht gebruik gemaakt worden van de volgende eigenschap van binaire gespiegelde cyclische codes:
Twee opeenvolgende codetekens die de eigenschap hebben dat ze dezelfde waarde hebben in een bepaalde bit, terwijl ze in diezelfde bit met de andere aangrenzende codetekens verschillen, kunnen gespiegeld ingevoegd worden tussen hun spiegelbeelden zonder dat cyclische eigenschap van de code verloren gaat.
9. De zogenaamde babyweegschalen zijn, meettechnisch gezien, niet voor hun doel geschikt.
10. De stelling van Posthumus: "Verzwarende van de exameneisen is niet oorzaak maar gevolg van de vergroting van de inspanning" is niet zonder meer juist.
Prof. Dr. K. Posthumus: Overlading, rendement, studieduur. Universiteit en Hogeschool 5 (1959), p. 341.
11. Volgens de Groot is de veronderstelling dat "de verschillen in relatieve bijdrage van verschillende milieus tot de studenten populatie niet verklaard kunnen worden door de combinatie van de factoren van aanleg en huiselijke milieu en dus door de daaruit resulterende verschillen in studiecapaciteiten, studiezin en -behoefte en tenslotte: eigen persoonlijke beroepskeuze "volstrekt niet bewezen. Dit is echter evenmin het geval met het tegenovergestelde.
Prof. Dr. A. D. de Groot: Behoeft aan democratisering-Misstand of misverstand? Folia Civitatis 16 no. 23 (1963).
12. Sommige woorden in de woordenlijsten van de Centrale Taalcommissie voor de Techniek zijn uitingen van een nutteloos purisme.
13. De eerste wet van Parkinson is dimensioneel niet in orde.
C. Northcote Parkinson: Parkinson's Law or the pursuit of Progress, John Murray, London (1961).

album 1427807

Disc. 1986189